REVIEW OF CANADIAN AERONAUTICAL FATIGUE WORK 2003-2005

Jerzy P. Komorowski, William Wallace
INSTITUTE FOR AEROSPACE RESEARCH
NATIONAL RESEARCH COUNCIL OF CANADA

SUMMARY

This paper provides a review of Canadian work associated with fatigue of aeronautical materials and structures during the period 2003 - 2005. All aspects of structural technology are covered including full-scale tests, loads monitoring, fracture mechanics, composite materials and non-destructive inspection.

Organisation Abbreviations Used in Text:
AMRL - Aeronautical and Maritime Research Laboratory (Australia)
APES - Analytical Processes and Engineering Solutions (USA)
ATESS - Aerospace and Telecommunications Engineering Support Squadron (DND)
CF - Canadian Forces
CSIR - Council for Scientific and Industrial Research, South Africa
DAES - Directorate of Aircraft Engineering and Support (DND)
DND - Department of National Defence
DTA - Directorate of Technical Airworthiness (DND)
FAA – Federal Aviation Administration
IAR - Institute for Aerospace Research
L-3 MAS - L-3 Communications (Canada) Military Aircraft Services (MAS)
NRC - National Research Council of Canada
QETE - Quality Engineering Test Establishment of DND
RAAF - Royal Australian Air Force
RMC - Royal Military College (DND)
SAAF - South African Air Force
SMPL - Structures and Materials Performance Laboratory
USAF – United States Air Force

TABLE OF CONTENTS

LIST OF ACRONYMS FOR TECHNICAL TERMS

ALEX	Aircraft Life Extension Program
AOA	Angle of Attack
ASI	Aircraft Sampling Inspection
ASIP	Aircraft Structural Integrity Program
BoC	Basis of Certification
CBRP	Centre Barrel Replacement Program
CDDT	Continuously Distributed Dislocation Theory
CFD	Computational Fluid Dynamics
CFSD	Corrosion Fatigue Structural Demonstration
CPBT	Corrosion Protection Breakdown Time
CPC	Corrosion Prevention Compound
CPL	Critical Parts List
CTH	Correlated Test Hours
CWH	Centre Wing Hours
DaDT	Durability and Damage Tolerance
DR-MMC	Discontinuously Reinforced Metal Matrix Composites
EBH	Equivalent Baseline Hours
ELE	Estimated Life Expectancy
EPD	Electrical Potential Drop
FE	Finite Element
FH	Flight Hours
FIP	Fuselage Improvement Program
FLAP	Fuselage Life Assessment Program
FLEI	Flight Loads Error Index
FLMP	Fatigue Life Management Program
FML	Fibre Metal Laminate
FSFT	Full Scale Fatigue Test
GIFTS	General Integrated Fatigue Tracking System
HAWSR	Hercules Airframe and Wing System Refurbishment
HUMS	Health and Usage Monitoring System
IAT	Individual Aircraft Tracking
IFOSTP	International Follow-on Structural Test Program
IMP	Incremental Modernization Program
IVD	Ion Vapour Deposition
LIF	Life Improvement Factor
LLI	Life Limited Items
MSDRS	Maintenance Signal Data Recording Set
NDI/NDT	Non-destructive Inspection/Testing
OEM	Original Equipment Manufacturer
OFP	Operational Flight Program
OIM	Orientation Imaging Microscopy
OLM	Operational Loads Monitoring
PLF	Parametric Loads Formulation
POF	Probability of Failure
RST	Residual Strength Test
PWHT	Post Weld Heat Treatment
SAR	Search and Rescue
SCMS	Structural Condition Monitoring System
SDRS	Structural Data Recording System
SEM	Scanning Electron Microscope
SESC	System Engineering Support Contract
SFH	Simulated Flying Hours
SIS	Structural Information System
SLAP	Service Life Assessment Program
SLMP	Structural Life Monitoring Program

SMP	Structural Maintenance Program
SRP	Structural Repair Program
TAM	Technical Airworthiness Manual
TEM	Transmission Electron Microscope
TLIR	Third Line Inspection and Repair
TRHH	Tail Rotor Half Hub
WDT	Wing Durability Test
WLG	Wing Landing Gear

INTRODUCTION

Canadian industry, universities and government agencies were solicited for information describing their fatigue technology related activities over the period 2003 to 2005. This review covers work performed or being performed by the following organizations:

Bombardier Aerospace

Department of National Defence (DND)
- Aerospace and Telecommunications Engineering Support Squadron (ATESS)
- Air Vehicles Research Section (AVRS)
- Canadian Forces (CF)
- Director for Technical Airworthiness (DTA)
- Director General Air Equipment Technical Management (Fighters and Trainers) (DGAEPM (FT))
- Quality Engineering Test Establishment (QETE)
- Royal Military College (RMC)

Goodrich Landing Gear
IMP Aerospace
L-3 Communications (Canada) Military Aircraft Services (MAS)

National Research Council of Canada
- Institute for Aerospace Research (IAR/NRC)
- Industrial Material Institute (IMI/NRC)

Carleton University, Department of Aerospace and Mechanical Engineering
University of Manitoba, Department of Mechanical and Industrial Engineering
Ryerson University, Department of Mechanical and Industrial Engineering

Names of contributors and their organizations are included in the text of this review.

Full addresses of the contributors are available through the Canadian National ICAF Delegate at:

J. P. Komorowski
Director
Structures and Materials Performance Laboratory
Institute for Aerospace Research
National Research Council of Canada
Montreal Road, Building M-13
Ottawa, ON, K1A 0R6, Canada
Phone: 613-993-3999
FAX: 613-993-6612
Email: jerzy.komorowski@nrc-cnrc.gc.ca

FULL-SCALE TESTING

F/A-18 Wing Fatigue Test (FT-245)– IAR/CF/Bombardier/L-3 MAS/RAAF

R.S. Rutledge, SMPL-IAR-NRC

The Structures Laboratory of the Institute for Aerospace Research (IAR) completed the wing fatigue test to 18256 simulated flight hours by October 29th 2004. The wing test is part of the F/A-18 International Follow-On Structural Test Programme (IFOSTP) to determine and extend the life of the aircraft for the Canadian Forces (CF) and the Royal Australian Air Force (RAAF). The test has been described in earlier ICAF reviews.

Figure 1. FT-245 Wing Fatigue Test

The fatigue cycling to three life times applied quasi-static loads in a sequential block. Each block represents 326 hours of CF aircraft flight. These loads were extracted from in-service aircraft measured data that represent average usage in a severe squadron. The spectrum accounts for manoeuvre, inertia, and some dynamic loads. The base data used to derive the spectrum had approximately 25 million end-point conditions and the final spectrum was truncated to about 155,000 with about 50,000 being unique load conditions. The lower level dynamic loads were truncated severely to obtain manageable test time. The objective is to determine the economic life of the F/A-18 IFOSTP aircraft wing structure and where possible obtain crack growth data to support management on a safety by inspection basis, validate repairs and modifications and obtain engineering data. This test is being conducted to demonstrate that the F/A-18 wing structure has a life equal to or greater than 6000 operational hours free of catastrophic failure. It is also required to verify the period decided upon for fleet structural inspections and to yield data on maintenance schedules, component replacements such as aileron and trailing edge flap fittings and repairs or modifications where applicable.

With fatigue cycling now complete the same rig will be used to test the fatigue test article and the transition structures to 120% design limit load conditions. These residual strength (RS) tests will be carried out to demonstrate the wing and control surface design loads can be sustained to ensure the operational limits can be met to retirement. Thirty-seven load cases have been planned with an expected completion in fall 2005. On successful completion of the initial phase of RS testing the specimen will be subjected to a second phase of RS testing with some induced damage and possibly an ultimate load case. On completion of the RS testing the specimen will be disassembled and inspected in a complete teardown. The examination of the damage structure will include quantitative fractography to obtain crack growth rates of significant cracks that occurred during fatigue testing. To date over 1138 damage sites have been reported in the structural information system database for the FT-245 wing test and 357 of these are located on the inner and outer wing test specimens. For each of the sites a disposition specifying the action taken and applicable depot level engineering report have also been recorded in the SIS. From the damage reporting and disposition record notices of structural deficiency have been created. These are used by the repair and overhaul contractor, L-3 MAS, to prepare repairs/modifications to the structure, schedule and carryout fleet structural inspections and to yield data on maintenance schedules.

Strain data trend monitoring has been used to identify areas where structural changes have occurred in the test specimen and several load calibrations have been carried out to measure the loads transmitted between the control surfaces and the wing box at connections where redundant load attachments occur. Monitoring of the strain changes throughout the test has lead to the discovery of much damage in the structure. Strains are monitored throughout each test block using a limited number of end levels and strain data has been recorded for full blocks following significant structural changes to aid in the interpretation of data.

Several significant failures have been discovered during the program. The most significant are: Trailing Edge Flap (TEF) wing half-hinge cracking; aft closure rib cracking, hole elongations and fastener problems resulting in structural reinforcements of the closure rib and aft closure rib using bonded titanium doublers; and Inboard Leading Edge Flap (ILEF) cracking at multiple locations and confirmation of cracking in the fleet ILEF's. The Bombardier / L-3 MAS structural modification to the ILEF that involves a confidence cut and shot peening has been successful since implementation with high strains indicated on the strip gauges but no cracks have been detected in the modified areas.

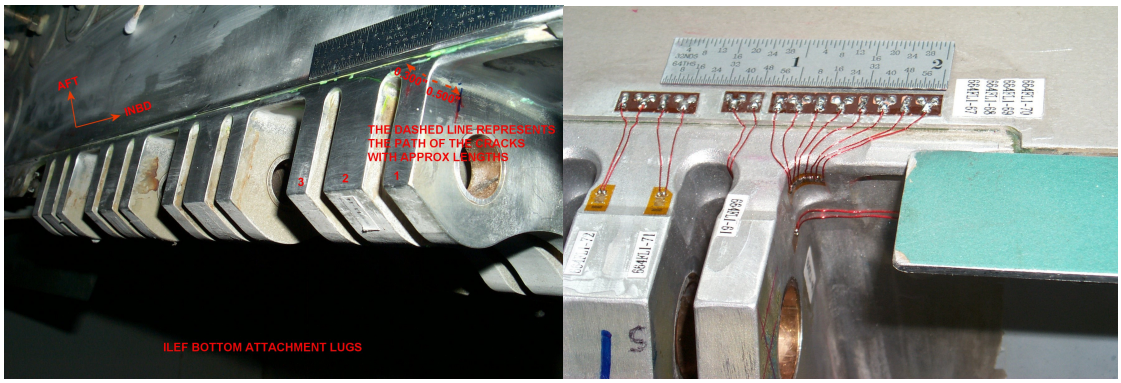

Figure 2. FT-245 Wing Fatigue ILEF Lug Cracks and Modified Instrumented Lugs

Also to date the structural cold working of holes 170-173 on the front spar of the inner wing at 3977 has been relatively successful. During level 1 inspection at 11,922 SFH a crack was detected aft of hole 172. The decision was to monitor the time to grow this crack to the front spar web, which would result a fuel leak situation for a fleet aircraft. Subsequently, a phased array ultrasonic inspection technique was developed to monitor the growth when the ILEF was removed. By 18,256 hours the growth forward toward the web at hole 172 had not significantly grown based on the phased array inspection. The slow growth or crack arrest at this location is likely due to the high compressive stress region due to cold work but this needs to be confirmed by teardown inspection. This location will be critical to the successful application of the residual strength load conditions. It is noteworthy that hole 172 on the port wing was also found cracked at about 7,000 SFH and this wing had approximately 3,600 hours of previous service. This crack was about 0.030 inches long at the time. To repair this crack the hole was reamed to remove the crack and an aluminum bushing was installed. Then a nominal size Radial-Lok expandable fastener was installed. Unlike the cold worked starboard wing in this area there has been no significant cracks found during the many subsequent inspections, including a level 1 inspection at 18,256 SFH and 21,900 total hours. Other areas of the wing box near the wing root have known cracks in the intercostals and closure ribs.

All cracks will be tested to residual strength loads that are 120% of design limit load. One of the residual strength test loading curves for the wing box and the associated wing root bending versus wing root torsion cross plot has been included below, Figure 3, along with the applied spectrum load levels.

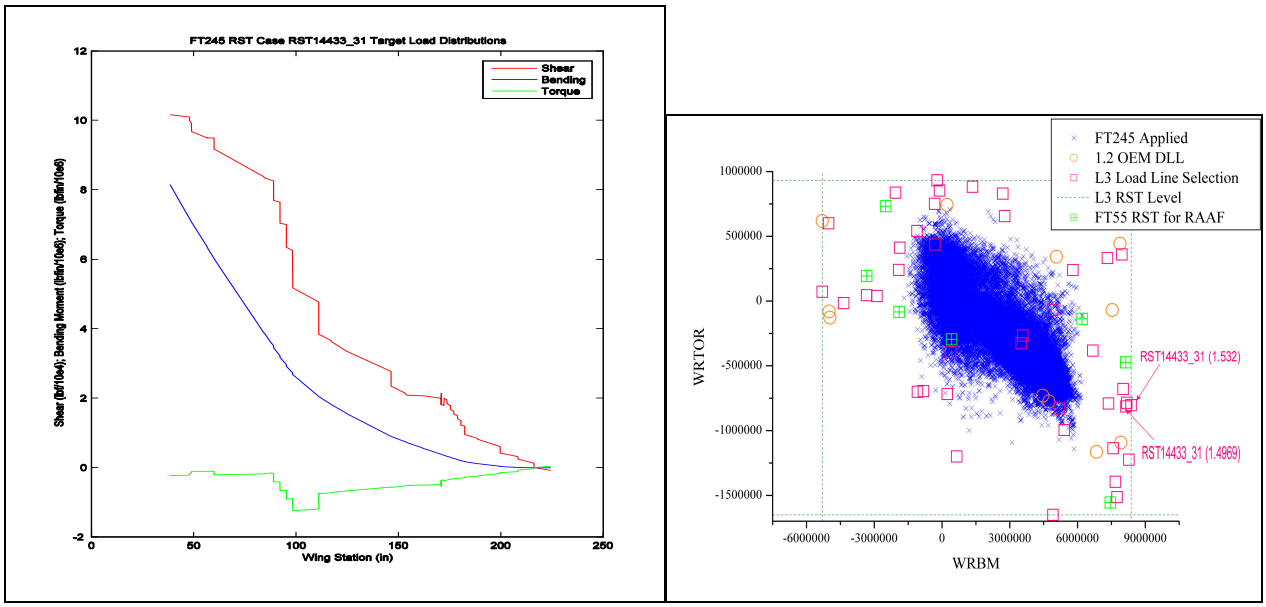

Figure 3. FT-245 Wing Fatigue RST Sample Load Distribution and Load Case Cross Plot

F/A-18 Extended Fatigue Test of Dynamically Loaded Wing Attachments - IAR/CF/ L-3 MAS

R.S. Rutledge, SMPL- IAR-NRC

FT-245, is the primary means of CF-18 wing structural certification. The test spectrum included dynamic loads caused by trailing edge and wing tip buffet, but the spectrum had to be severely truncated, particularly in terms of control surface attachment and wing tip loads, to complete the test in an appropriate time. Some areas of the wing may therefore be under-tested. In addition, the CF Lifing Policy has recently been revised such that areas subjected to dynamic loads must be tested to five times the required service life. Therefore, the CF decided to perform additional component testing to ensure that no failures to the lug attachments and wing tip would occur in five lifetimes of testing or 30,000 simulated flight hours. The IAR-NRC was tasked to carry out this testing during the next year.

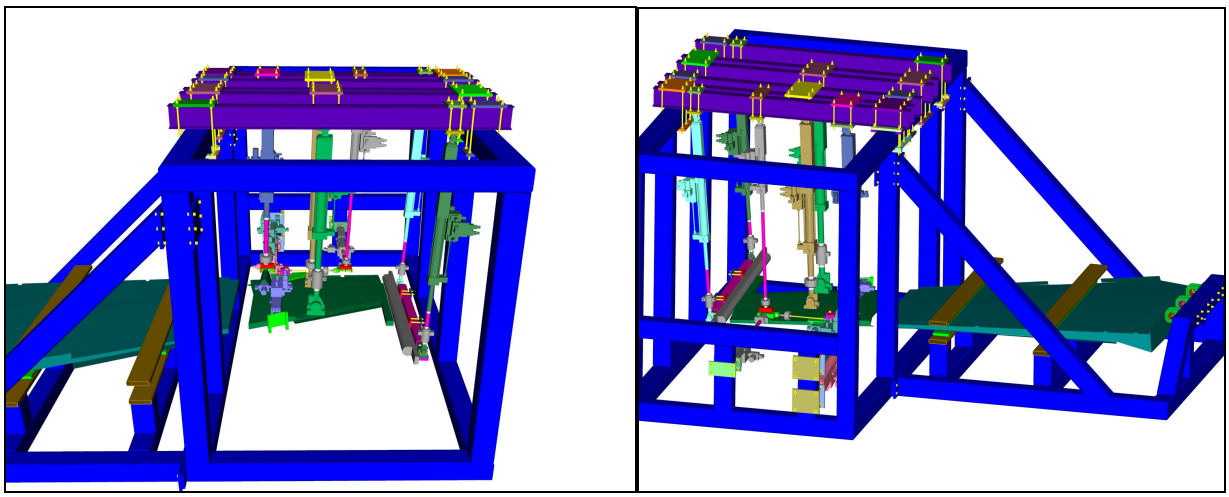

Figure 4. FT-193 Extended Fatigue Test Set-up

The objective of the project, identified as FT-193, is to test the outer wing tip, the wing-side aileron outboard lug, wing-side aileron inboard lug and wing-side aileron actuator attachment in phase 1 of the test. In phase 2 the wing-side trailing edge flap outboard lug and localized back-up structure will be tested. Both test phases will apply an equivalent of 30000 simulated flight hours of CF-18 usage. Due to anticipated long spectra length for these tests the Structures Laboratory will utilize developmental software that has been developed to increase fatigue-testing speeds. The rig developed for this test is shown schematically in Figure 4. This work is also described separately in the ICAF review.

F/A-18 International Follow-On Structural Program (IFOSTP-FT-55) Center Fuselage Test

J. Dubuc, L-3 Communications (Canada) Military Aircraft Services (MAS)

In November 2003, L-3 Communications (Canada) acquired the Military Aircraft Services (MAS) division from Bombardier Aerospace Defense group. Since 1987, L-3 MAS has been under contract by the Canadian Forces (CF) to conduct System Engineering Support (SESC) on their CF-18 fleet. This contract includes the conduct of all aspects of the ASIP program and of all related depot level structural maintenance. Since 1998, a major life extension effort has been in place under the Aircraft Life Extension (ALEX) program to ensure that the aircraft could reach their original design life of 6000 hours.

The teardown of IFOSTP FT-55 centre fuselage test article (Figure 5,[1]) was completed. Quantitative fractography performed by the Quality Engineering Test Establishment (QETE) and the Aeronautical and Maritime Research Laboratory (AMRL) in Australia provided important data on the various cracks that were excised from the test article. Microscopic examination of the fracture faces defined the crack initiation sites and growth rates that were key inputs to the ASIP and SRP programs.

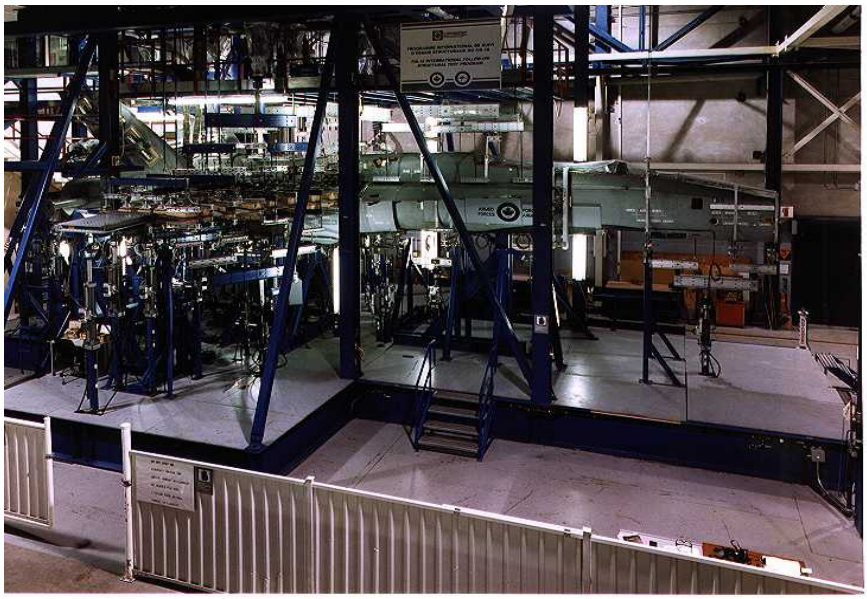

Figure 5. FT-55 Full scale fatigue test at Bombardier Military Aircraft Division, now L-3 Communications

Significant effort has also been spent to improve the accuracy of the IFOSTP derived fleet spectrum loads (designated 99LD). This has resulted in improved predictions of wing root, wing fold, and wing tip torsion interface loads with a better definition of dynamic loads caused by buffeting at high angles-of-attack (AOA). Nearly all of the outer wing and trailing edge control surfaces interface loads are subjected to dynamic effects. As noted above, a scatter factor as high as 5 (compared to as low as 2.4 for traditional low-cycle fatigue areas) is required for dynamically affected components. L-3 MAS has proposed and evaluated various configurations of the testing set-up for the purpose of optimizing test fidelity, test speed, and cost. As described above, the final development of the selected set-up is now underway at the NRC where the test will be performed. L-3 MAS will provide engineering support, including the responsibility to derive and truncate the final actuator load spectrum.

Instrumentation of a Fatigue Full-Scale Test Article

Dany Paraschivoiu, L-3 Communications (Canada) Military Aircraft Services (MAS)

A summary has been provided of the purpose and procedures used in the instrumentation of a full-scale fatigue test with emphasis on strain gauges, accelerometers and displacement gauges. The methods used on the CF-18 full-scale fatigue test (FT-245) at IAR-NRC are given as examples. Instrumentation fulfils several criteria and needs, including ground calibration comparisons, flight test correlations, comparisons with previous fatigue test results, loading assessment, analyses and component life assessment, FEM validation, test safety, inspection support and component calibration (if required). Full details are available in [2].

Regional Jets DaDT Testing and In-Service Issues

P. Newman, M. Jolicoeur, Bombardier Aerospace (BA), Regional Jets

The continued success of Bombardier Regional Jets is best illustrated in Table 1, which shows that as of May 2005 there were over 1,200 aircraft in-service. In order to ensure continued safe operation of these aircraft Bombardier has been involved in extensive fatigue testing. Much of the program was described 2 years ago in the previous Canadian National Review [1]. An update will be provided below.

Table 1. CRJ fleet statistics

As of May 2005	CRJ 100/200	CRJ 700/900
Number of aircraft in service	994	219
Number of Operators in service	40	12
Cumulative flight cycles	10.3 million	661,229
Average flight - minutes	71	80
High time aircraft cycles	26645	7585

CRJ200 Fleet Leader Program - Complete Airframe Fatigue Test (CAFT)

Service aircraft was acquired in October 2002, by this time it has accumulated 21580 cycles in service. Test Objectives are as follows:

- To confirm the durability and residual strength of the airframe
- Allow for early Identification of Structural Issues
- Avoid Aircraft-on-the-Ground (AOG)s and reduce Operators costs by allowing the scheduling of preventive modifications with planned maintenance activities
- Allow Bombardier Aerospace to plan corrective action for aircraft in production
- To validate repairs for service and assess Structural Repair Manual (SRM) repairs

Service aircraft was acquired in October 2002, by this time it has accumulated 21580 cycles in service. Test Objectives are as follows:

- To confirm the durability and residual strength of the airframe
- Allow for early Identification of Structural Issues
- Avoid Aircraft-on-the-Ground (AOG)s and reduce Operators costs by allowing the scheduling of preventive modifications with planned maintenance activities
- Allow Bombardier Aerospace to plan corrective action for aircraft in production
- To validate repairs for service and assess Structural Repair Manual (SRM) repairs

Test started in August 2003 and by December 2004 completed 80,000 flight cycles (in-service cycles + test cycles). Test setup is shown in Figure 6.

Figure 6. CRJ200 Fleet Leader CAFT.

CRJ700/CRJ900 DaDT Testing

The purpose of the DaDT Test Program is to ensure that catastrophic failure, due to fatigue or accidental damage, will be avoided throughout the life of the aircraft. The program will achieve this by:

- Identifying fatigue critical areas within the airframe.
- Providing test data for substantiation of analysis predictions.
- Developing inspection and maintenance procedures.

The test program will also demonstrate that, at the completion of 2 lifetimes of testing, there is no widespread fatigue damage present which will degrade the residual strength of the structure. With the implementation of Standard Structural Repairs and Inspection Procedures at the beginning of the program, repair integrity and inspection techniques can also be validated.

Various generic/standard repairs were incorporated in the DaDT test articles to substantiate the SRM repairs. The repairs include:

- Flush and non-flush repairs
- Dents
- Blends
- Oversize fasteners
- Oversize bushings

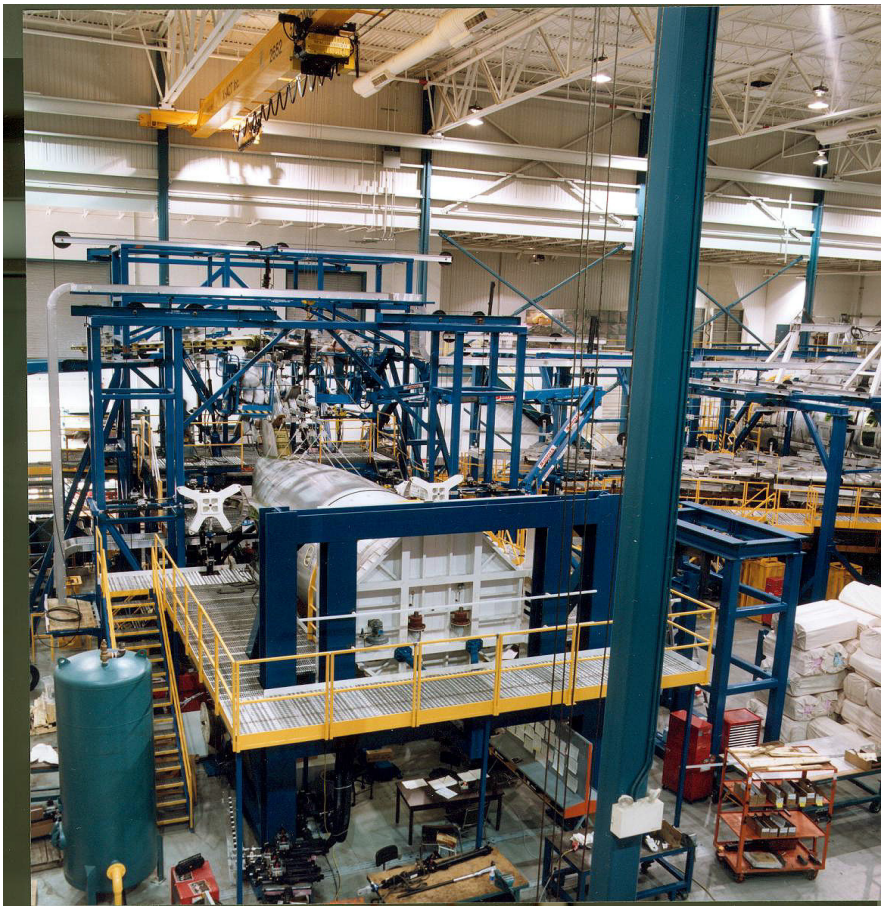

Figure 7. CRJ700 DaDT aft fuselage/empennage test.

As was reported in the previous Canadian Review [1] the CRJ700/900 DaDT full scale test is being done in 4 sections: CRJ700 forward fuselage, center fuselage/wing, aft fuselage/empennage test (Figure 7), and CRJ900 center fuselage/wing.

The status of the large sections tests is shown in Table 2.

Table 2. CRJ700/900 DATA test status – all have target of 160,000 cycles

Test section	Start Date	Status (cycles completed)	Number of artificial damages
CRJ700 Forward fuselage	April 2000	111050	42
CRJ700 Center fuselage/wing	March 2000	100806	83
CRJ700 Aft fuselage/empennage	March 2002	120,000	97
CRJ900 Center fuselage/wing	March 2002	80,000	38

In addition to these full-scale sections large number of components is undergoing testing (Table 3)

Table 3. CRJ700/900 DaDT test specimens status as of May 2005.

DaDT Specimen	Flight Count (cycles)
Slat Track 1-2 Deployed	160,000
Slat Track 1-2 Retracted	160,000
Aileron	160,000
Rudder	160,000

Multi Functional Spoiler	160,000
Inboard Flap	160,000
Inboard Slat Body	160,000
I/B Flap H/Box WS 128.00	160,000
O/B Flap H/Box WS 264.00	160,000
O/B Flap H/Box WS 220.00	160,000
Winglet	160,000
Ground Spoiler	160,000
Slat to Track 1-3 Attach.	160,000
MLG Trunnion	103,264
Elevator	160,000
Fwd Engine Mounts	120,000
Slat #3	120,000

All DaDT test programs, typically involve (i) introduction of artificial damage, (ii) monitoring of crack growth, (iii) residual strength tests.

Bombardier has developed a resin transfer molded (RTM) CRJ200/700/900 outboard flap (Figure 8). The development required a building block test approach based on MIL-HDBK-17-1E – from materials characterization, design allowable, sub-component to full-scale component tests.

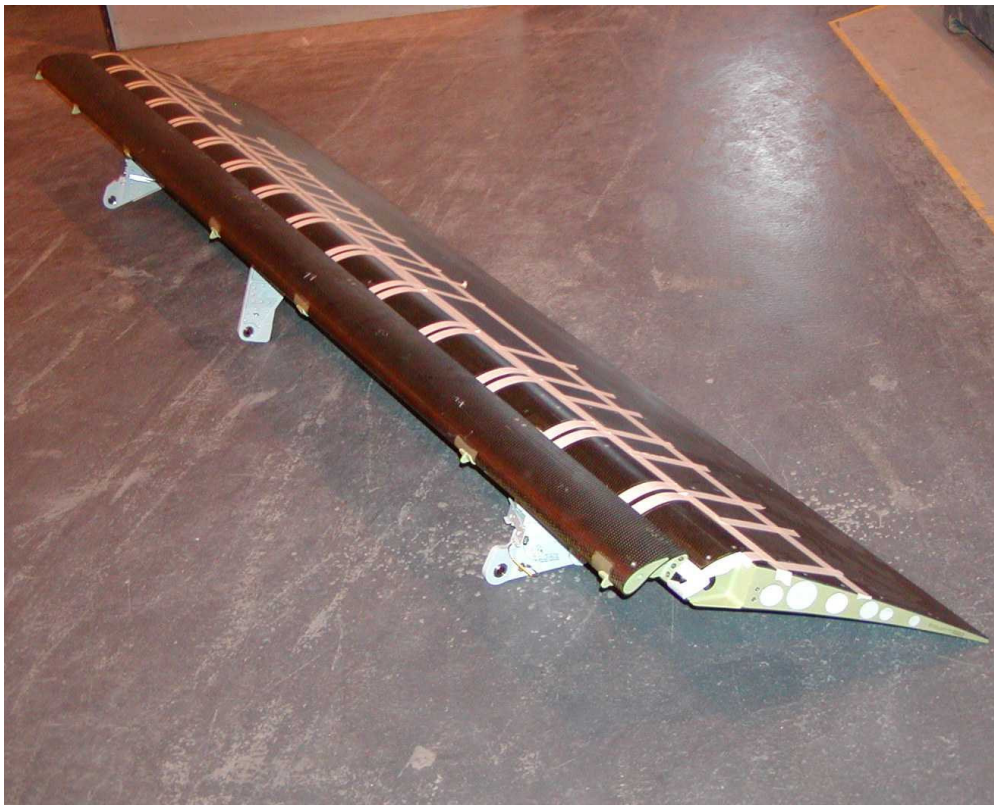

Figure 8. CRJ200/700/900 RTM outboard flap.

Four flap full scale test articles have undergone testing: birdstrike, metallic flap static and DaDT, composite flap static and DaDT, and flight testing. The composite ground tests required environmental enclosure around the specimen (Figure 9).

Figure 9. CRJ200/700/900 RTM outboard flap undergoing DaDT testing.

Challenger 300 Structural Certification Test Program

M. Milekic, Bombardier Aerospace

The Bombardier's Challenger 300 (BD-100) is a super mid size corporate jet which entered service in 2003. Challenger 300 is a transcontinental range eight-seat corporate jet which sits in the company's model line-up between the Learjet 60 and Challenger 604. It was developed for a non-stop 5471km (3100nm) mission with a load of eight passengers and National Business Aviation Association (NBAA) Instrumented Flight Rules IFR reserves.

The Challenger 300 has a primarily light-alloy structure, with composites used for some non-structural items. The fuselage is of a semi-monocoque construction with frames and stringers. The wing has two spars.

Structural certification test program consists of:

- Static Test Program (Bench Tests & CAST)
- DaDT Test Program
- Residual Strength Testing
- Bird Strike Tests
- Tire Fragment Wing Access Cover Impact Test

The first three components are described below.

The static bench tests involved multiple components loaded to limit and ultimate loads:

Fwd & Aft Engine Mounts and Thrust Link (AIDC)
Aft Engine Mount Static Test (Honeywell/GKN)
Aileron Static Test (MHI)
Rudder Static Test (AIDC)
Winglet Static Test (MHI)
Thrust Reverser Static Test (Honeywell / GKN)
Fwd Engine Mount Static Test (Honeywell/GKN)
Flap Static Test (MHI)
Elevator Static Test (AIDC)
Spoilers Static Test (MHI)
Pitch Trim Actuator Attachment Static Test (AIDC)
Gear Tab Static Test (BA)

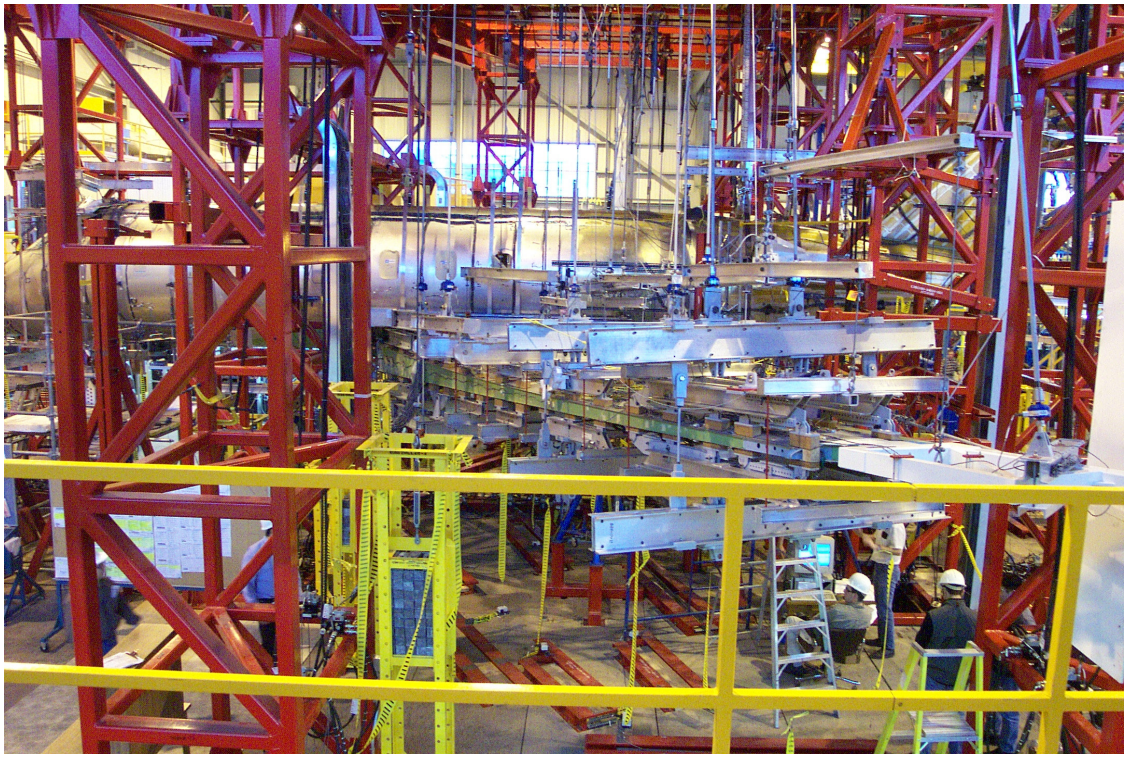

Figure 10. Challenger 300 CAST.

Complete airframe static test (CAST) – consisted of 19 limit load and 22 ultimate load test cases. The test article was instrumented with 2234 strain gauges: 1759 axial (E), 371 shear (S), 104 rozettes (R), 14 load cells, 101 displacement transducers (LVDT). The CAST is shown in Figure 10.

As part of the structural certification a complete Challenger 300 FEM was created with: 27113 nodes and 60132 elements. FEM verification procedure involved several steps:

- Replacing flaps, ailerons, elevators etc. with modeled dummy components
- Modeling loading straps and pads as per CAST specimen
- Discretizing for 1G internal loads
- Applying 1G free-float loads
- Applying load case pad/strap loads
- Comparing strain gauge and deflection measurements from CAST with output data from the model and analysis based on model output.

Certification DaDT Test Program involves bench test components and complete airframe DaDT test. The bench test components were:

Engine Mounts (Fwd & Aft) & Thrust Link (AIDC)
Fwd Yoke DaDT Test (Honeywell / Westland)
Aft. Yoke DaDT Test (Honeywell / Westland)
Aileron Tabs DaDT Test (Bombardier)
Aileron DaDT Test (MHI)
Elevator DaDT Test (AIDC)
Rudder DaDT Test (AIDC)
Spoilers DaDT Test (MHI)
Flap DaDT Test (MHI)
Flap connections DaDT Test (MHI)

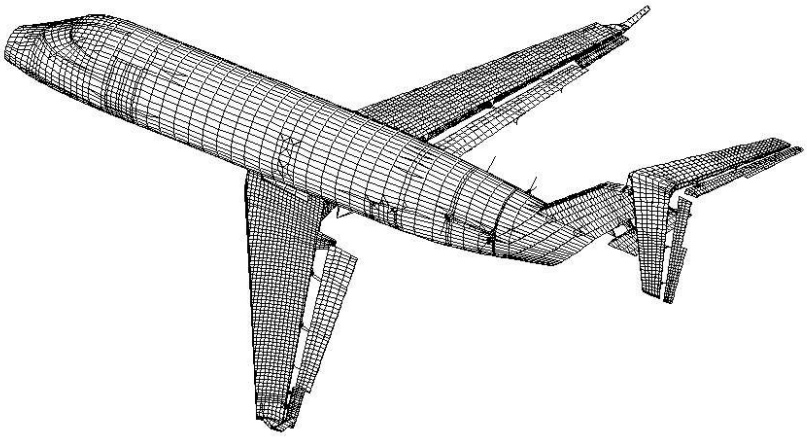

Figure 11. FEM model of Challanger 300.

All static and DaDT bench tests were completed as was the CAST.

Complete airframe full scale DaDT test article is being subjected to two and a half lifetimes of fatigue testing (15,000 + 15,000 + 7,500 = 37,500 flights) (Figure 12). The certification requirement is two lifetimes only (30000 flights). As of Nov 15, 2004, the full scale DaDT test article has completed one life (15,000 flights) crack free and has undergone scheduled inspection after 5,625 flights in second life (total flight completed 15,000 + 5,625 = 20,625 flights). As of May 10, 2005 DaDT test has accumulated 27,500 cycles. The goal is to achieve 2.5 lifetimes (37,500 cycles).

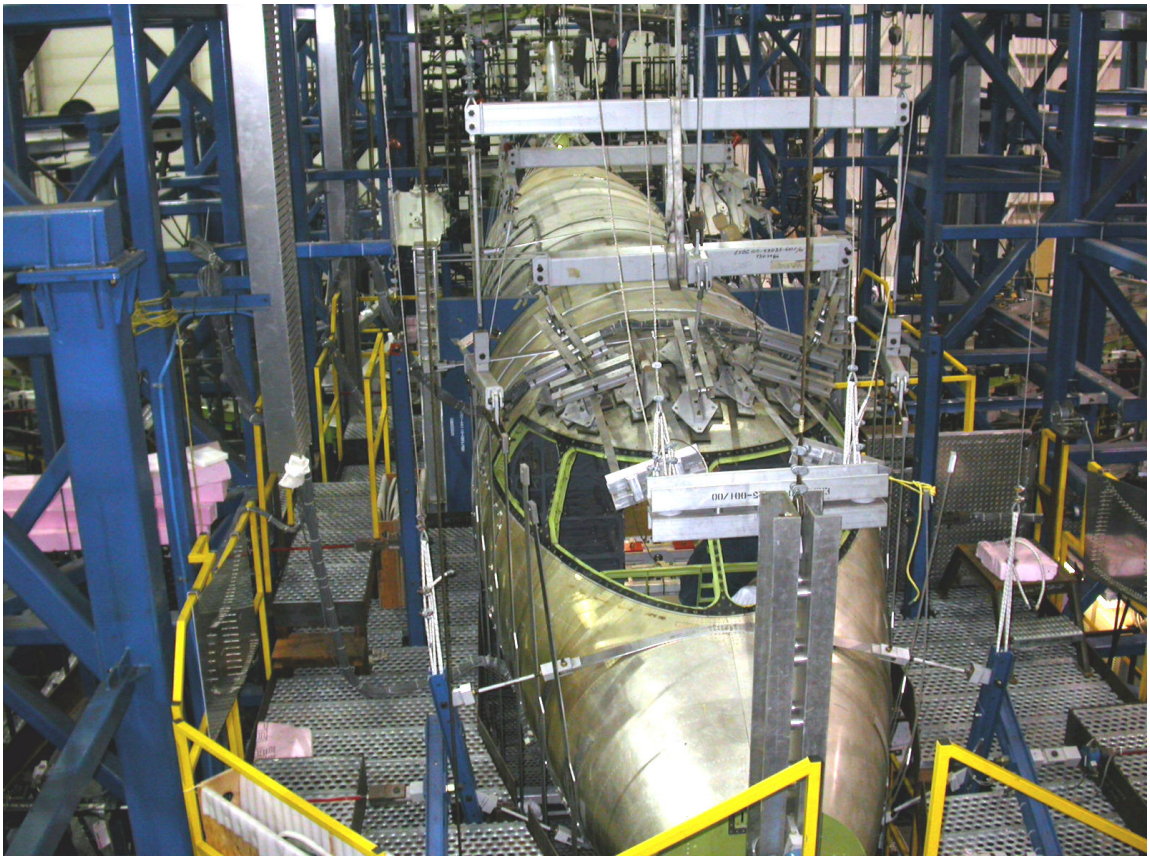

Figure 12. Challaenger 300 DaDT test article.

Full-scale Structural Fatigue Testing Technology

R. Hewitt, SMPL-IAR-NRC and MTS Systems Corporation

Full-scale aircraft structural fatigue tests are extremely complex from a control systems viewpoint. There are usually a large number of actuators with significant interactions between them and control is made more difficult because the load cells usually move with the actuators. As reported in previous ICAF reviews, a model of a full-scale structural test system has been developed at IAR with the aim of improving the understanding of the complete structural test system. It has been used to investigate some typical problems within full scale testing as well as methods for increasing test speed.

As reported in the last ICAF review, IAR and MTS Systems Corporation entered into a collaborative research program to develop a full-scale structural test system test bed at IAR. This currently consists of a horizontal stabilizer from a Canadian Forces CT114 (Tutor) aircraft with two actuators applying loads to the starboard side as shown in Figure 13.

This facility has been used to validate a method for increasing test speed that came out of the modeling work. By using information about the complete test system that can be obtained from a relatively simple structural response survey, test speed increases of more than a factor of 4 have been obtained under spectrum type loading. Details of the technology are proprietary to IAR.

Figure 13. Two-channel test bed

IAR and MTS Systems Corporation have recently extended their collaborative research agreement to demonstrate this technology on the extended testing of the CF-18 wing, FT-193, described elsewhere in this review. IAR has incorporated the technology within MTS's AeroPro™ control software and has demonstrated it on the two-channel test bed. Implementation on the extended test is expected later this year.

LOADS AND USAGE MONITORING

CF-18 Fatigue Life Management Program (FLMP)

J. Dubuc, L-3 Communications (Canada) Military Aircraft Services (MAS)

Aircraft fatigue management is a key requirement of the structural integrity policy implemented by the Canadian Forces (CF) to ensure continued safety of flights and operational readiness of its fleets. The Fatigue Life Management Program (FLMP) encompasses all the elements needed to fulfill this requirement for the CF-18 fleet. This includes the on-aircraft Maintenance Signal Data Recording Set (MSDRS) and Structural Life Monitoring Program (SLMP) from which flight-flight derived, strain sensor based, fatigue life indices are computed. See previous ICAF summaries for further details. FLMP has been in effect since the early operation of the fleet in the late 80's. Two significant improvements have been completed recently. First, an update of SLMP to remain compatible with the new avionics and software (i.e. Operational

Flight Program (OFP) 17C) implemented during the on-going Incremental Modernization Program (IMP) and second: improvement to the strain drift derivation from operational flights.

Strain sensor readings at wing root are known to drift with time due to local effects at wing-fuselage assembly. To assess this phenomenon and make appropriate adjustments to strain sensor readings, calibration flights are performed following any aircraft maintenance action that could potentially impact on sensor drift. The experience demonstrated that this approach is not efficient from both economical and logistical perspectives. Several studies have been conducted recently to investigate the possibility of using operational flight manoeuvres instead of calibration flight manoeuvres for the calculation of the wing root strain drift. The studies showed that acceptable drift factors could be obtained using the Parametric Loads Formulation (PLF), and that the error in calculated FLEI is within acceptable limits. A methodology was developed, implemented in a test version of SLMP, and tested on a significant amount of historical data of a randomly selected aircraft. The results showed that quasi-identical FLEI are obtained over the period.

CT-114 Tutor Operational Loads Monitoring Program

J. Dubuc, L-3 Communications (Canada) Military Aircraft Services (MAS), R. Kaufman DTA

The Tutor aircraft is mainly used in the Snowbirds (air show) role. Since April 2004, all twenty-one (21) aircraft have been equipped with an Operational Loads Monitoring (OLM) system (i.e. four (4) flight parameters and four (4) strain gauges).

Following the decision to replace the horizontal stabilizer brackets (due to the difficulty of developing a proper inspection at this critical area) on several horizontal stabilizer components, a new component/location was created in the General Integrated Fatigue Tracking System (GIFTS). This brings the total number of components/locations of the aircraft, where usage tracking is performed, to twelve (12).

On-going OLM data processing is performed and results are presented on a monthly, semi-annual and annual basis to the fleet manager to assist in aircraft rotation, component swapping and aircraft retirement decisions. Safety-by-Inspection results for the wing critical locations are presented in the annual report.

Strain gauge problems were observed after about 5 years of the OLM system installation. In 2001, strain gauges were replaced on four (4) aircraft. Even with the new strain gauges installed, intermittent problems were still observed. After investigation, the strain gauge switch (used to toggle from primary to backup position) was suspected and was replaced in 2004 on some aircraft.

CT-133 Silverstar Operational Loads Monitoring Program:

J. Dubuc, L-3 Communications (Canada) Military Aircraft Services (MAS), R. Kaufman DTA

The CT-133 aircraft is now mainly operated at the Aerospace Engineering and Test Establishment (AETE). Only four (4) aircraft remain in operation. All aircraft are equipped with an OLM system. Only one aircraft is instrumented with strain gauges and the others have only four (4) flight parameters.

On-going OLM data reduction is performed with GIFTS to track the aircraft usage severity. Results are gathered in the form of semi-annual and annual reports and presented to the fleet manager.

A coupon test program was conducted at the Royal Military College of Canada (RMC) between November 2003 and April 2004. This program consisted of deriving the material properties of the aluminum alloy 2014-T6 extrusion. Coupons were machined from used and unused wing spars of the CT-133 aircraft. The most significant finding in the comparison was that the used wing material had higher strength and faster crack growth rates than the unused wing. It is suggested that differences in material processing at the time of manufacture were responsible for the observed differences.

LANDING GEAR

Qualification Testing of the Airbus A380-800 Wing and Body Landing Gear

Neil Walker, Goodrich Landing Gear

Figure 14. The A380 super structural test rig

Goodrich Landing Gear has been responsible for the design, manufacture and testing of the wing and main body landing gear of the Airbus A380-800 aircraft. The qualification test program ensures that these gears meet stringent requirements for aircraft safety and structural integrity. The tests include a series of landing simulations (drop tests) to demonstrate and quantify the energy absorption characteristics and behaviour of the gears during landing. Strength testing ensures that the envelopes of extreme load conditions expected in service are safely within the structural capability of the gears. Fatigue testing ensures that the complex spectrum of daily service loading does not result in fatigue failures in future service. Endurance testing ensures that the retraction equipment of the gears will perform as designed throughout the life of the aircraft. These landing gear tests required over two years of careful preparation –including the construction of a new lab and enormous rigs, Figure 14, to support the test equipment, and new developments in test application technology.

Strength testing is performed to demonstrate that the actual structural capability of the landing gear meets the design load criteria. There were two qualification tests and two development tests within the strength test program:

The photo-elastic test consists of the same load conditions used in limit loading, but at 50% to 75% magnitude. Photo-elastic coating on the gears was used to identify high stress concentrations. The locations of these hot spots were strain gauged and monitored during limit and ultimate load tests.

The limit load qualification test consisted of a series of 10-20 load cases representing the outer envelope of all service loads. The gear must sustain the limit loads without yielding.

The stiffness development test consisted of a series of safe loads used to measure landing gear stiffness in various directions and conditions.

The ultimate load qualification test consisted of the same load conditions used in limit loading but at 1.5X magnitude. This represents a safe margin on the landing gear structure. The gear must sustain ultimate loads without rupture.

Figure 15. Wing landing gear test rig.

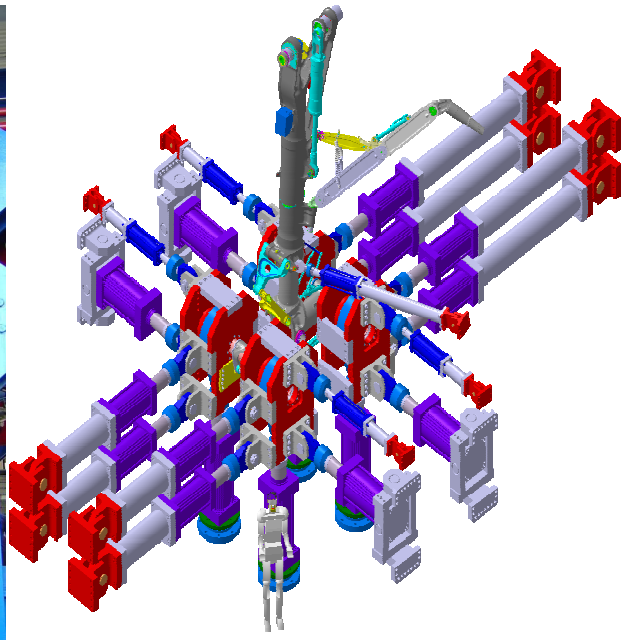

Figure 16. Wing landing gear fatigue loading

Fatigue testing was performed to prove that the landing gear design was adequate to sustain a full life of service load conditions. The test article was subjected to 5 lives of equivalent, flight-by-flight service loads. These loads included:
•Ground loads, including taxi, takeoff, landing, braking, steering, were applied through the dummy wheels.
•Up-lock loads, including lock, unlock, and in-flight cycling, were applied to the up-lock roller on the shock strut cylinder.
•Retract/extend loads induced by the aircraft Retract and Unlock Actuators, were applied by production actuators at the actuator attach points.
•Bogie pitch trimmer loads induced by a simulated Bogie Pitch Trim Actuator, were applied to the actuator attach points on bogie and shock strut cylinder.
•Piston out-stop loads, were applied by pressurizing the shock strut at full extension, and exerting a downward vertical force on the dummy wheels.

The WLG Fatigue test looks superficially like a strength test. The landing gear was installed in a test bay in the Super-rig. Dummy wheels installed on the axles were attached to loading rams, or actuators, grounded on the test rig frame. Loads were controlled in PID closed-loop by a load control system.

Whereas the strength test applied only the relatively few extreme design cases to test static strength, the fatigue test applied a long spectrum of load conditions that simulate normal service loads rather than extremes, to test resistance to fatigue cracking. The flight-by-flight spectrum was a simulation of a full life of approximately 20,000 flights, each consisting of taxiing, ground handling, takeoff, landing, turning and braking. Each simulated flight consisted of ~110-140 load combinations and events, applied in sequence over approximately 5 minutes. A wide variety of different flight conditions were simulated, including heavy landings, hard braking, etc. However, the nature of fatigue is such that a single life of testing is not sufficient proof of full life survival for all production landing gear. Consequently, the fatigue test was run through 5 lives of testing, with periodic NDT inspections to detect any incipient cracking.

An Equivalent Uniaxial Fatigue Stress Model for Analyzing Landing Gear Fuse Pins

K. Narayan, K. Behdinan, Ryerson University, and P. Vanderpol, Goodrich Landing Gear

Landing gear fuse pins are subject to a biaxial state of stress in the fuse groove. This biaxial state comprises a combination of shear stress that is usually the largest stress in the fuse pin by design, and a compressive stress that is needed to keep the half-section of the fuse pin in equilibrium. Local bending also contributes to this compressive stress. Conventional fatigue

analysis techniques have utilized an equivalent uniaxial stress, based on the Von-Mises stress of a pure-shear condition. This model predicts fatigue damage that is far greater than the damage obtained from fuse pin cyclic tests. A new equivalent uniaxial fatigue stress model has been proposed [3] that includes the additional compressive stress as a relief on the fatigue damage in the fuse groove, thereby explaining the observations from fuse pin tests. The model is used in conventional uniaxial strain-life fatigue software (for instance, Goodrich Aerospace's Fatigue Life V2) to predict the fatigue damage on a sample landing gear fuse pin with a sample load spectrum. The results are then compared to the pure shear model, and to a biaxial Finite Element (FE) fatigue analysis of the same fuse pin using nCode® FE-Fatigue™. The damage predicted by the proposed model was about twice that predicted by FE-Fatigue™ while the proposed model was far less conservative than the conventional pure shear model. The Von-Mises results for a sample fatigue load are given in Figure 17, and as expected, the maximum Von-Mises stress is in the fuse groove. It was found that the proposed model predicted the fatigue damage in the sample fuse pin conservatively when compared to FE-Fatigue™, while still being far less conservative than the conventional analysis.

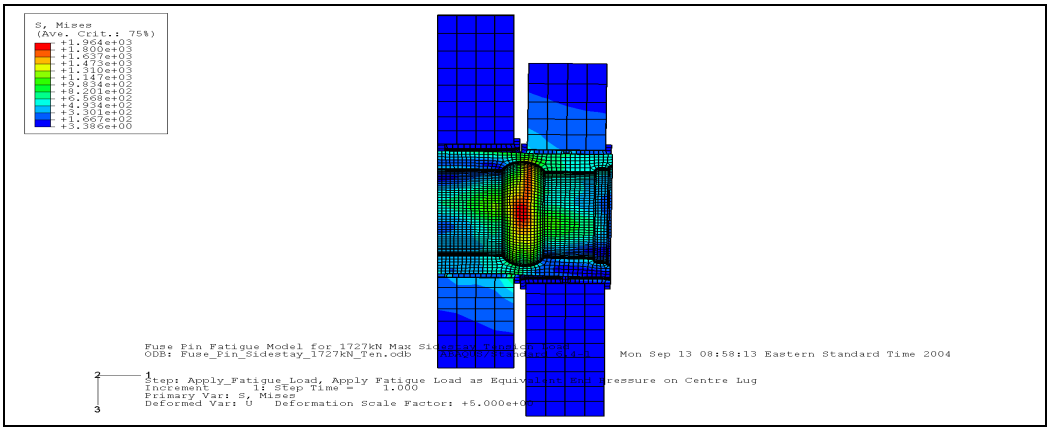

Figure 17. Assembly Von-Mises Stress Contour Plot, Top View (Sample Fatigue Load)

FATIGUE LIFE PREDICTION AND ENHANCEMENT

Effects of Exfoliation Corrosion on Residual Strength and Remaining Fatigue Life of Aircraft Materials and Structures.

Min Liao, SMPL-IAR-NRC

Exfoliation corrosion (exfoliation) is a significant maintenance issue plaguing many of today's aging aircraft. The current "find-it-fix-it" maintenance approach is very costly while the effect of the maintenance on structural integrity is not well understood. A new corrosion management philosophy has been proposed with the intent of anticipating, planning, and managing corrosion, which stands in sharp contrast to the current "find-it-fix-it" approach. To implement this new philosophy, analytical models need to be developed to evaluate the impact of exfoliation on structural integrity.

The objective of this project was to develop an analytical framework/tool to evaluate the effects of exfoliation on residual strength and remaining fatigue life of aircraft structures, and provide appropriate guidance for the repair action. Extensive test programs have been carried out using pristine and corroded specimens manufactured from naturally exfoliated 7075-T6511 wing panels. These included static tension and compression tests, compression strength tests Figure 18, bearing strength tests, and fatigue tests. Both thermographic (from the damaged side) and ultrasonic (from the undamaged side) non-destructive inspections (NDI) were performed to determine the maximum depth and three-dimensional (3D) profiles of the exfoliation damage. In the static tests, the strain/stress changes due to exfoliation were measured using strain gauges, photo-elasticity, and digital image correlation techniques. In the fatigue tests, crack origins were determined with the aid of a scanning electron microscope and the mechanisms of fatigue cracking in exfoliation regions were summarized. Progressive polishing and optical observations were carried out on failed specimens to quantify the depth of intergranular corrosion. In parallel, an analytical model was developed based on a 'soft inclusion' technique and 3D finite element (FE) modeling. The 3D FE model was first verified using the test results from the pristine specimens. For the corroded specimens, a technique to automatically generate the 3D geometry of the 'soft inclusion' (damage zone) from the NDI input was developed using the PATRAN Command Language (Figure 19). Non-linear FE analysis was also performed to

analyze the non-linear bending effect due to exfoliation. Once calibrated, the 'soft inclusion' based FE model was used to quantify the effects of the exfoliation on the residual strength (yielding strength and buckling). Based on engineering considerations, a simplified fatigue model was also developed for estimating the remaining fatigue life of the exfoliated specimens. The fatigue model used a semi-elliptical surface crack model based on the damage depth determined from NDI and the local aspect ratio of the damage (Figure 20).

The important results from these studies are:

- Exfoliation may NOT necessarily have a detrimental effect on the residual strength in the elastic and near plastic regimes, such as compressive yield (Figure 18) and bearing strength, but may have an effect in the plastic region, such as ultimate compression strength. In addition, exfoliation may have a greater effect on buckling.
- Effects of exfoliation on local strain/stress concentration are more significant than those on residual strength.
- The 'soft inclusion' based FE modeling was calibrated and verified using the experimental results, and was capable of quantifying the effect of exfoliation on residual strength (Figure 19).
- The developed engineering fatigue model could give a good estimation on the range of the remaining fatigue life, based on conventional NDI inputs (Figure 20).

Full details are provided in References [4, 5, 6, 7, 8].

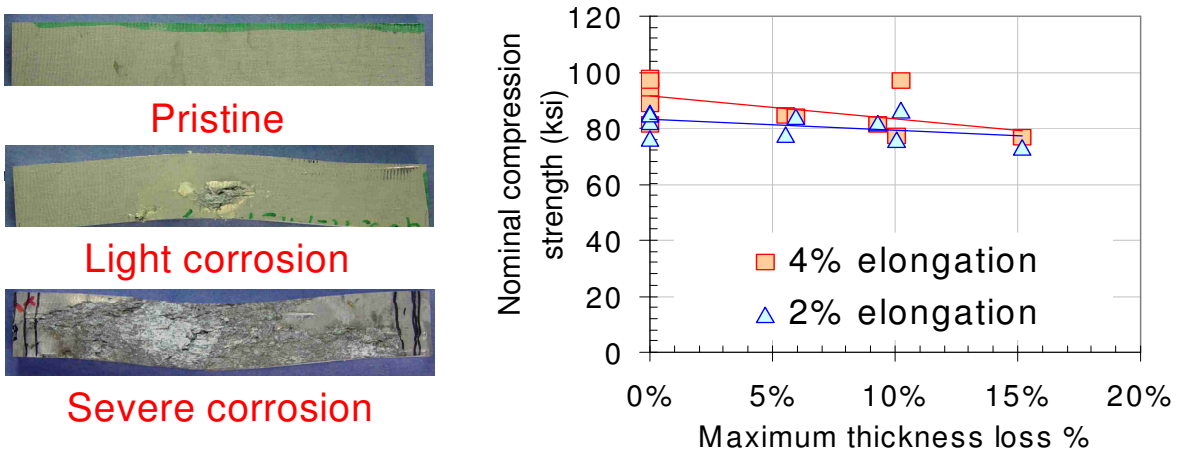

Figure 18. Typical static test: compression strength test and results.

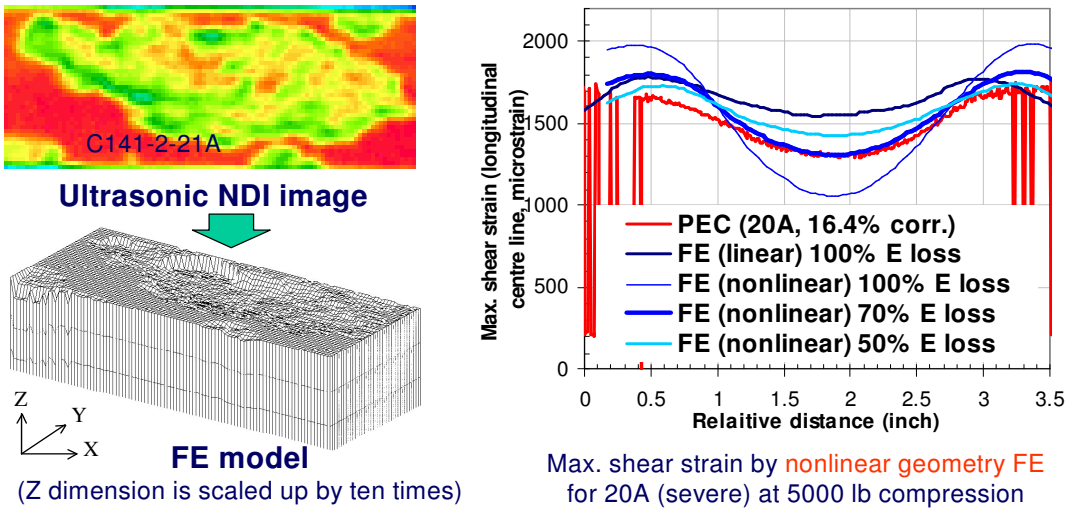

Figure 19. FE modeling process using NDI inputs and modeling results (Young's modulus E loss was calibrated in between 50-70% by non-linear FE analyses).

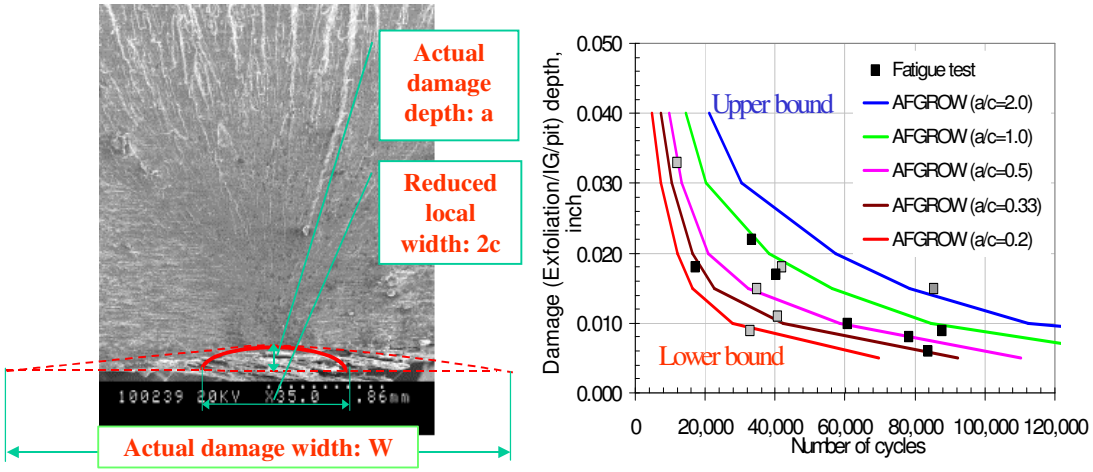

Figure 20. Fatigue cracking model in IG/exfoliation and remaining life estimation

Exfoliation Fatigue Tests Results

N. Bellinger, SMPL-IAR-NRC

To determine the effect of exfoliation corrosion on the fatigue life of wing skins, a specimen based on the ASTM E647 standard was designed so it could be machined from Boeing 707 exfoliated 7178-T6 upper wing skins. The back-face stiffener was removed leaving only a small portion of the flange around the fasteners to form a washer around the nut. Those holes that were not affected by the exfoliation were cold expanded and an interference fit steel plug was inserted to prevent premature failure.

All the tests were carried out under constant amplitude compression dominated cyclic loading, with a maximum gross section stress of 82.7 MPa (12 ksi) and a minimum gross section stress of 137.9 MPa (20 ksi). The specimens were tested to failure in laboratory air at a frequency of 10 Hz and the results are presented in (Figure 21). The maximum depth of the exfoliation was measured using ultrasonic inspection carried out after failure from the back face of the specimen. Figure 21 shows the majority of the specimens failed by fretting fatigue. A black residue was present on most of the fracture faces suggesting that fretting fatigue took place.

Although exfoliation was present around the holes where failures occurred, the primary nucleation site for most specimens was a small pit, or pits, along countersunk holes. A failure investigation on one of the failed specimens revealed tested to 9692,865 cycles revealed two cracks, Figure 22. A single pit or scar was found to be the nucleation site for the primary crack, which was located along the countersink, Figure 23.

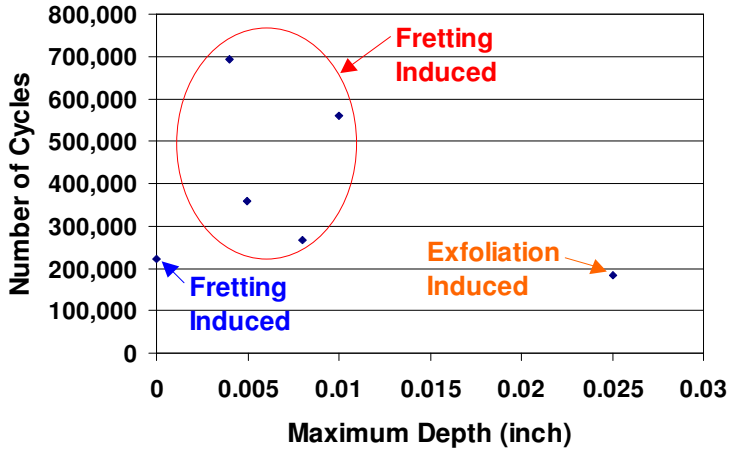

Figure 21. Results from fatigue tests carried out on coupons containing various levels of exfoliation.

The secondary crack, however, on the side of the hole that contained the exfoliation had five nucleation sites, three of which were present along the countersunk hole away from the exfoliation damage, Figure 24. Given the sizes of these cracks, it appears that the primary nucleation site was located at the maximum depth of the exfoliation (labeled 4 in the figure).

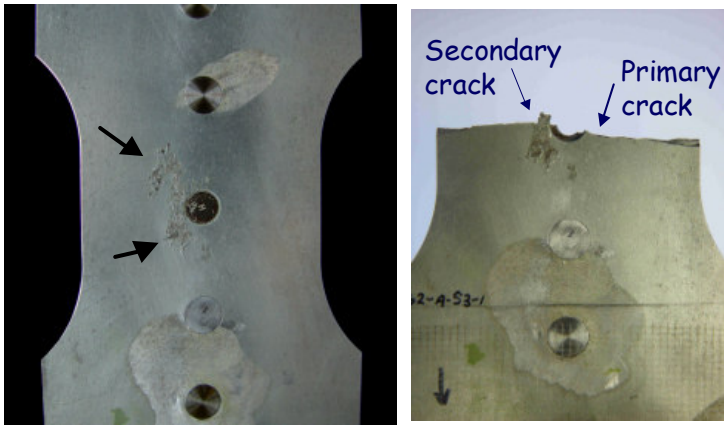

Figure 22. Optical photograph showing location of exfoliation and primary and secondary cracks.

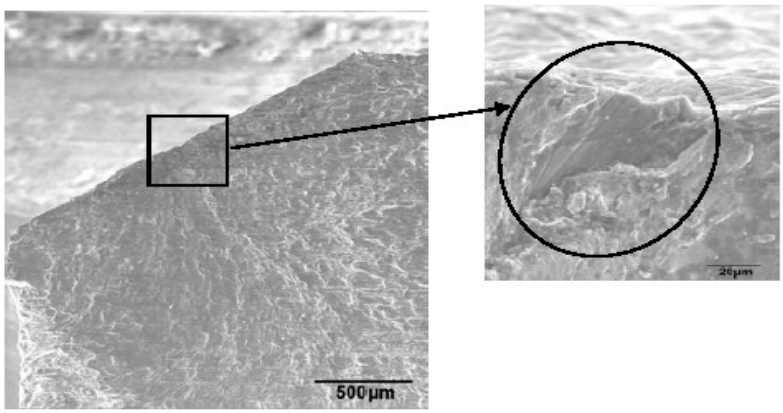

Figure 23. Micrographs of primary nucleation site that was located along countersunk hole.

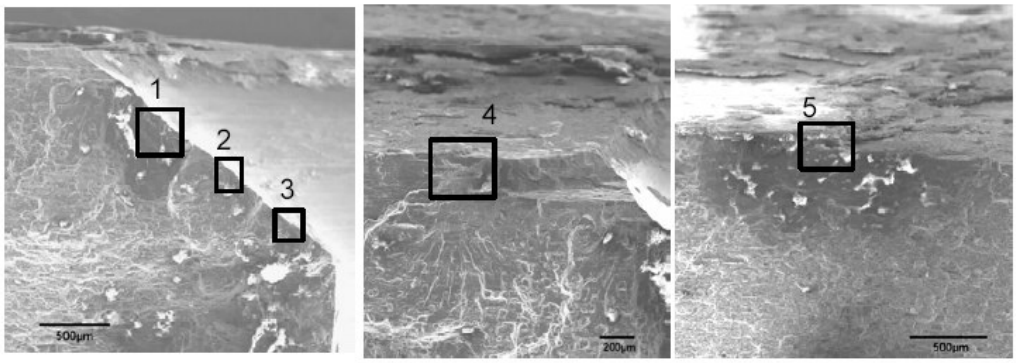

Figure 24. Micrographs showing location of nucleation sites for secondary crack. Note that crack 4 and 5 were located within the exfoliation.

When another specimen with exfoliation spanning two holes (arrows in Figure 25), was subjected to the compression dominated load, an area below the visible exfoliation was observed to buckle (circle in Figure 25b). This buckled area was found to contain exfoliation that was 0.01 inch deep while the visible damage was only 0.005 inch deep. This specimen failed at 560,465 cycles.

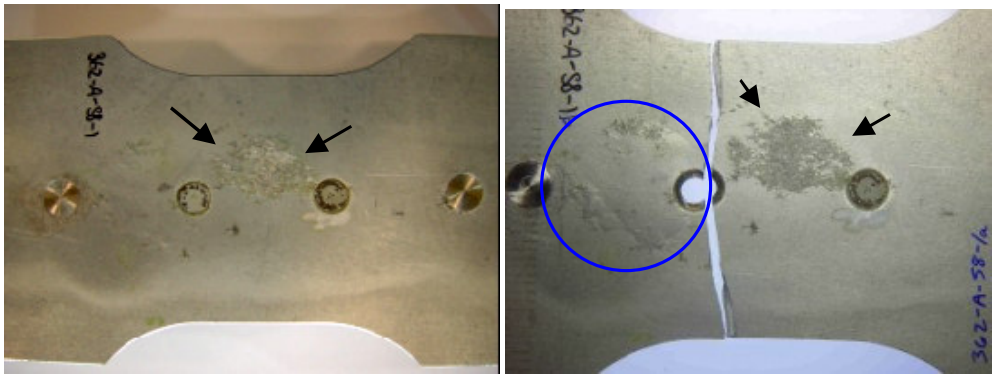

(a) Condition of outer surface prior to testing. Arrows shows visible exfoliation.

(b) Condition of outer surface after failure. Circle shows area at which local buckling occurred during loading.

Figure 25. Optical photographs of a specimen showing location of visible as well as hidden exfoliation.

For this particular specimen, exfoliation (red arrow in Figure 26), was present on the primary fracture surface. This exfoliation was not extensive and consisted of intergranular cracking that propagated parallel to the outer surface. The nucleation site, however, did not occur at the exfoliation but along the countersink. Once again a black residue was present on both fracture faces.

The results presented in Figure 21 were obtained from tests carried out using compression dominated constant amplitude loading. Since this type of loading was not representative of the load applied to an upper wing skin, it was decided to carry out a test using a truncated upper wing skin spectrum. The specimen chosen was inspected to determine that the depth of the exfoliation was 29%. Since it was anticipated that this specimen could be subjected to a significant number of load cycles, tabs were bonded to the ends of the specimen to prevent premature failure, Figure 26.

During testing an x-ray inspection was carried out, under a slight tensile load, at the end of each pass of the spectrum to determine if a crack was present. The specimen successfully completed 20 passes of the truncated spectrum, which represents 2 lifetimes, with no observable cracking. This suggests that for the spectrum loading used, the significant level of exfoliation present in the specimen did not affect the fatigue life of the material.

After this test was completed, the specimen underwent a simulated repair, in that the exfoliation was ground out in accordance with repair guidelines. Prior to testing an ultrasonic inspection from the back face of the specimen was carried out to determine the depth of the grind-out, which had a maximum thickness loss of 30%, Figure 27.

Once again this specimen successfully completed 20 passes of the truncated spectrum (2 lifetimes) without any evidence of cracking. As in the previous test an x-ray inspection was carried out after each pass to detect the presence of cracking. It should be pointed out that this specimen successfully completed 4 lifetimes (using a truncated spectrum) without cracking.

Once again this specimen successfully completed 20 passes of the truncated spectrum (2 lifetimes) without any evidence of cracking. As in the previous test an x-ray inspection was carried out after each pass to detect the presence of cracking. It should be pointed out that this specimen successfully completed 4 lifetimes (using a truncated spectrum) without cracking.

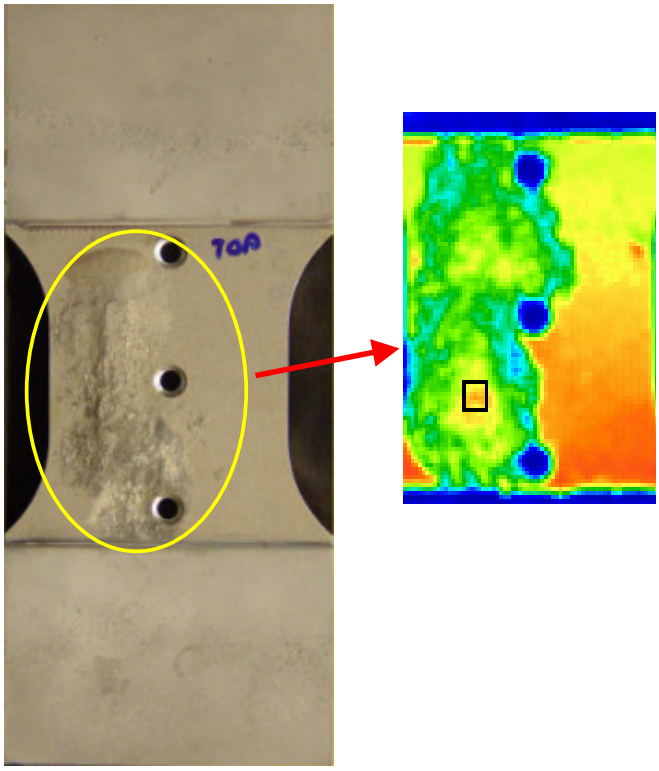

Figure 26. Photograph of exfoliated specimen and ultrasonic inspection showing location of maximum depth.

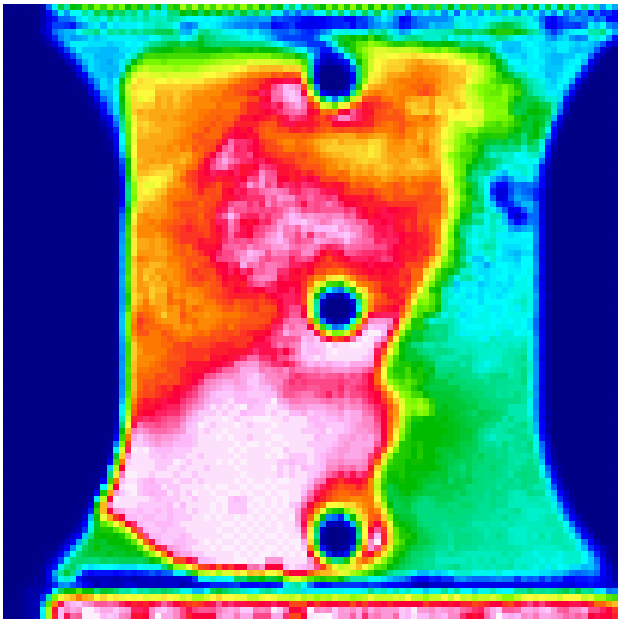

Figure 27. Ultrasonic image showing maximum depth of the repaired specimen.

Nucleation and Short Fatigue Crack Growth Behaviour of 2024-T3 Aluminium alloys

A. Merati, SMPL-IAR-NRC

Nucleation and short crack growth make up a majority of the fatigue life of aluminium alloys. In the short crack growth regime, local microstructural features such as grain boundaries and grain size, inter-particle spacing, and

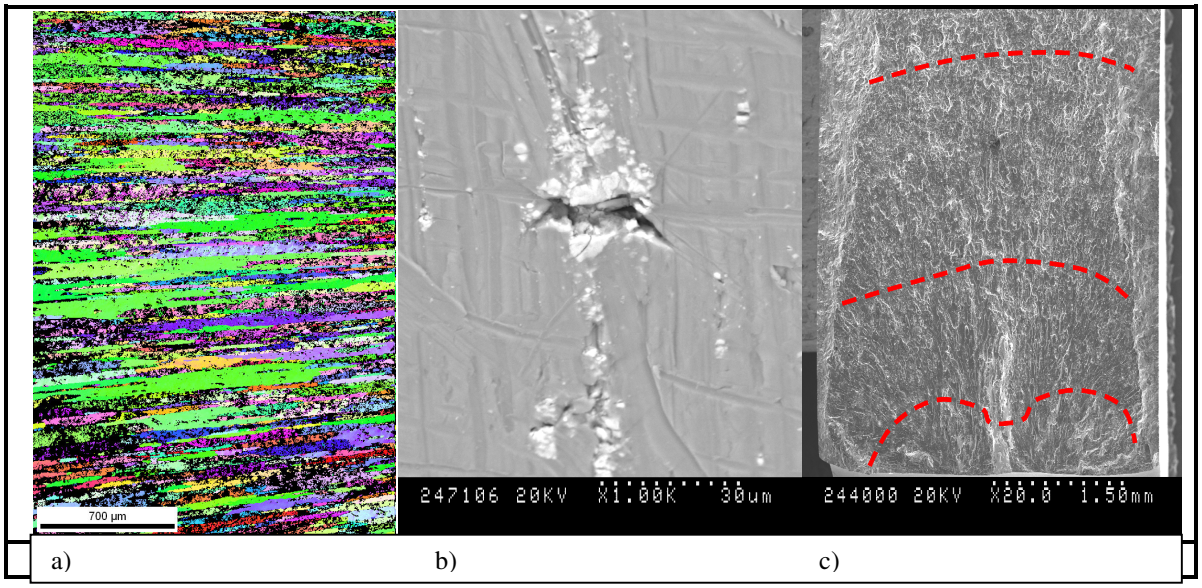

Figure 28. Microstructural features such as constituent particles, grains size and orientation play key roles in nucleation and propagation of short cracks in AA2024-T3, a) grain orientation using OIM, b) particles acting as the main fracture origin, c) marker bands were used to characterize the growth pattern.

texture play the primary roles. An extensive study [9] has been carried out to evaluate the main factors affecting the fatigue crack nucleation process and to characterize the growth of physically short cracks. In this work, different crack detection and monitoring techniques such as surface replication, marker bands, and electrical potential drop (EPD) have been used. Fatigue samples were prematurely overloaded at different stages of the fatigue life in order to help develop a more basic understanding of the microstructural features that influence the growth rate and pattern of short cracks in the aluminium alloy. Extensive fatigue testing, fractography and metallographic examinations are near completion.

As shown in Figure 28, it was observed that almost all the fatigue failures originated at constituent particles and microstructural features such as grain boundaries and grain orientation influence the early crack growth patterns. A novel hypothesis for the short crack mechanism has been developed.

Analysis of Bolt/Hole Interference and its Influence on Fatigue Life

M. Oore and A. Muise, IMP Aerospace, Halifax, Nova Scotia

Fastener/hole configurations are most common in aircraft structures and have been analyzed by many investigators. The purpose of the present work was to study the effects of some basic parameters in such configurations and to assess their influence on fatigue life. The approach has been to use simple two-dimensional finite element modeling to gain insight that will aid in the analysis, design and repairs involving such configurations.

First, a probabilistic analysis was used to account for the tolerance effect on the level of interference. Then, some levels of interference were used in geometric non-linear NASTRAN FE analyses of a hole with an interference bolt (with gap elements) to determine stresses under the combination of applied cyclic load and the interference stresses. The resulting max-min stresses were used with the MIL-HDBK-5H S/N curves data to calculate fatigue life. The results of fatigue lives for various interference levels are shown in Figure 29 below. A verification of the finite element modeling has also been performed.

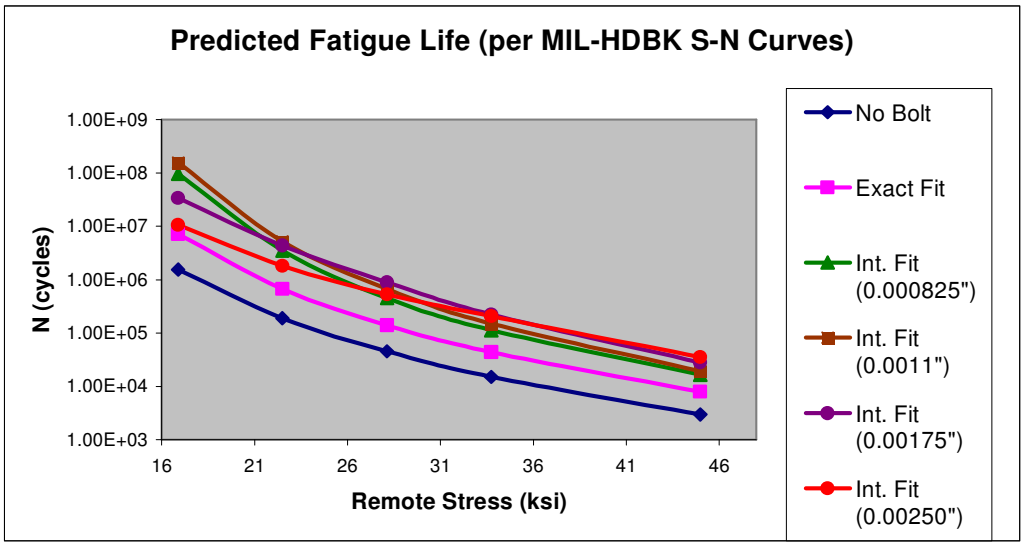

Figure 29. Fatigue life curves for different interference fit fasteners.

Fatigue Failure of Adhesively Patched Clad and Bare Aluminum Alloys

D.L. DuQuesnay, Royal Military College of Canada.

The fatigue behaviour of adhesive patches used for repairing aircraft components has been investigated [10. Adhesive patches were simulated using single lap shear specimens on clad and bare 7075-T6 and 2024-T3 aluminum alloy substrates. Stress-life curves were generated under constant amplitude loading at three stress ratios: R= -1, 0, and 0.5. Typical results are shown in Figure 30. In the bare materials, failure always occurred in the adhesive itself, leaving the substrates intact. At fatigue lives below about 100,000 cycles, the clad alloy specimens also failed in this manner. However, at lower stress levels, the clad alloys failed by cracks initiating in the cladding layer along the end of the lap and subsequently propagating through the substrate, Figure 31 and Figure 32. The fatigue strength of the substrate, due to the adhesive patch on the clad materials, was reduced by an order of magnitude compared to Military Handbook values.

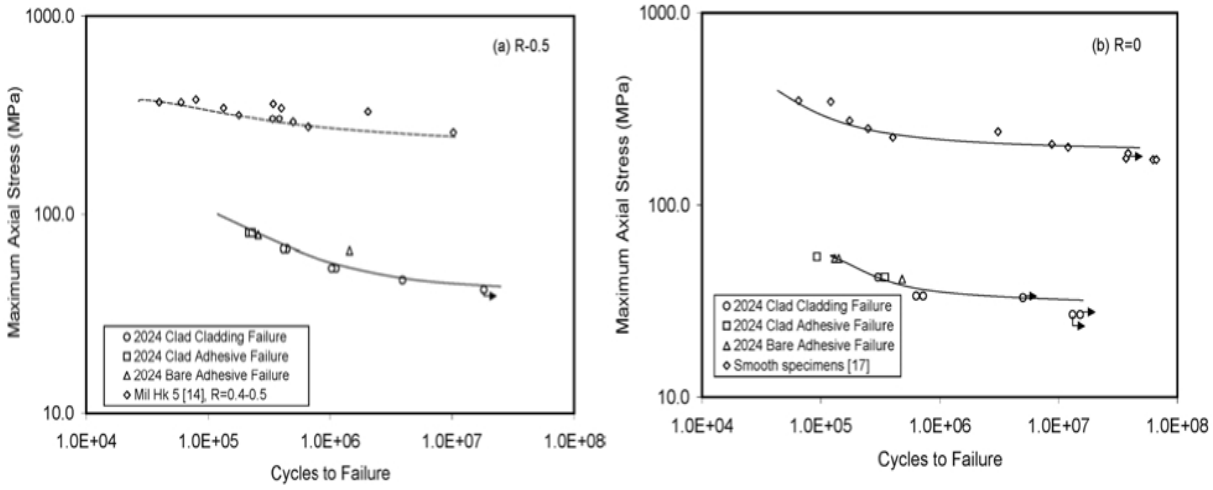

Figure 30. Shear stress versus fatigue life data for single lap shear specimens of 2024-T3 tested at (a) R=0.5 and (b) R=0. Data from bare 7075-T6 has been added for comparison.

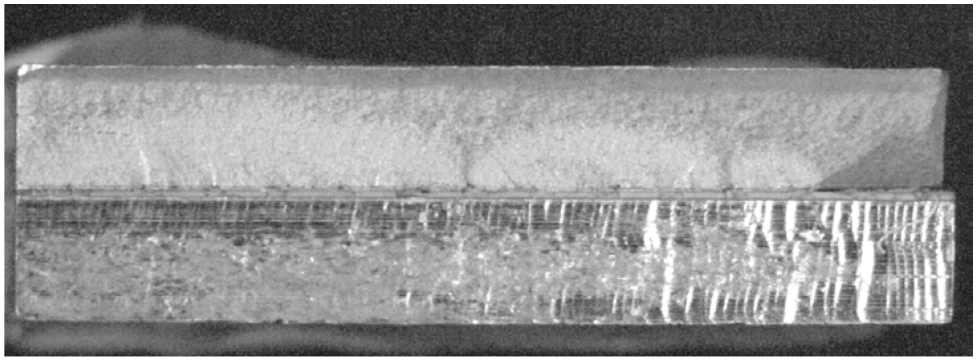

Figure 31. Fracture surface of clad 7075-T6 specimen tested at R=0.5 with a maximum shear stress of 20 MPa showing multiple fatigue cracks initiated in cladding layer (specimen shown approximately full size).

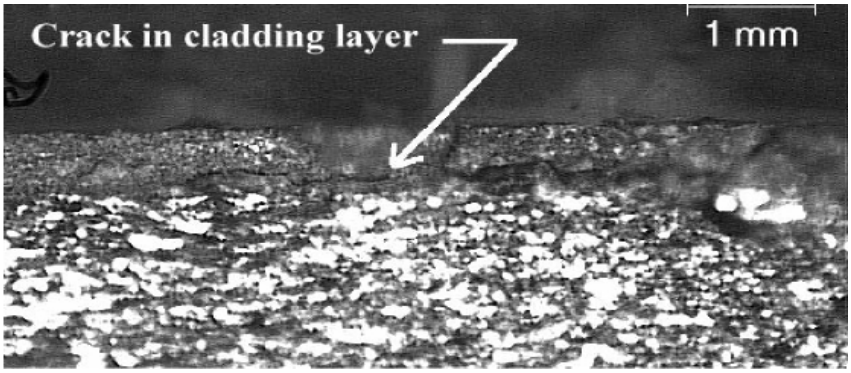

Figure 32. Cracks in cladding layer for adhesive failure in a 7075-T6 lap shear specimen.

Compression Testing of Composite Patch Repaired C-141 Lower Wing Panels

M. Yanishevsky, G. Renaud, G. Li and G. Shi, SMPL-IAR-NRC

C-141 Lower Wing Panels were tested in compression in support of the USAF study on Aircraft Corrosion Control and Coatings. The tests were intended to determine the ability of composite patch repairs to restore the residual strength of wing panels that have been reworked beyond normal limits to eliminate exfoliation corrosion. Exfoliation corrosion is a major problem facing USAF aging transport fleets. The efficacy of composite repairs where the structure is loaded primarily in tension has been determined for many cases; however, for structures and components dominated by compression loading, little actual test data is available. Although the three compression tests conducted do not completely answer all questions about the efficiency and reliability of composite repairs, they do provide important comparative data for a typical repair.

Three configurations of the C-141 Lower Wing Panels were tested: “pristine”, “damaged” (simulated by a centrally milled out “Z” section to a maximum depth of 80% of the panel thickness) and “damaged and repaired” (simulated by the same milled out section repaired with boron composite patches). The volume of material machined away for the latter tests simulated a worst-case scenario of what may be required to remove significant exfoliation or other corrosion damage and addressed concerns about grind-outs affecting bending and torsional stability.

Loading of the specimens was accomplished using a custom designed fixture, shown in schematically in Figure 33, to allow the application of compressive loads on the ends of the wing panels. The design incorporated two rib supports attached to the panels at stations approximately 30 inches apart. C-channel anti-buckling stiffeners were installed along the edges of the panels on the lower wing surface to simulate the support normally provided by adjacent wing panels, and to preclude premature failure due to unrepresentative buckling at the free edges.

Fifty strain gauges were installed to determine the strain distribution for comparison to FEM analyses. Ten LVDT displacement transducers (nine out of plane and one axial) were used to measure deflections in the wing panels, and to

measure the overall movement between the two end fixtures. In addition, photo-elastic sheets were bonded to the outer skin of the wing panels to capture the large field strain distribution as compressive loads were incrementally applied. Photos of the panels prior to and post compression testing are provided in Figure 34 to Figure 36.

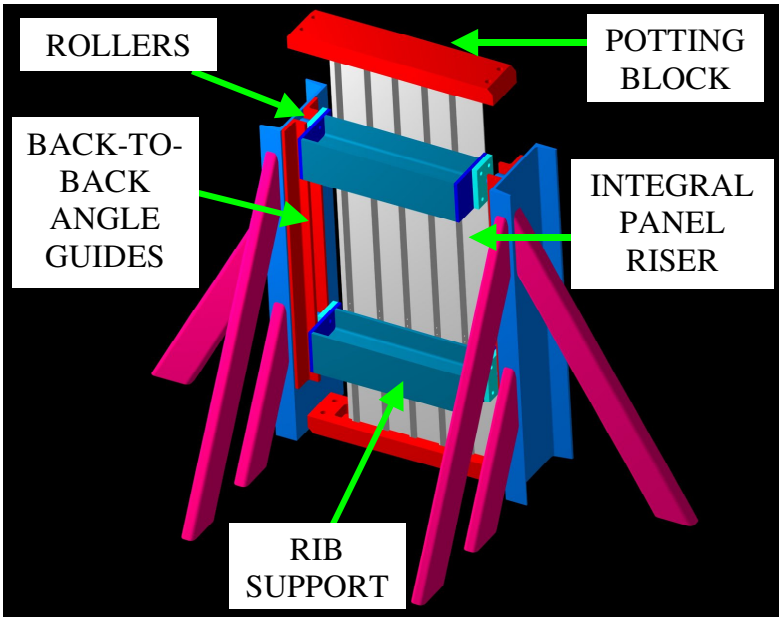

Figure 33. Overall CAD conceptual drawing of the test panel installed in the loading fixture.

Outer Skin of the Pristine Panel Prior to Testing

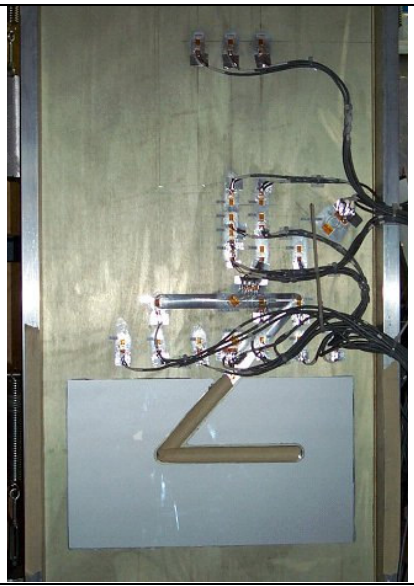

Outer Skin of the "Z" Damaged Panel Prior to Testing

Outer Skin of the "Z" Damaged and Bonded Patch Repaired Panel Prior to Testing

Figure 34. Comparative views of the three wing panel inner skins prior to compression testing showing some strain gauge locations and photoelastic coatings used to record/monitor the tests to failure.

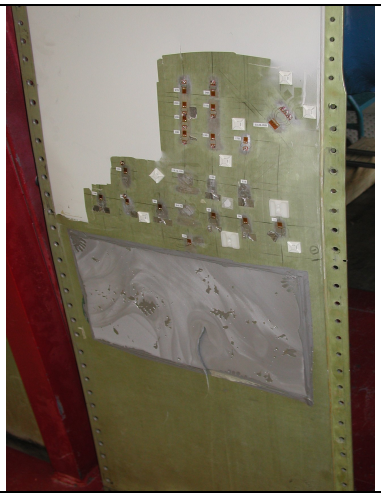		
Outer Skin of the Pristine Panel After Failure.	Outer Skin of the "Z" Damaged Panel After Failure.	Outer Skin of the "Z" Damaged and Bonded Patch Repaired Panel After Failure.

Figure 35. Comparative views of the three wing panel outer skins after failure.

Assuming a yield failure criterion, the pristine panel performed best, and the damaged panel performed worst. However, in terms of final failure, the damaged panel carried the most compressive load while the repaired panel carried the least. The central risers failed first in the pristine and repaired panels, leading to catastrophic failure. The “Z” damage encouraged the load to bypass the central risers in the absence of a repair. Strain gauge measurements indicated that the patch caused a very large gradient between the lower surface of the outer patch and the top of the riser, encouraging early riser buckling and riser / inner skin failure.

		
Inner Skin of the Pristine Panel After Failure.	Inner Skin of the "Z" Damaged Panel After Failure.	Inner Skin of the "Z" Damaged and Repaired Panel After Failure.

Figure 36. Comparative views of the three wing panel inner skins after failure.

Finite element analysis suggested a different ordering in the panel performances. Assuming both yield and final failure, the repaired panel gave the best results and the damaged panel the worst, contrary to what was observed in the test, especially for the repaired case.

A numerical post-cure effects investigation suggested that the thermal residual strains might increase the final failure load and modify the post-cure behaviour. A preliminary patch design parametric study suggested that the patch should shift the assembly neutral axis inward, which would be more aligned with the loads. Initial indications showed that the thickness of the patching material on the inner surface should be higher than the outer surface. The opposite was present in the provided repaired test panel.

The work has been reported in references [11, 12, 13, and 14].

The Effect of Mean Strain on Fatigue Damage Caused by Fully Open Loading Cycles

A.E. Nolting and D.L. DuQuesnay, Royal Military College of Canada, Kingston, Ontario.

The effect of mean strain and mean stress on fatigue damage caused by fully open loading cycles have been examined for SAE 1045 steel, 2024-T351 aluminium alloy and Ti-6Al-4V titanium alloy [15]. The loading spectra contained periodic compressive overload cycles which caused the crack opening stress to remain below the minimum stress of subsequent constant amplitude small cycles, Figure 37. The mean strain and mean stress of the small cycles were varied between tests and the results were compared on the basis of equivalent fatigue lives (Neq) of the small cycles. A decrease in fatigue life was observed with increasing mean strain and mean stress. Typical results are shown in Figure 38.

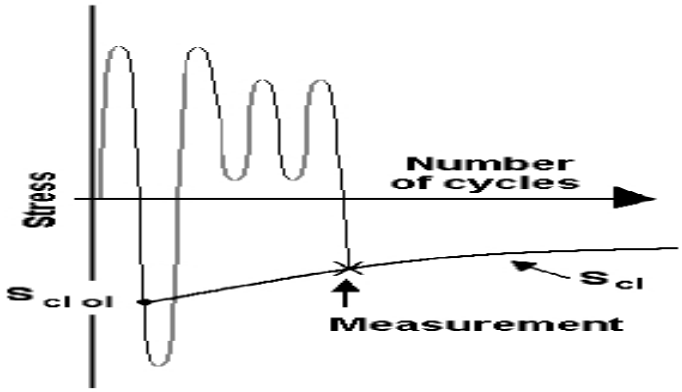

Figure 37. Schematic of crack closure measurements taken at 2 cycles following a compressive overload cycle.

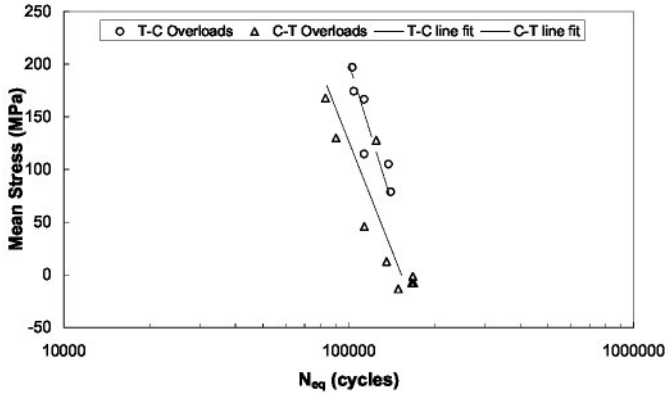

Figure 38. Equivalent fatigue life vs. mean stress, C-T and T-C overload SAE 1045 steel data.

Modeling of Low Cycle Fatigue in MMCs

Q. Zhang and D.L. Chen, Ryerson University.

There has been an increasing interest in characterizing the fatigue resistance of discontinuously reinforced metal matrix composites (DR-MMCs) because of their high specific modulus, specific strength, wear resistance, and reasonable cost.

While DR-MMCs have superior high cycle fatigue resistance compared to the corresponding un-reinforced counterpart, their resistance to low cycle fatigue (LCF) is less satisfactory. To improve the LCF resistance of these composites, much work has been done with respect to the effects of the microstructural parameters, such as the volume fraction, size, shape and distribution of the reinforcing particles, bonding force between the matrix and particles and aging conditions. The influence of the particle size on the LCF life of DR-MMCs has been widely studied. However, the mechanisms of such effects have not been fully understood, since different authors reported different or contradictory results. This would be partially due to the lack of a quantitative model describing how the particle size influences the LCF life of DR-MMCs. Recently, an analytical model relating the particle size to the LCF life of DR-MMCs has been developed [16]. In that model the LCF life was related to the yield strength of the

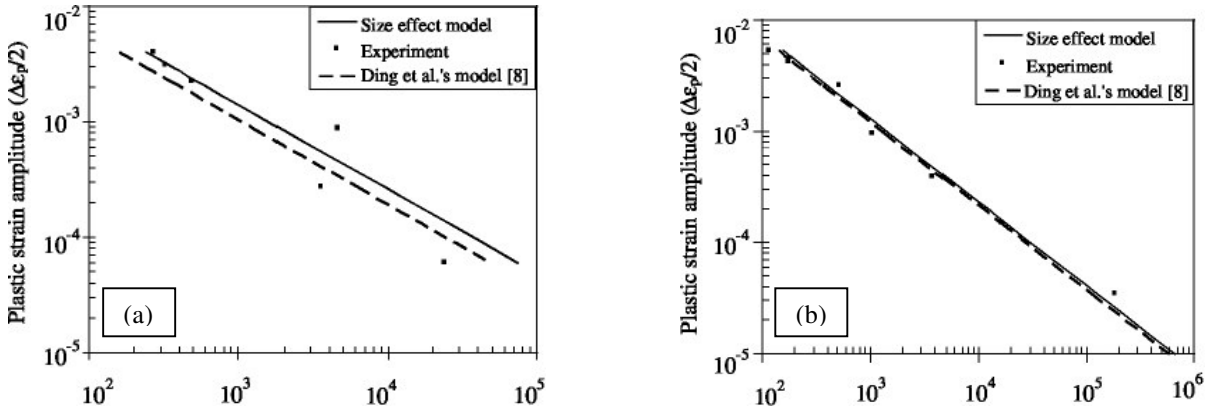

Figure 39. Plastic strain amplitude vs. reversals to failure for the Al2O3 particulate reinforced AA6061 composite material. (a) Vf = 15%, d = 15 µm, -30 °C, (b) Vf = 20%, d = 12.8 µm, 25 °C.

composite, which was strengthened by the modified, shear lag and enhanced dislocation density effects. The model predicted that fine reinforcement particles had a beneficial effect on the LCF life of DR-MMCs. However, the effect was not so apparent, especially at high plastic strain amplitude levels. During the derivation the modified shear lag effect factor was assumed to be a constant of 0.5, which might not always be appropriate according to recent experimental data. Therefore, an alternative LCF life prediction model was proposed via linking the modified shear lag effect factor to the volume fraction of reinforcing particles in the composites. It was shown that a decreasing particle size resulted in an increasing LCF life of DR-MMCs, Figure 39, especially at low plastic strain amplitude levels and under a critical particle size of about 5 µm. The proposed model was found to be in good agreement with the experimental data reported in the literature.

A model for low cycle fatigue life prediction of discontinuously reinforced MMCs.

Q. Zhang and D.L. Chen, Ryerson University.

An analytical model for predicting the crack initiation life of low cycle fatigue (LCF) of discontinuously reinforced metal matrix composites (DR-MMCs) has been proposed on the basis of Gibbs free energy law. The formation of a fatigue crack was considered to be associated with the reduction of the internal energy that could be expressed as a part of the area of the saturated hysteresis loop. The effects of the volume fraction V_f of reinforcement, cyclic strain hardening exponent n' and cyclic strength coefficient K' on the LCF fatigue crack initiation life of DR-MMCs were analyzed at different levels of plastic strain amplitude.

A higher level of plastic strain amplitude led to a shorter fatigue crack initiation life, and the higher the volume fraction of the reinforcement particles the shorter the fatigue crack initiation life, Figure 40. The cyclic strain hardening exponent had only a weak or little effect on the low cycle fatigue crack initiation life when $n'<0.26$. However, the low cycle fatigue crack initiation life increased strongly with increasing cyclic strain hardening exponent when $n'>0.26$.

With increasing cyclic strength coefficient, the low cycle fatigue crack initiation life first increased, and then decreased. The maximum crack initiation life appeared at $K' \approx 1840$ MPa, which seemed to be independent of the applied plastic strain amplitude.

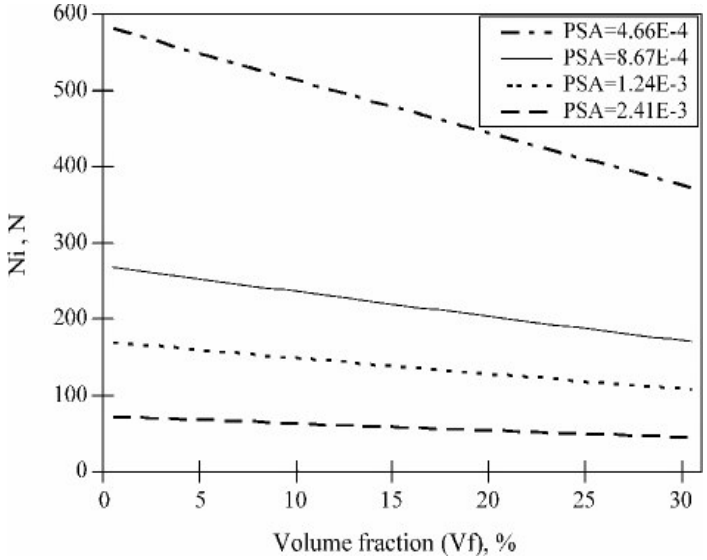

Figure 40. Effect of the volume fraction (Vf) on the number of cycles for the fatigue crack initiation (Ni) in the Al2O3 particulate-reinforced, AA6061 aluminum alloy based MMCs tested at 25 °C, with consideration of the variation of Ec, n', K' and ft with the volume fraction.

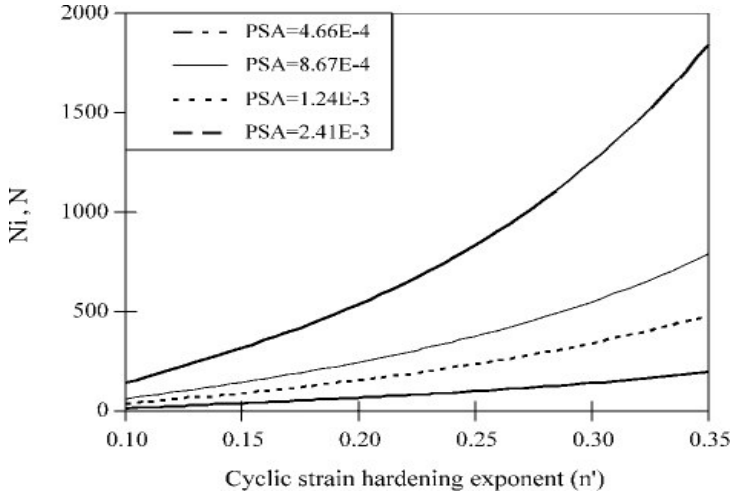

Figure 41. Effect of the cyclic strain hardening exponent (n) on the fatigue crack initiation life (Ni) in the Al2O3 particulate-reinforced, AA6061 aluminum alloy based MMCs tested at 25 8C, without consideration of the variation of Ec, Vf, K' and ft. These quantities are defined in [17]

The theoretical predictions based on the proposed crack initiation model, in conjunction with the crack propagation model of Ding et al, were found to be in good agreement with the experimental data reported in the literature for a number of particulate-reinforced MMCs. Since both processes of the crack initiation and propagation have been taken into consideration, the accuracy of predicting the total LCF life of DR-MMCs was improved [18].

Articulated Robots for Structural Modifications

J. Dubuc, L-3 Communications (Canada) Military Aircraft Services (MAS)

A robotic shot peening system has been developed at L-3 MAS to provide optimum peening conditions in hard to reach locations. This system has been used, in the last few years, to peen the tapered web on one of the wing carry-through

bulkheads on the CF-18 as well as the lugs of the inboard leading edge flaps [1]. Several in-service commercial aircraft have also been peened using this system both in Europe and at different locations in North America.

More recent R&D activities at L-3 MAS have focused mainly on expanding the capabilities of the robotic system to perform surface renewal on areas already submitted to fatigue damage. Most of the major structural components on the CF-18 are covered with an Ion Vapour Deposited (IVD) aluminium layer for protection against corrosion. Before this IVD is applied, an etching is performed to maximize the bonding of the aluminium to the structure. This etching introduces inter-granular pits from which cracking usually initiates. Removal of this thin layer of damaged material is often necessary to ensure an optimum life improvement due to shot peening. This is very difficult to do by hand since accurate control of the depth removed is complicated and often inaccurate.

To remove a layer of material in a uniform manner from the surface of a part, a relative approach was used. It consists in the use of two end effectors: a touch probe and a spindle. The trajectory of the cutter is based on surface mapping previously performed with the touch probe. The repeatability of the robot is exploited and placing the probe styli at the same location as the cutter minimizes the calibration error of the robot. It is important to select the appropriate machining parameters to avoid chatter problems. These parameters and others were therefore investigated to determine the combination that would allow maximum material removal without the risk of tool vibration, see Figure 42. The project has demonstrated that a robot is not as efficient as a CNC machine in terms of precision, surface finish and rapidity. However its portability allows for on-aircraft machining which is very important on the CF-18 since the parts cannot be removed from the aircraft and installed on a CNC machine.

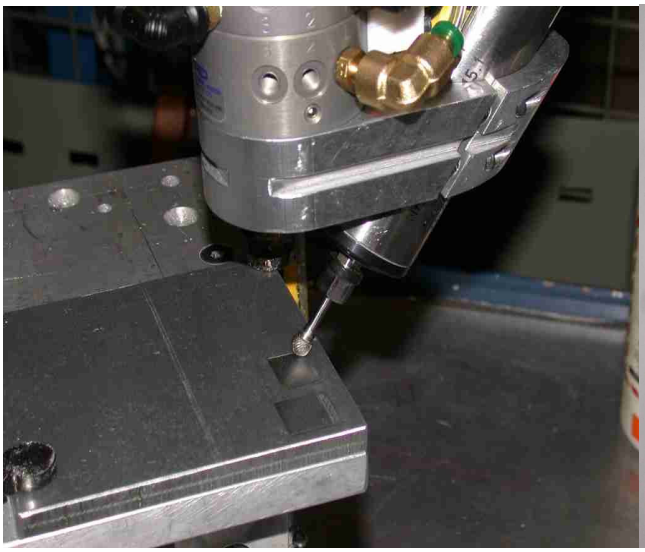

Figure 42. Robotic Machining Test.

Figure 43. Robotic Material Removal Modification on the CF-18

The new robotic material removal capability has been successfully used in the development of a new CF-18 modification. For this modification, the material removal area is very difficult to access as illustrated in Figure 43. The robotic application has allowed material removal following an optimum profile that reduces the stress and ensures a longer period before crack re-initiation. Because of accessibility, a technician cannot do this modification. The alternative is to remove and replace the complete frame. This option is much more expensive than the development of a robotic material removal modification.

FRACTURE MECHANICS AND CRACK PROPAGATION STUDIES

Fatigue of As-machined and Shot Peened Coupons Under a Predominantly Compressive Spectrum

M. Sova and M. Roth, QETE, DND

Several locations on the CF-188 wing are subjected to loads that are mostly compressive. Although cracking under compressive loads was not expected, cracks have been found in some of these locations, such as the upper inboard leading edge flap lugs, the inner and outer wing fold ribs, and the 68% spar shear tie lug. The preferred modification consisted of shot peening the surface to introduce compressive residual stresses, but concerns have arisen whether the effects of shot peening were beneficial or detrimental, when the loading is predominantly compressive. Yielding could occur when compressive loads are superimposed on the shot peening compressive residual stresses as this combination might result in tensile residual stresses that could cause cracking with small tensile loads. A test program was set up and coordinated with L-3 MAS to investigate the effects of a predominantly compressive spectrum on the fatigue life of as-machined and shot peened specimens [19].

Simple 2 in. wide flat coupons made of 0.25 in. thick 7050-T7451 aluminium alloy plate with semi-circular edge notches of 0.25 in. radius, providing a gross Kt (theoretical stress concentration factor) of 3.13, were selected. This geometry is somewhat representative of the bottom of a lug. Coupons, as machined and shot peened (Almen A 0.008 in. intensity), were fatigue tested to failure using a spectrum block simulating 326 flight hours. In that spectrum, the maximum compressive load was -1.205 times the maximum tensile load. The testing was performed at two stress levels, referred to as 70 ksi and 80 ksi and corresponding to the maximum tensile stress in the specimen.

Two shot peened coupons and two as-machined coupons were tested to failure at the 80 ksi stress level. The shot peened coupons failed after a slightly higher number of blocks (i.e. 38.9 and 40.0 blocks) than the as machined coupons (i.e. 35.0 and 37.0 blocks). This suggested a slight beneficial effect of shot peening. Two shot peened coupons and two as-machined coupons were tested at the 70 ksi stress level. The scatter in the number of blocks to failure was larger. The lives of the shot peened coupons (i.e. 76.4 and 83.5 blocks) were between those of the as-machined coupons (i.e. 73.9 and 93.0 blocks). In this case the benefits of shot peening were questionable except for a possible reduction in the scatter in the number of blocks to failure.

The crack growth rates were measured in the four as-machined coupons. Repeat patterns, which could be associated with crack growth during a loading block, were observed over large areas of the crack surfaces, despite the high compressive loads in the spectrum (Figure 44). Cracks initiated at both radii in all the specimens at slightly different times at the beginning or early in the tests. The initial crack growth rates were slow up to crack depths of about 0.040 in., and then one crack started to propagate faster than the other (Figure 45). The crack growth curves of the two coupons tested at the higher stress level were similar. For the coupons tested at the lower stress level, the crack growth rates varied from specimen to specimen when the cracks were larger than about 0.040 in. with the result of a larger scatter in the lives to failure.

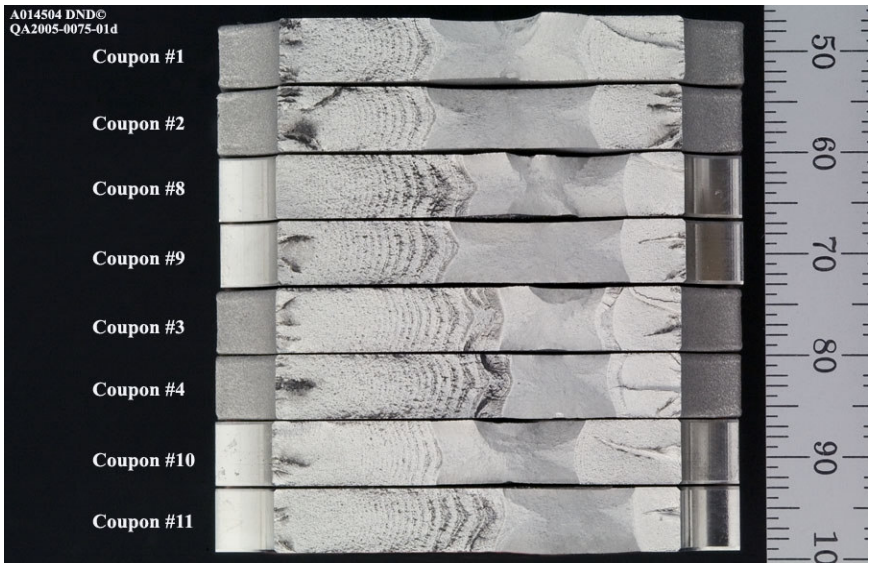

Figure 44. From top to bottom: Fracture surfaces of the shot peened coupons #1 and #2, and as machined coupons #8 and #9 tested at the higher stress level (i.e. 80 ksi); of the shot peened coupons #3 and #4, and as machined coupons #10 and #11 tested at the lower stress level (i.e. 70 ksi), all oriented with the larger crack at left and the smaller crack at right (mm scale).

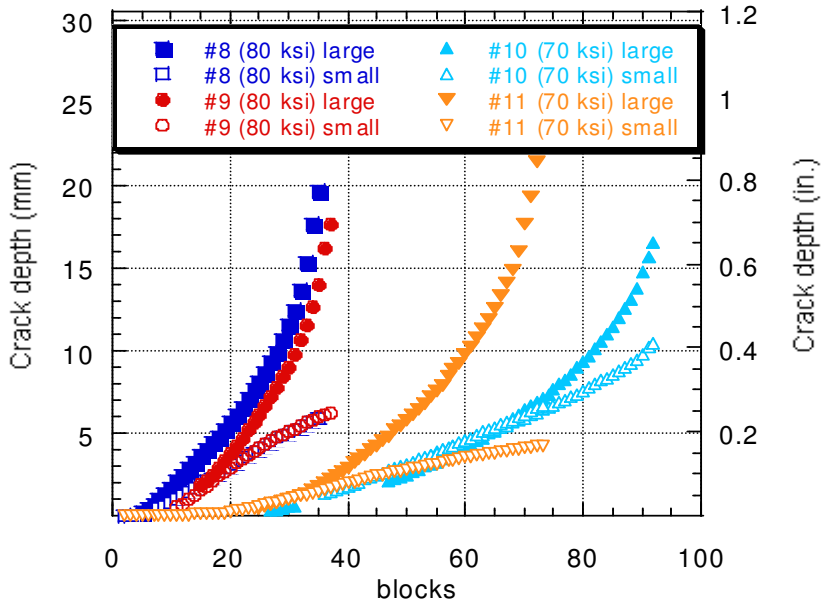

Figure 45. Crack growth curves as a function of spectrum blocks for the large cracks (filled symbols) and small cracks (open symbols) of the as machined coupons tested at each of the stress levels (linear crack depth scale).

FAILURE INVESTIGATIONS

Fractographic Investigation and Determination of the Rate of Growth of Cracks from the F/A-18 IFOSTP and the P-3C SLAP Full Scale Fatigue Tests

M. Roth, QETE, DND

Canada is participating in two collaborative full-scale fatigue test (FSFT) programs. The first one is the F/A-18 International Follow-On Structural Test Program (IFOSTP) where Canada is testing the centre fuselage and the wings, and Australia the rear fuselage and empennage. The aim of the program is to demonstrate the F/A-18 original design life of 6000 hours. The other is the P-3C Service Life Assessment Program (SLAP) involving the US Navy, Canada, Australia and the Netherlands. The objective of the fatigue test is to identify fatigue related life-limiting factors and to determine what measures must be undertaken for continued safe and economic operation of this aircraft designed in the mid-1960s.

Within both programs, fatigue crack growth data is required to establish appropriate inspection intervals, maintenance actions, or modifications. QETE has been performing detailed fractographic investigations to determine the rate of growth of selected cracks found during or at the completion of the tests. The fractography performed for each program differed because of differences in the selection of the types of spectra used for the two FSFT. In the case of the F/A-18 IFOSTP, a spectrum of variable amplitude loads simulating 325 flight hours was repeatedly applied until reaching the desired life (i.e. 16636 simulated flight hours for the fuselage). In the case of the P-3C SLAP, the wing/fuselage test article (which had accumulated close to 11000 flight hours) was tested to simulate 38,000 flight hours of the 85th percentile mission profiles using a randomized flight-by-flight spectrum representing one design lifetime of 15,000 flight hours. The spectrum was then repeated for a total of 2.5 lifetimes. To facilitate the fractographic work, six marker blocks were introduced during the test.

The F/A-18 IFOSTP spectrum was relatively short and repeated many times in the course of the test. Because of a relatively small advance of the crack front per block, it is expected that two consecutive spectrum blocks will leave similar striation patterns. If these repeating patterns can be identified, the distance between them will provide the crack growth per spectrum block. AMRL in Australia found that it was often possible to observe repeat patterns from the crack origin to the

end of the crack using optical microscopy. QETE has been applying the same technique to determine the growth rate of cracks from the Canadian fuselage and wing tests and has found that optical microscopy works well in the case of small cracks or in the early stages of crack growth in the case of larger cracks (Figure 46). Examination using the scanning electron microscope (SEM) was preferred for deeper cracks. An area showing a characteristic sequence of striations is selected and the corresponding crack depth measured. The specimen is then moved slowly forward or backward until a similar sequence of striations is observed and the corresponding crack depth measured, and so on (Figure 47).

To facilitate the fractographic crack growth measurements in the case of the P-3C SLAP, marker bands consisting of sequences of constant amplitude loads were introduced at 3000, 10000, 15000, 21000, 27000, and 33000 simulated test hours (STH). They were of three types, Type A at 3000 STH, type B at 10000 and 15000 STH, and type C at 21000, 27000, and 33000 STH. The test ended at 38000 STH. The purpose of these marker bands was to introduce fractographic features different from those resulting from variable amplitude loading and identifiable by microscopic examination of the crack surfaces. The surfaces of the selected cracks were first examined using the SEM at magnifications in the x1000 to x3000 range to detect the periodic features of the marker bands (Figure 48). This approach was partially successful, but quite slow. During the course of the investigations, it was found that sometimes a small number of beach marks could be seen using the stereomicroscope when a ring light obliquely illuminated the crack surface (Figure 49). SEM examination of these shiny beach marks confirmed that most of them were indeed marker bands. The preferred procedure for detecting the marker bands was to look first for shiny marker bands using a stereomicroscope and oblique illumination, and then to confirm using the SEM that these beach marks were marker bands. This approach worked very well with wing plank cracks, but was less successful with spar cap cracks. The P-3C SLAP crack growth measurement techniques are discussed in detail in References [20, 21 and 22].

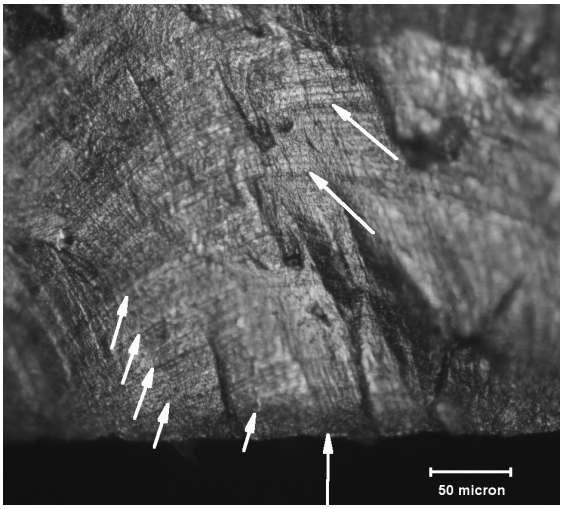

Figure 46. Repeat patterns (inclined arrows) close to the origin (vertical arrow) of an F/A-18 Y543 bulkhead crack seen using an optical microscope. The curvature of the crack front suggested that some material had been removed from the surface.

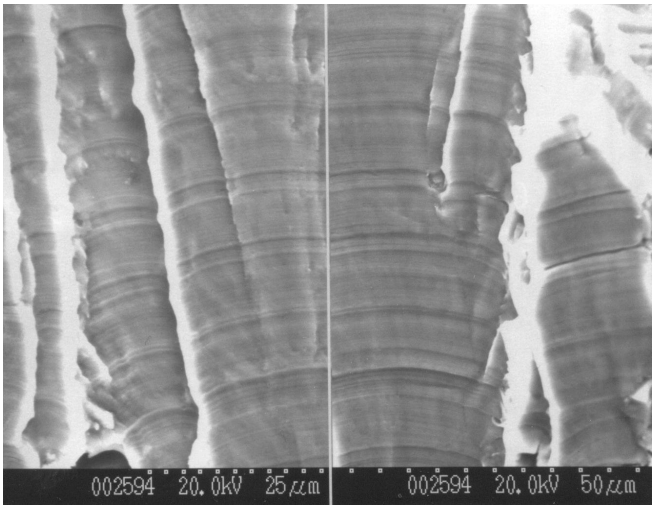

Figure 47. EM fractograph of repeat patterns from spectrum blocks 27 (left) and 33 (right) showing their similarities. Note that the original magnification was x1200 on the left and x1000 on the right.

In the case of the F/A-18 IFOSTP, a large number of spectrum blocks were applied to the test articles. If repeat patterns associated with many of these blocks can be identified, the coordinates of the repeat patterns are recorded sequentially starting as close to the origin as possible and travelling in as much a straight line as possible to the end of the crack. The crack depth is then plotted as a function of simulated flight hours (SFH) or blocks (Figure 50). This approach requires a detailed and sometimes time consuming examination of the whole crack, but can provide crack growth data from the beginning to the end of the test. In the case of the P-3C SLAP, a maximum of six marker bands can be observed, but in practice the first two were rarely found. The crack growth curves were often limited to the later stages of crack growth, but occasionally crack growth from 3000 STH to the end of the test could be plotted (Figure 51). Finding the marker bands was a relatively rapid process when they could be visualized optically using side illumination, otherwise a thorough and time consuming examination of the crack surface using the SEM was required.

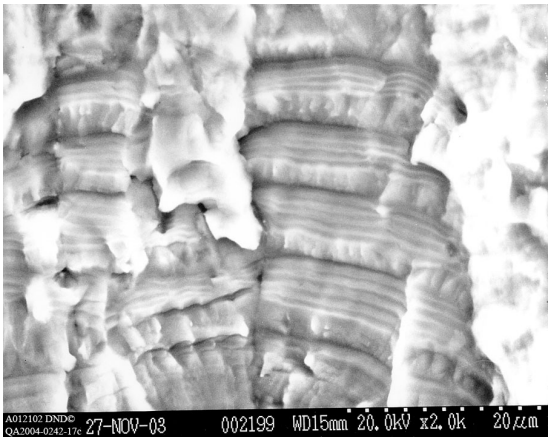

Figure 48. 33000 STH marker band in a P-3C SLAP forward spar cap crack.

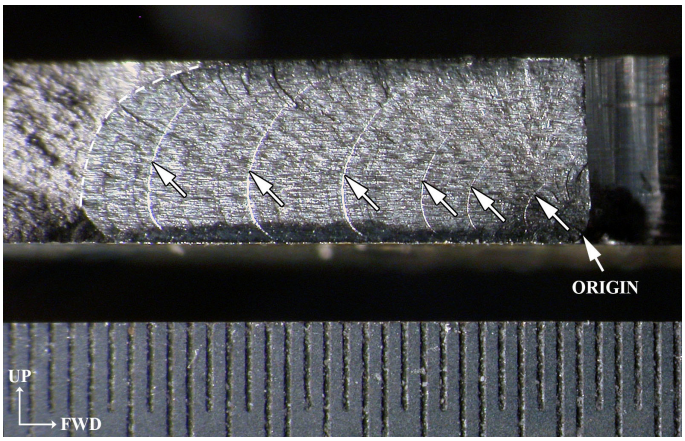

Figure 49. Overall view of a 0.26 in. long crack from a P-3C SLAP lower wing panel. The arrows point to the six marker bands clearly visible using side illumination and also observed using the SEM.

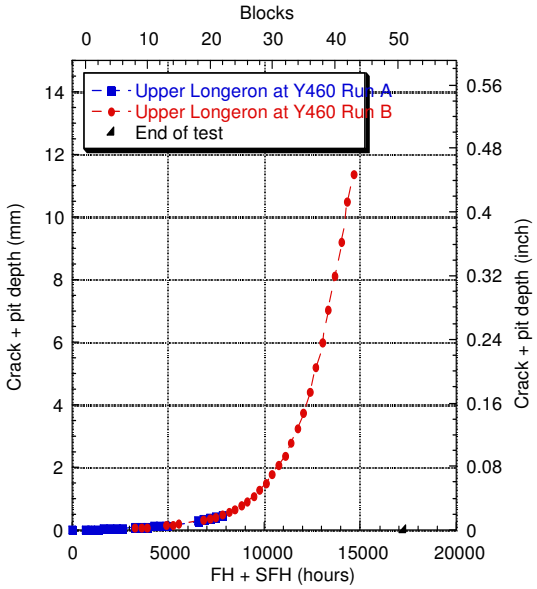

Figure 50. Crack growth curve for two sets of repeat patterns for a F/A-18 IFOSTP upper longeron crack as a function of flight hours (FH) and simulated flight hours (SFH).

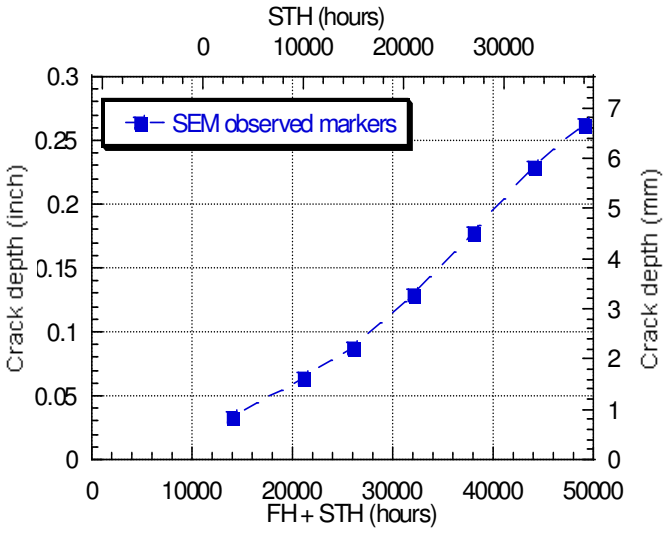

Figure 51. Crack growth curve as a function of flight hours (FH) and simulated test hours (STH) for the P-3C SLAP crack shown in Figure 49.

The F/A-18 IFOSTP centre fuselage test and wing test cracks from the following main areas have been investigated since ICAF 2003:

- Center fuselage -Y453 bulkhead [23], Y488 bulkhead [24], and longerons [25],
- Wing front spar [26].

The main findings were that:

- Cracking often initiated very early in the component life at small surface pits, which were formed during the etching step preceding the deposition of the ion vapour deposited (IVD) aluminium corrosion preventative coating applied to the 7050 aluminums alloy of the F/A-18 structure.
- Crack propagation was initially slow and then increased markedly usually between 6000 and 10000 SFH (Figure 50).

The fractography reports for the 22 P-3C SLAP right hand wing cracks investigated at QETE are included in the P-3C SLAP right-hand wing teardown final report detailing the logistics involved, the teardown plan, the conduct of the teardown, the findings and conclusions, and the disposition of parts [27].

Investigation of a tail rotor failure at the origin of a CH-146 crash

M. Lottes, Quality Engineering Test Establishment, DND.

The crew was conducting a SAR mission about 100 NM from Goose Bay when RCC Halifax cancelled the mission because the target had been located. The weather was marginal VFR and the crew started the return leg to 5 Wing. At about 350ºM at 40 NM from Goose Bay, while in normal cruise flight at 200-300 feet AGL, the tail rotor departed the aircraft. About 400 meters down track, the aircraft crashed into hilly, tree-covered terrain. Both pilots were killed instantly and the SAR technician was seriously injured when the aircraft struck the ground with high vertical speed. Although the flight engineer was seriously injured he was able to render first aid to his crewmates. He used a satellite phone to report the accident to RCC Halifax. A 444 Squadron rescue helicopter arrived on scene to evacuate the survivors to medical facilities within 3 hours. The aircraft was destroyed (Figure 52).

Figure 52. Overall view of the crashed CH146420.

The main tail rotor section was found 280 meters up track from the crash site with one complete tail rotor blade attached but the other blade was missing the outboard 18.5 inches. The 18.5-inch section had fragmented into one large piece and two smaller pieces that were found a further 100 meters up track. Examination and analysis of the tail rotor pieces by QETE identified the tail rotor blade had failed due to fatigue cracking (Figure 53 and Figure 54). The initiation site for the fatigue failure was a 0.008-inch deep nick, Figure 55. Analysis of debris on the surface of the nick indicated material consistent with stone.

Examination of the blade fracture surface showed that the fatigue zone extended to about 65 percent of the cross section of the blade structure. Based on a striation count, it was estimated that the fatigue crack grew from initiation to catastrophic failure in 50 to 70 flying hours.

As a result of these findings, the Canadian Forces instituted a visual inspection of the tail rotor blades for nicks and cracks every 12.5 hours of helicopter operation. Based partly on information from the preliminary report on the Canadian accident the FAA issued Special Airworthiness Information Bulletin SW-05-10 on 5 Nov 2004. The bulletin advises operators of the Bell 412 helicopter of the possibility of tail rotor blade failure and recommends a visual inspection every 25 hours.

Figure 53. Root portion of the failed tail rotor blade viewed from the tip end. The ruler is situated on the inboard side of the blade. The yellow arrow indicates the origin of the initial fatigue crack at a 0.008-inch deep nick. The green line indicates the fatigue portion and the red line the final overload zone.

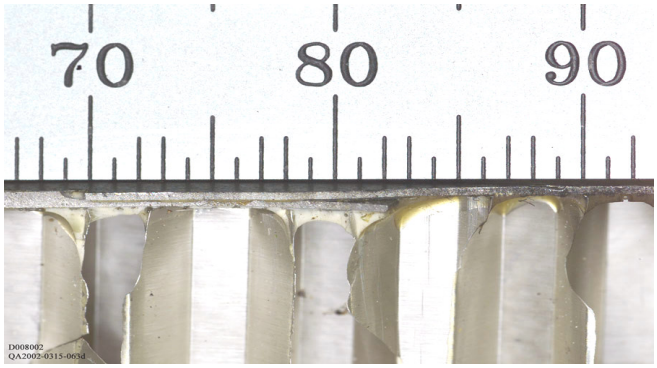

Figure 54. View of the fatigue initiation point and the crack that led to failure of the rotor blade.

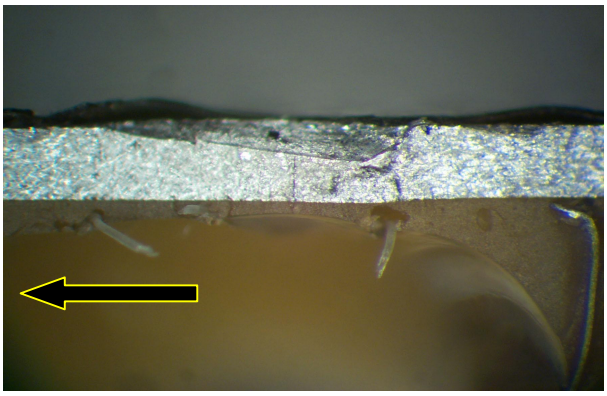

Figure 55. High magnification view of the fracture surface in the skin showing the initiating defect. The arrow points in the direction of the leading edge.

Cormorant Tail Rotor Half Hub Fatigue Testing

M. Roth, QETE, DND.

Cracking was discovered in the Cormorant Tail Rotor Half Hub (TRHH) after very few hours of service life. The TRHH is a composite material structure consisting of glass/epoxy, carbon and titanium plate. QETE has initiated a simple coupon test program in an effort to gain an understanding of the failure mechanisms involved under various cyclic loading conditions.

Test specimens were extracted from the area underneath the titanium plate of the Cormorant Tail Rotor Half Hub. Constant amplitude, compressive loading was applied in a three-point bend test configuration. Marker loads were introduced in one coupon to assist in cycle counting under SEM examination. This investigation is on-going.

PROBABILISTIC AND RISK ANALYSIS METHODS

Risk-based Corrosion Assessment of Aircraft Structures

Min Liao, SMP-IAR-NRC

From previous work [28, 29], it was found that existing risk analysis codes, such as USAF PROF and Bombardier PRISM, have major limitations in performing risk assessment of aircraft structures with corrosion damage. Since these codes do not take into account environmental effects, corrosion and fatigue interactions are not addressed. Consequently, some key corrosion related random parameters, such as corrosion growth rate, corrosion protection (CP) breakdown time, nondestructive inspection (NDI) for corrosion, etc. are not included in these codes. Complex corrosion mechanisms found on aircraft structures, such as pitting, exfoliation, crevice, and environment assisted cracking, essentially add more difficulties for risk assessment.

Research has been carried out at NRC to develop a risk-based corrosion assessment framework/tool for aircraft structures to evaluate the corrosion impact on structural integrity. A NRC in-house program, ProDTA (Probabilistic Damage Tolerance Analysis), was developed for corrosion risk assessment, in which the Holistic Structural Integrity Process (HOLSIP) age degradation models and mixed probabilistic techniques were integrated to calculate the probability of failure (POF) of aircraft structures. ProDTA was linked to ECLIPSE of APES and AFGROW of USAF for damage tolerance analysis. Compared to the existing risk analysis codes, the unique capabilities of ProDTA are, 1) ability to include more environment related random variables, such as corrosion growth rate (CGR), corrosion pit depth (PD), thickness loss, and corrosion protection breakdown time (CPBT) in a risk-based life cycle assessment; 2) abilty to include both NDI results for cracks and corrosion in a structural risk assessment.

ProDTA was first compared to PROF and PRISM in structural risk analyses without age degradation effects. Figure 56 presents the single flight POF results from PROF, PRISM, and ProDTA in two benchmark examples, which indicate that ProDTA produced the same results as PROF and PRISM.

To demonstrate the capability of ProDTA to quantify the effects of corrosion maintenance on the damage state and risk level, a risk analysis was carried out on a typical Boeing lap joint that contained fatigue and corrosion. In this analysis, both crack and corrosion maintenance was simulated. Four types of corrosion maintenance actions were assumed (in order of increasing severity and cost); 1) no repair, 2) CPC application, 3) groundout and CPC application, and 4) replacement. The risk analysis, shown in Figure 57, indicates that a high performance CPC (75% reduction in corrosion growth rate) could extend the life by a factor of 2.12, while a low performance CPC (25% reduction) would extend the life by only 1.16 while maintaining a POF less than 10^{-7}.

Moreover a study was carried out to quantify the effect that corrosion NDI uncertainty has on a risk analysis. This was accomplished using a more fundamental measurement on corrosion NDI uncertainty than POD, NDI error distribution, which was developed at NRC by determining the errors between the measured and actual variable of interest for a given NDI technique. In the simulation shown in Figure 58, it was assumed that, at year 30, a 16% average thickness loss (due to corrosion) was found in the first layer of the lap joint using both advanced (data fusion) and traditional NDI techniques. The results indicate that the single flight POF would reach 10^{-7} at about 47 years and 53 years by using the inputs from traditional and advanced NDI, respectively. In other words, given that the two NDI techniques determined the same average value for thickness loss, the advanced NDI technique could 'gain' 6 more years for the lap joint structure before costly corrosion maintenance has to be done.

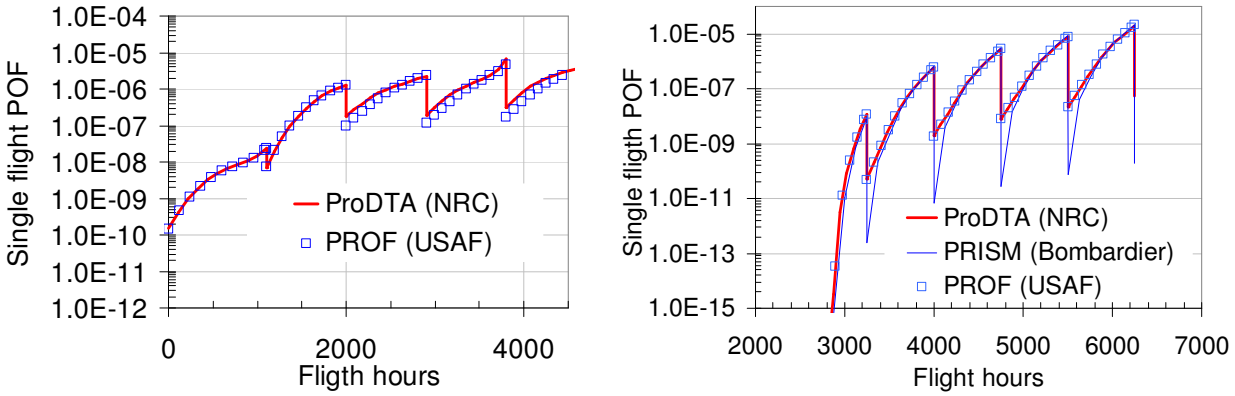

(a) Fastener hole on the lower wing skin of T38 (PROF benchmark example)

(b) Fastener hole on upper outboard longeron of CF18 (PRISM benchmark example)

Figure 56. Single flight POF results by PROF (USAF), PRISM (Bombardier), and ProDTA (NRC).

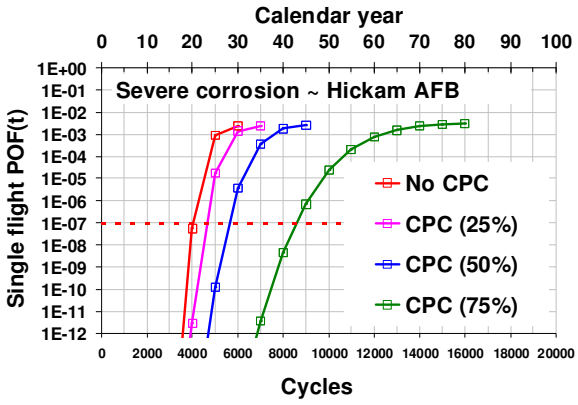

Figure 57. Effect of CPC performance on POF.

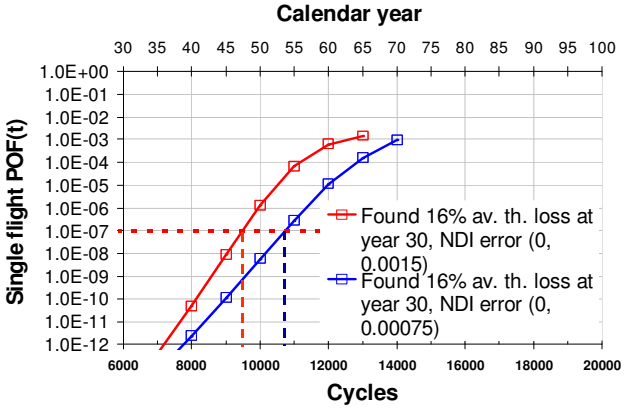

Figure 58. Effect of corrosion NDI uncertainty on risk assessment.

A comprehensive summary of risk analysis research at NRC can be found in References [30, 31].

AGING AIRCRAFT ISSUES

CF-188 Hornet

Maj. J.J.P.J. Brosseau and Capt. B.S.Thibeault, DAES, DND.

Since 1998, a major life extension effort has been put in place under the ALEX (Life Extension) program in order to ensure that aircraft will reach the original design life under the CF spectrum (fatigue life expenditure index (FLEI) of 1.0). With this program, aircraft go through third line maintenance 2 or 3 times in their lifetime. At these stages, structural modifications are carried out to correct or prevent failures. Inspections of critical locations are also completed to mitigate risk or to gather ASIP information.

The CF18 is mainly managed as a safe life aircraft. However, a few years ago, the failure criteria was changed from crack initiation to the crack length that would sustain 1.2 design limit load. The safety by inspection concept has also been introduced and is now used in selected locations. The fleet averages have reached 4100 airframe hours and 0.55 FLEI. The CF is therefore at the mid point life of the fleet.

Recently, a few aircraft reached the second ALEX phase (CP2 at 0.645 FLEI). Approximately 70 items (modifications or inspections) are encompassed by this package. These new structural modifications have been implemented for the first time on fleet aircraft at the third line level. These modifications will ensure that the jets maintain a safe level of airworthiness up to FLEI of 0.78 (CP 3).

ASIP efforts are now oriented towards phase 3 of the ALEX program. Numerous life limited items (LLIs) will be regarded, binned and assessed. Up to now, 23 items have been judged as critical for this third phase. The safety by inspection concept will be seriously investigated during this stage.

Center barrel replacement (CBR) has been reduced to 13 aircraft. The ALEX modifications in the centre fuselage have proven to be far less expensive than the CBR option. The possible extension beyond the retirement life of the CF18 is no longer an argument in the life management cycle. There are 3 aircraft left to receive the CBR.

Lately, the CF fleet has experienced cracks in the dorsal longerons between the vertical stabilizers. These findings are unexpected. A special inspection determined that approximately 25% of the fleet is crack in this location. The OEM modification (splice) for this failure is fairly complex and labour intensive. L-3 MAS, the third line contractor, proposed an alternative solution in the form of an internal strap. Preliminary analysis shows that the repair could be full life and lower cost than the OEM splice option. First fleet aircraft installation will begin shortly.

Early configuration wings are also providing their share of trouble. The lower spar cap located near the inboard leading edge flap lugs is not certified full life. Front spar replacement was planned as the solution for CP3. However, for economic reasons the CF has selected a wing swap strategy. Retired wings from non-modified aircraft will be used to replace early production wings at CP3. Safety by inspection and the result from the upcoming residual strength test of FT-245 will be required to manage these life limited items.

A significant number of coupon tests are scheduled to begin shortly and are expected to identify the exact life improvement factor (LIF) of critical locations rework. Assessment will be focused on surface renewal (shallow blend), shot peening and IVD removal. The results are expected to certify certain ALEX modifications to full life status. The present lifing policy dictates a LIF (life improvement factor) of 1.5 for shot peening and approximately 3 for cold working. Surface renewal is not covered by this policy.

DND is eager to complete the residual strength test of FT-245. Positive test results will allow DND to introduce a damage tolerance approach for the wing structure. The early configuration wing problems identified above could consequently be eliminated.

CF-188 Aircraft Structural Integrity (ASIP) and Life Extension (ALEX) Programs

J. Dubuc, L-3 Communications (Canada) Military Aircraft Services (MAS)

As part of the service engineering support contract, L-3 MAS conducts a full-fledged ASIP program on the CF-18 fleet on behalf of the CF. Most of the recent and current efforts are dedicated towards interpretation of the IFOSTP test series and fleet findings in order to update the Structural Maintenance Program (SMP) of the aircraft, more specifically, the so-called ALEX Program (see details below).

L-3 MAS has recently completed the definition and development of the second phase of the ALEX program, designated as CP2, using mainly full-scale fatigue test results from the IFOSTP FT-55 Center Fuselage and FT-46 Aft Fuselage tests. The main objective of these activities is to identify all structural deficiencies that could affect the CF fleet and define corrective measures that will allow the fleet to meet its targeted ELE (Estimated Life Expectancy). In this aim, IFOSTP results have been complemented with a very aggressive Aircraft Sampling Inspection (ASI) program. In many instances, cracks were found in the fleet earlier than anticipated based on test results and usual scatter. Reasons for this are numerous but are usually not predictable on a case-by-case basis. Sometimes, variations compared to the test loading itself or the environment can be in question. Often the presence of manufacturing or maintenance induced surface defects is an aggravating factor as it creates scatter, which is beyond that seen otherwise.

Given the scope and complexity of the ASIP program, L-3 MAS has adopted a stage-gate approach to this task (ref. ICAF 2003) and has developed a series of unique engineering tools and processes including:

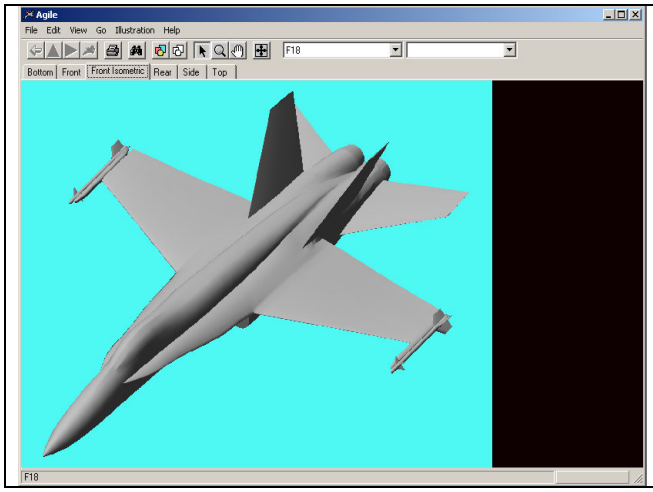

Figure 59. A typical screen from the Structural Information System (SIS).

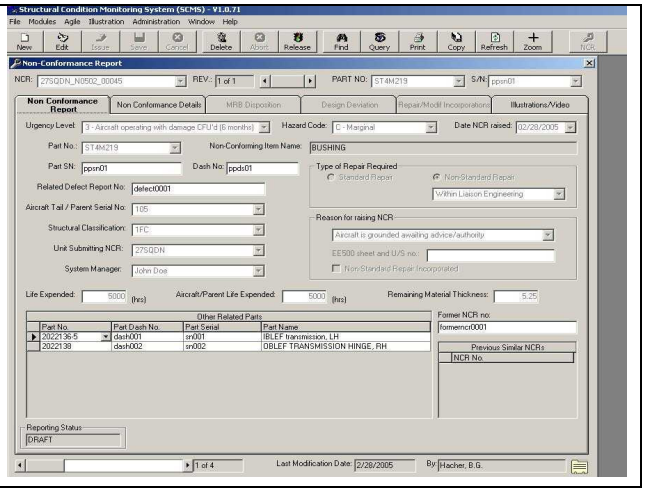

Figure 60. A typical screen from the Structural Condition Monitoring System (SCMS).

- Structural Information System (SIS)
- Analytical Tools, namely the Spectrum Generation software *Specgen*
- Risk Assessment process

Structural Information System (SIS): L-3 MAS has developed an application to efficiently track all structural problems on the CF-18 fleet. The system is called SIS for Structural Information System, it consists of a repository of relevant CF-18 structural information and as such forms the backbone of the documentation process for the CF-18 ASIP program. SIS includes the life-limited items, fleet and test failures, modification data, inspection data, fleet usage data as well as all full-scale structural test data (instrumentation, inspection cards and schedules, failures, etc.). Data is linked, where appropriate, which allows the user to visualize all related fleet and test information. This also allows the user to perform queries using almost any type of data. The system periodically interfaces with external database to update the aircraft modification incorporation status and with the fatigue usage database to update the aircraft usage data.

L-3 MAS was awarded a contract to customize SIS for the RAAF F/A-18 fleet requirements. The RAAF has procured a regular version of SIS as an interim tool for their fleet management and have initiated the development of new software modules that will form the Structural Condition Monitoring System (SCMS) once integrated to SIS. One of the key objectives of SCMS is to provide powerful reporting capabilities, to depict the spread of damage, corrosion namely and associated trend monitoring features over the airframe and operational conditions. A new graphical 2D engine included with SCMS allows technicians to locate non-conformances on the aircraft structure each time a defect is reported. Typical SIS and SCMS application screens are shown in Figure 59 and Figure 60.

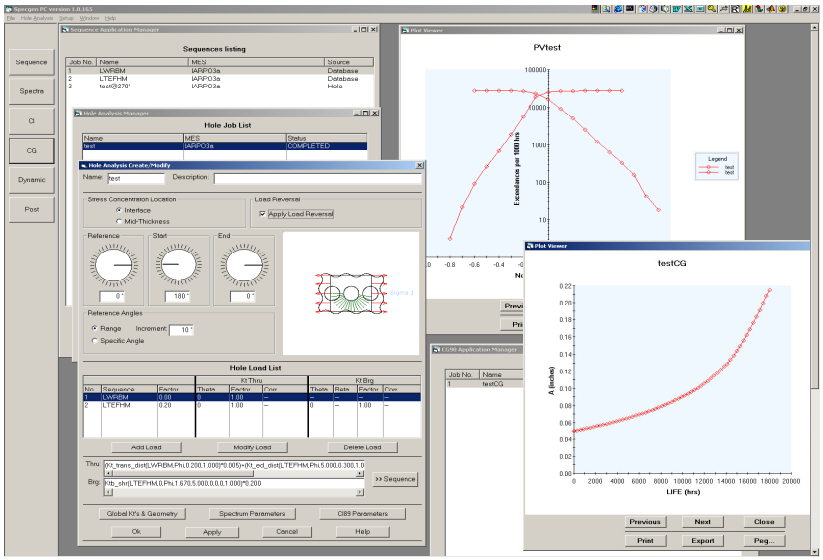

Figure 61. Typical screens from the Specgen software.

Analytical Tools: The test interpretation phase of ASIP entails use of a variety of engineering tools such as finite element models (FEM), strain gauge data from full-scale and flight test as well as fatigue and crack growth prediction software. L-3 MAS uses the CI89 and CG90 software acquired from Boeing, in the late 1980's, integrated into an in-house developed software, Specgen. *Specgen* integrates all spectrum generation utilities and common stress concentration (or intensity) solutions under the same umbrella along with CI89 and CG90. It allows easy access to a variety of design and test spectra and provides for linear combinations for mixed loading. In benchmarking performed with complex loading cases, Specgen yielded time-savings as high as 80% compared to the non-integrated software suite.

One portion of *Specgen* that has been greatly enhanced within the last year has been the development and integration of various tools and databases for dynamically driven zones on the aircraft. As is well known, various areas on the F/A-18 aft fuselage such as the empennage and engine support structures are largely driven by dynamic/buffet loading. The same is true for several areas on the wing. A substantial effort was performed to review and compile an extremely comprehensive database of flight test data from the CF, RAAF and US Navy programs for these areas of the aircraft. Various filters and signal processing tools have been developed to allow engineers to use the data for test interpretation relative to in-service

aircraft. Given the high sample rate of the flight test data and embedded modes of vibration within typical signals, the tools and methodologies developed have been key in providing a means to extract and manipulate the data. Most importantly, the tools allow the generation of line-by-line fatigue spectra, which include manoeuvre and buffet loads for subsequent analysis by CI and CG programs. Typical screens from *Specgen* are shown in Figure 61.

Risk Management Processes: The ASIP stage-gate process culminates with the risk assessment and management phase. These sub-processes allow the CF and L-3 MAS to establish risk acceptance and/or mitigation plans for each specific life limited item of the airframe according to its probability of failure and criticality. The CF has an airworthiness risk management process that is normally used to manage risks as they occur in the fleet. L-3 MAS has integrated this process as part of ASIP and applies it up front to eliminate or mitigate the risk before the probability of occurrence reaches an unacceptable level.

L-3 MAS also uses a so-called logistic risk assessment process to assist the CF in making the best value-for-money decisions for their fleet. This process is based on the CF Maintenance Policy Statements and it takes into account the operational aspect, i.e. loss of aircraft availability due to repair or maintenance and the cost of the mitigation compared to the financial risk exposure. As the ALEX program progresses to its second (CP2) and third (CP3) phases, an increasing number of life-limited items are managed by inspection. The key aspect of the decision to opt for inspections rather than preventive modifications is usually the logistic risk as for many areas of the airframe it is relatively straightforward to maintain safety-of-flight through a periodic inspection.

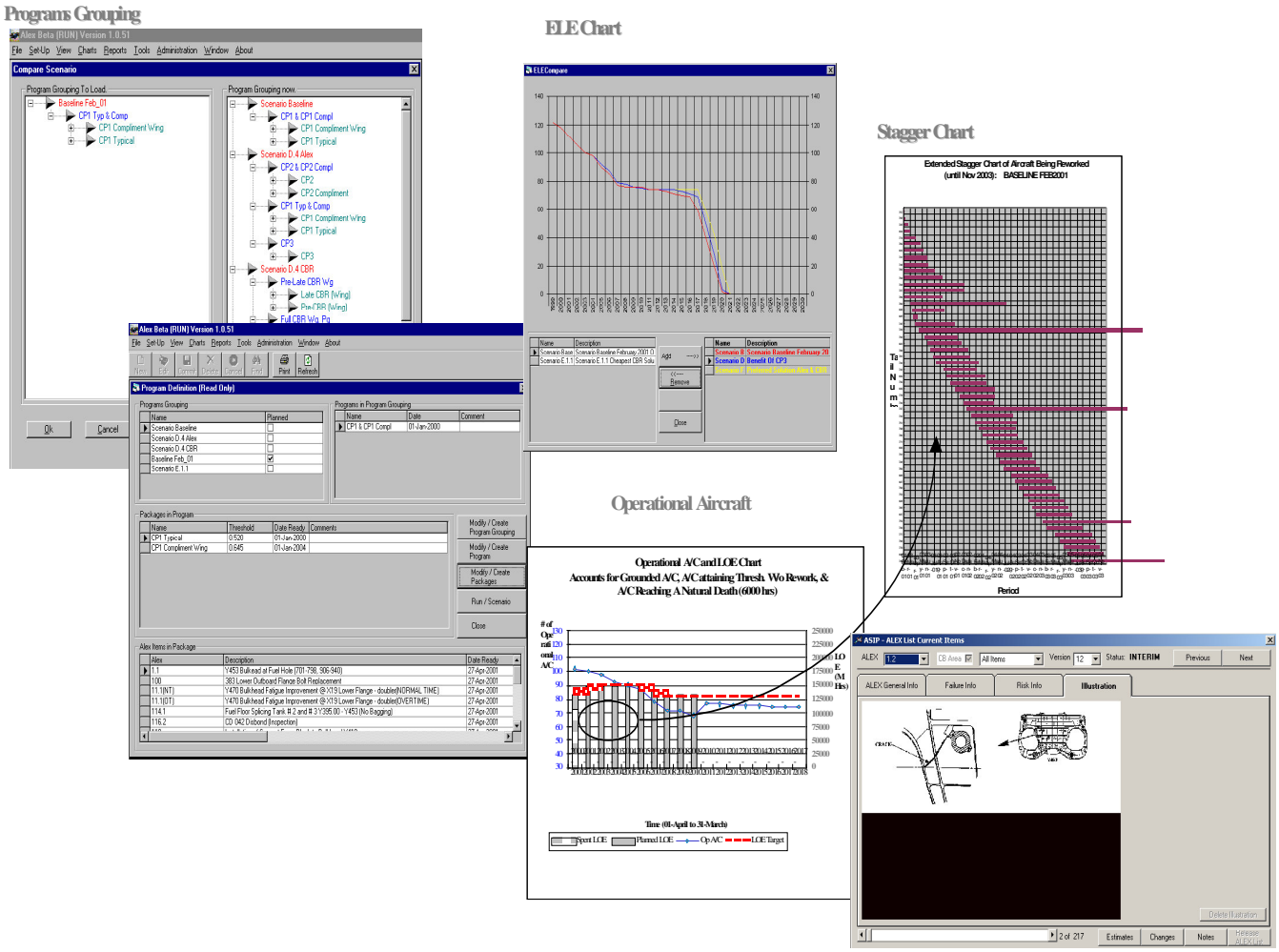

Figure 62. Typical Screens from the Alex Planner Fleet Management Software.

ALEX is a three-phase structural program aimed at progressively upgrading the fatigue resistance of the airframe and repairing existing cracks. As of the end of 2004, most of the CF-18 fleet has received the ALEX CP1 package at the L-3

MAS' depot level facility in Mirabel, Quebec. The CP1 package contains approximately 35 structural modifications, mostly situated in the centre fuselage area. A complementary program to extend the life of the fleet has also been developed in parallel, involving a major disassembly of the aircraft and replacement of the "centre barrel". This is the structural heart of the aircraft, the three highly loaded wing carry-through bulkheads that have demonstrated the most significant structural fatigue problems. The Centre Barrel Replacement (CBR) program will apply to about 15 aircraft; the ALEX program will address the rest.

Considerable efforts have taken place over the last two years to develop modifications and inspections for the ALEX CP2 package. CP2 comprises 70 modifications and inspections and encompasses various locations in the centre fuselage, Wing and Aft Fuselage. The majority of items under the ALEX program consist of structural modifications. Such modification items consist of the application of life improvement techniques such as cold working and shot peening. Most modification items include stress reduction features such as installation of fittings or doublers and in some cases re-profiling of existing geometry through various machining techniques. Many items require the removal of accumulated fatigue damage. Such damage removal is achieved by over-sizing fastener holes or micro-machining thin layers of material from high stress regions. Analytical and experimental techniques are used to demonstrate qualification of each modification against the aircraft specification. CP2 is currently in prototype at the L-3 MAS Mirabel facility and is planned for full production deployment in June 2005.

To assist the CF in the fleet management activities of the CF-18, L-3 MAS has developed an integrated fleet management tool referred to as the *ALEX Planner*. In essence, this tool provides an electronic/live version of a structural maintenance plan encompassing all structurally significant items on the CF-18, including the required thresholds of implementation. The database is linked to production cost breakdowns for the embodiment of modifications and/or inspections as well as to various operational databases for all aircraft (embodiment status, various operational usage parameters for the aircraft). With the integration of these databases, *Alex* can forecast and assemble all required modification packages for each aircraft in the fleet and allow for proactive planning that accounts for airworthiness requirements of the aircraft as well as provide tools to allow planning and resource or budget allocations. Typical screens from *ALEX Planner* are shown in Figure 62.

CC-130 Hercules

Major J.Y. Caron and T.W. Cheung, DAES, DND.

The CF CC-130 Hercules fleet consists of 32 aircraft, of five configurations (E, H73, H84, HT90 and H30), ranging in age from 13 to 40 years, and between 4000 and 44500 airframe hours. CF usage, as calculated by mission code base severity, has been climbing steadily since 1997. From the historical severity factor tracking, the CC-130 fleet is currently flying two times as severe as the 1980 baseline usage.

Due to increasing fatigue damage and the severe usage of the aging CC-130 fleet (over 40 years), service life for the centre wing has been evaluated by mapping in-service damage with the results from the wing durability test (WDT) employing statistical prediction. The in-service crack length found at each representative critical location is calculated to the same crack length that was found in the WDT. With the same crack length, the in-service life (in hours) can be correlated to the wing test hour (CTH). Comparison to the WDT allows the life remaining to be determined before the predicted onset of widespread fatigue damage dependent on current usage. The newly established service life on the centre wing is incorporated into the basis of certification and ASIP Master Plan update. In fact, most of the CW damage sights are located at the lower skin (stations 61, 178 and 220). Individual Aircraft Tracking (IAT) is continuously monitored to determine usage and damage, and each individual aircraft is assessed separately to determine the remaining service life.

One 'E' model centre wing is scheduled for teardown this year and the findings will be used to confirm the presence or absence of multi-site damage or multi-element damage. All crack findings will be used to develop a long-term structural strategy that will include revising the critical locations, the inspection intervals, the NDI techniques and the CWH/EBH ratio (CF Centre Wing Hours /Equivalent Baseline Hours from the WDT).

One of the major activities, during this period, focussed on repairing cracked holes at the vertical flange of the front spar lower cap at CWS 174. The USAF and the CF have jointly developed the titanium angle repair for restoring static and fatigue strength of the FS lower beam cap. Lockheed Martin is tasked to perform the damage tolerance analysis for the repair and a full-scale component fatigue test is planned. A new NDI technique will be developed to detect any cracks emanating from fastener holes at the vertical flange of FS lower cap that is sandwiched between the repair angle and the web. Fastener removal will not be considered as a requirement for completion of the inspection.

To date, six aircraft have been installed with new replaced parts and cold working has been embodied as part of the HAWSR fuselage and wing improvement programs. Rainbow fittings, spar webs and wing to fuselage attach angles have been replaced and most of the holes in the vertical flange of the spar cap have been cold worked for better fatigue life.

To satisfy the continuous airworthiness requirements for repairs or design changes, damage tolerance analysis and assessment is required. A CFD model for the complete airframe has been constructed and a full-scale airframe fatigue test (wing and fuselage) is to be completed in the UK. It is planned that the CF, the RAF and the RAAF will jointly fund the testing. A global finite element model was developed in the USA and funded by the CF and the USAF. The model can be used for structural loads validation and stress analysis.

Fuselage Service Life for the Canadian Forces CC-130 Hercules

Jason Scott, L-3 Communications

The worldwide C-130 Hercules community has recently focussed on Centre Wing Service Life issues. The Canadian Forces are seriously considering CW replacement on a portion of their fleet, including E-models with 40k FH and almost 40 years of service. Since the outer-wings were previously replaced, the CF expects the fuselage to become the life-limiting factor after the centre wing. With the centre wing replaced, it may be possible to extend the fuselage life to 60k FH, but this will probably require extensive replacements and corrosion control. An extensive review of fuselage experience of the CF fleet has been carried out with focus on known problem areas, such as the corrosion and cracking in the wheel well, underbelly and aft fuselage.

The C-130 Hercules, was initially designed in the 1950s as a tactical transport. In later years its role expanded to include strategic airlift, air-to-air refuelling, search-and-rescue and many other more specialized missions. The aircraft is a high-winged pressurized vehicle equipped with four Allison T56 turbine engines. It has a maximum gross weight of 155,000 lbs, including up to 65,000 lbs of fuel stored in a wet wing and external tanks, and can carry a maximum payload of 45,000 lbs or 92 troops, 64 paratroops or 74 litters. It is 98 feet long with a wingspan of 132 feet and a top speed of 320 kts. The fuselage is low-slung with an uplifted tail and narrow-track large-tyred landing gear tied directly into the fuselage structure. The centre fuselage is the cargo compartment area of the airplane, providing a clear volume that measures 9 ft. high, 10 ft. wide and 40 ft. long, which matches the internal dimensions of a railway boxcar. The aft fuselage is equipped with a ramp, which lowers to the ground and a door that rises into the crown to provide access for loading of personnel or cargo, including vehicles.

The centre-wing of the C-130 Hercules has been the subject of increasing investigation for several years. In particular, cracking of the forward beam lower cap at WS174, just inboard of the inboard engines, has focussed the attention of the OEM and operators on the service life of the centre-wing, which is currently poorly understood. However substantial test and in-service data is available, and the OEM is making a concerted effort to establish service lives for the centre and outer wings, both of which have been replaced by most operators, including the Canadian Forces.

The Canadian Forces initially operated four B-model aircraft in the early-1960s. These were replaced by 24 E-model aircraft in the mid and late 1960s. Attrition and small acquisitions since then have brought the fleet to 32 aircraft. The fleet includes five aircraft equipped for air-to-air refuelling of aircraft such as the CF-188. The stretch configuration aircraft, acquired from the OEM in 1997, are equipped with 100- and 80-inch forward and aft fuselage plugs to increase cargo capacity. The centre- and outer-wings were replaced on the E-models in the 1970s and 1980s respectively. The H-models are equipped with original wings.

While substantial changes have been made to the wings, primarily in the 1960s and 1970s, to address in-service fatigue problems, very little has been changed in the fuselage since the original A-model. The most significant improvement has come in the form of material substitutions to address corrosion. The fuselage frame is constructed largely of 7075-T6. The original 0.025” (min) 7075-T6 skins were changed to 0.050” (min) 2024-T3 from the B-model. The cargo floor was changed from extruded 7178-T6 to hat-stiffened 2024-T4 sheets at the same time.

In the late 1990s a Fuselage Life Assessment Program (FLAP) was initiated to assess the life of the fuselage and establish options for extending the life to 50 000 FH and 2010. The study reviewed all available analysis data to identify potential damage locations, which were then compared to in-service results. Two fuselage sampling inspections were undertaken to gather data on infrequently inspected structure. The analytical and in-service data were consolidated to identify locations

requiring improvemens, and improvement options were identified. Improvements ranged from fastener replacements and cold-working through addition of straps or doublers to replacement with new parts, in some cases including detail design improvements (e.g. to increase edge-distances or open fillet radii). The results of the FLAP study evolved into a Second Fuselage Improvement Program (FIP2) that is now being implemented. FIP2 consists of inspections, improvements, some directed replacements, and extensive corrosion prevention and control. FIP2 is being implemented as part of the Hercules Airframe and Wiring System Refurbishment (HAWSR), which began with a prototype in 2001-2002.

CC-115 – Buffalo

Major J.Y.Caron and A. Taylor, DAES, DND

Approval to have the Buffalo fleet life extension to the year of 2010 was granted at the end of 2002. A wing full scale DaDT (Durability and Damage Tolerance) test was contracted to the OEM in 1985 to substantiate the life extension to the year 2010 (estimated 30,000 flight hours). Today, it is estimated that the highest-time airframe/wing fleet will accumulate no more than about 24,313 flight hours based on the current usage of 450 FH per year. All centre wing rear spars have been replaced with improved material (7075-T73) to provide a predicted endurance life of 37,500 FH. All six airframes in the fleet have completed one cycle of corrosion surveys and a collation of structural repairs is underway in an attempt to document and track pre-existent structural repairs, some of which have not been recorded previously. Since the corrosion survey fleet cycle occurred over a period of almost 5 years, a new cycle of corrosion surveys is due to be scheduled.

The last review on the ASIP master plan was performed in 1985 and shall be re-assessed for SSI locations, severity factor in CPL (critical parts list) and usage spectrum. It is important to note that the usage spectrum recorded in 1987/88 was different from the baseline (assumed) wing DaDT test spectrum, particularly under 'training' and 'SAR' missions. It is proposed to review the fleet usage in order to qualify the effectiveness of the current ASIP program and for TAM compliance.

For corrosion (being time dependent), a tear down inspection on one Buffalo aircraft stored at Trenton, Ontario, is being considered. However, previous inspection results reveal no major corrosion problems. So far, there are no major repairs on the Al 7079-T6 structural components (centre wing skins and front spar web) that are susceptible to corrosion. A bonded repair option is being studied to determine whether this solution may be appropriate for a 7079 material.

Cracks have been and continue to be found in lower fuselage frames (floor support structure) in the fleet. In some cases, to relieve the load and provide a secondary load path for the lower cracked frame, the maintenance contractor has installed an angle doubler. These crack growth rates have been carefully monitored to determine their interaction effects on adjacent structure and between adjacent frames. The OEM was tasked to investigate the possible cause of the cracks and recommend corrective repairs.

CC-138 – Twin Otter

Major J.Y. Caron and A. Taylor, DAES, DND

The basis of the CC-138 ASIP is the commercial maintenance program recommended by the OEM. There are four CC-138 aircraft in service in the CF. Today, the maximum accumulated flying time is 25,500 hours (with 850 hours annually) and the aircraft is designed for a lifetime of 35,000 flight hours. The ELE 2010 plan is being considered but has not yet been approved. In 1992, the flying mission was changed from SAR to the transport operation. While this has been a change from a more severe to a benign mission profile, the previous effects (cumulative fatigue damage) of this change of operations while on SAR missions on the BoC and overall fatigue life has not been assessed.

During the design and development stage, the damage tolerance concept was not applied to the CC-138. To comply with ASIP requirements, 55 CPL items were identified and 10 most critical locations were chosen to perform the damage tolerance analysis using the CC-138 fleet average mission mix spectra.

No major structural or corrosion problems were reported in the past years. All the structural repairs were reviewed and instructed by the OEM. An overall structural and corrosion review is scheduled for the fleet upon completion of the TLIR. Since the usage mission was changed in 1992, the ASIP Master Plan has to be reviewed and updated with the current mission profile.

The number and extent of structural repairs applied to the control surfaces are of concern, e.g. flaps and ailerons which in many cases result in the surfaces being entirely re-skinned while other cases result in one-sided or off-set skin thickness distributions. This causes a modified structural behaviour due to the different stiffness distributions. Much reliance is placed on the surfaces being properly re-balanced. However it is worthwhile noting that the Twin Otter suffered from flutter of aileron and elevator surfaces in some conditions during its initial certification process, so that these areas require close scrutiny.

CT-142 – Dash 8

Major J.Y. Caron and A. Taylor, DAES, DND

The CT-142 fleet (4 aircraft) has been approved to for a life extension up to 2011. The ELE 2021 plan has been submitted for airworthiness approval. To date the fleet has accumulated an average flight time of approximately 9000 hours. Due to the introduction of a new training syllabus (low altitude), a load survey was performed between 1999 and 2001 to assess the impact to the current ASIP. The OEM was tasked to determine whether any reduction in the inspection intervals is required due to the change in mission. From the DaDT analysis, the OEM concluded that there is a damage ratio of 2.16 per flight between CT-142 and commuter Dash 8 airplanes. A 'half-life' threshold and repeated cut-offs were also incorporated in the maintenance program following the OEM recommendation. A team has been working to incorporate the differences in the maintenance programs between the commercial and CT-142 fleets. Results have not yet been received. All structural repairs were tasked to the OEM for instructions.

CH-146 Griffon

Sqn. Ldr. A.D. Armstrong, and M.N. Crawley, DAES, DND

Significant progress has been made with the generation and implementation of the Aircraft Structural Integrity Program (ASIP) for the CH-146. An ASIP was not part of the Griffon procurement since the OEM, Bell Helicopter Textron Canada Limited (BHTCL) agreed to support the helicopter. When a gap analysis was carried out to reconcile the ASIP and DND Technical Airworthiness Manual (TAM) requirements for the CH-146 fleet, available information was found to be deficient in a number of areas including knowledge of the baseline flight spectrum for the Bell 412CF as operated by the CF, structural usage monitoring and structural condition monitoring.

The task to validate current military usage with the original procurement assumption that usage would fall within the civilian design spectrum is nearing completion with data from approximately 11,000 flights in 7 basic roles between October 2002 and October 2003. A report will be issued in 2005 that will include an assessment of component fatigue lives based of the CF usage spectrum. The validation was carried out using parameters defined in the cockpit voice and flight data recorder and the development of maneuver recognition software. The CH-146 Aircraft Structural Integrity Management Plan was due to be completed in May 2005 with its main function being to describe the structure of the CH-146, outline activities that demonstrate compliance with the TAM structural integrity requirements, and a statement of the plan of action for achievement of compliance with the TAM wherever deficiencies exist.

Since the accident investigation for the Griffon crash of July 2002 due the fatigue failure of the tail rotor blade a range of work has been completed and planned to mitigate the airworthiness risk.

Inspection: Information since the introduction of the enhanced 12.5 hr inspection (vs. OEM directed 25 hour) has been compiled. Since implemented, the enhanced inspection has resulted in a ten-fold increase in detected damage indicating an increased Probability of Detection (POD) as compared to procedures used prior to the crash of CH-146420.

New damage limits: BHTC has issued Change 4 to the CH-146 maintenance manual. There has been clarification added to the inspection and repair guidelines. Of note, the limits for acceptable damage depth have been reduced in some areas (maximum damage for nick/scratch and sharp dent reduced from 0.005" to 0.003"), the critical zone has changed, and overlapping repairs are no longer allowed.

Probability of Detection (POD) Study: The NRC conducted this study, which was performed in two phases. In the first phase, NRC studied flaws and investigated techniques to accurately create flaws of known sizes and types in a tail rotor blade. The flaws had to be representative of defects/damage found in service. In the second phase, defects were introduced in four tail rotor blade segments with different paint schemes (2 white with black stripes, 2 olive with

red/white/red stripes) and an inspection reliability trial was performed. The tail rotor blades were mounted on CH-146 helicopters and technicians performed the inspections according to the maintenance manual for the CH-146. It is important to note, the units use a two-stage inspection method when the aircraft is at base. That is, the aviation technician assesses potential defects beyond limits and an aircraft structures technician is called to measure the damage and confirm its classification. Away from base, reliance is upon the flight engineer only until the aircraft returns to base. Significant findings were as follows:

- The damage limits in the maintenance manual are specified solely in terms of depth. The detectability of nick/scratch discontinuities is not a function of depth, but length, and so no POD could be determined. This is considered unacceptable and further work is required to address the problem.
- The current inspection procedure is in effect a two-stage process. The inspection looks for, and attempts to detect all visible discontinuities. It then classifies the discontinuities and measures them for depth with the use of a micrometer. Based on the result, the blade is repaired or returned to the repair and overhaul contractor. The key impact of this additional verification is that the visual inspection is simplified, as the inspection is only required to find visible discontinuities.
- Sharp dents were detected and correctly classified at only about 50% POD at 0.005" depth, and 80% POD at 0.015" depth (0.005" and 0.015" were the maintenance manual limits for repair when the study was conducted). Even assuming that the second inspection with the measuring device can be used to correctly classify errors, the inspection only achieves about 75% POD at 0.005" depth and 95% POD at 0.015" depth. These PODs are not considered acceptable and further mitigating actions should be pursued to raise the POD to an acceptable level.
- Although the original black paint scheme was not evaluated during this test, it was concluded through observation and interviews with inspectors that both the green and white paint schemes are superior from a visual contrast criteria. It was recommended that the original black paint scheme be removed as soon as possible.

Tail Rotor Vibration: The importance of paying special attention to any reported tail rotor vibrations (as reported by the aircrew or through HUMS analysis) was re-emphasized. In particular, close inspection of the entire tail rotor assembly is called for in advance of any action to damp out the vibration. Changes to the HUMS procedures have been carried out including trouble-shooting information, a requirement for a visual inspection prior to balancing, and a lowering of the criteria for when Tail Rotor vibration give early warning indications.

Defect Measurement Tool & Blade Mapping: An optical micrometer was provided to each CH-146 unit to make sure that a precise tool is used to measure any defects in the blades. A more detailed damage tracking and damage history record has been implemented to develop a better understanding of flaws types found in service, the effectiveness of the prescribed inspection techniques, and problems detecting and classifying damage. In addition, proper mapping will eliminate the possibility of overlapping repairs and to comply with the new requirements of the maintenance manual.

CH-124 Sea King

Sqn. Ldr. A.D. Armstrong and M.N. Crawley, DAES, DND

The CH-124 is working on the implementation of a new ASI Program that will involve the development of a Structural Usage Monitoring Program. This program has been initiated with the aid of Sikorsky Helicopters to track flight parameters and to define a baseline usage spectrum. This program is expected to continue to the estimated life expectancy (ELE). The ASIP program also includes the development/usage of a structural condition monitoring activity focusing on primary structure as well as the capability to assess recurring damage, modifications and repairs.

CT-114 Tutor

Maj. J.J.P.J. Brosseau and Capt. A.J. Gallant, DAES, DND.

The Canadian Forces CT-114 Tutor aircraft fleet, procured in 1962, has been retired from its current role as lead-in fighter trainer. However, the CF has decided to continue operating several of these aircraft in the Snowbird aerobatic role. The CT-114 Tutor aircraft was originally designed, monitored, and maintained according to the safe life philosophy. Recent re-analysis of current aircraft/fleet usage data from on-board operational loads monitoring and individual aircraft tracking systems, as well as recent field detection of cracks in fuselage and wing structures, indicated that the safe life of the fleet in general has been consumed. Bombardier, the CF Director of Technical Airworthiness and QETE organizations have collectively developed and conducted a safety-by-inspection program to keep selected aircraft from the Tutor fleet operational using damage tolerance and crack growth principles. Since the fuselage and tail structures have recently undergone a full-scale durability and damage tolerance test, it was urgent to generate component level spectrum data to

validate that the change from the safe life to the damage tolerance philosophy for the wing attachment fittings was indeed possible. Analysis, service experience, and results from previous full-scale tests identified five locations that were most critical. Three aircraft were decommissioned in order to recover components for testing purposes. Electro-discharge machining was used to introduce damage in critical design details of these components to simulate worst-case unsuccessful inspections. These components were then monitored to establish crack growth behaviour while being fatigue tested in uniaxial servo-hydraulic test frames. The components were subjected to the current Snowbird aerobatic usage spectra to develop and validate a safety-by-inspection program for formation and solo aircraft. To date, most locations have been demonstrated to satisfy the life extension requirements. Only one location has required a repair doubler designed and implemented to allow the wing front spar lower cap to achieve its expected life. Additional tests will not be performed on a final specimen, since the original testing where initial damage was introduced was "too severe". The CT-114 Tutor fatigue-testing program has now been terminated.

CT-133 Silverstar T-Bird

Maj. J.J.P.J. Brosseau and Capt. A.J. Gallant, DAES, DND.

Following the fleet reduction in April 2002, the CT-133 aircraft is now mainly operated at the Aerospace Engineering and Test Establishment (AETE). Only four (4) aircraft remain in operation while six (6) were put in storage as spares. All aircraft are equipped with an Operational Loads Monitoring (OLM) system. Only one aircraft is instrumented with strain gauges and the others have only four (4) flight parameters. The fleet was due to be retired by April 2005, and final closeout activities were planned for that time. These aircraft perform numerous missions varying from executive transport, training, chase plane and more recently as an ejection test bed. The ejection test bed aircraft will not be employed for any on-going ejection trials and will be retired with the remainder of the fleet.

The CT-133 fleet has not been monitored on a regular basis since entry into service in 1958. An Operational Loads Monitoring (OLM) system was used to track the relative damage experienced by the wing and the carry-through components for comparison to the Lockheed full-scale fatigue test spectra. On-going OLM data reduction was performed with the L-3 Communications (MAS) General Integrated Fatigue Tracking System (GIFTS) to track the aircraft usage severity. Results were gathered in the form of semi-annual and annual reports and presented to the fleet manager. Since no fatigue baseline exists for this fleet, the Canadian Armed Forces decided to manage the aircraft on a safety by inspection basis. The wing was believed to be the key life-limiting structural element. Consequently, a coupon test program was performed for wing critical locations WS 32 and WS 126 to ensure appropriate inspection intervals. Fracture mechanisms and fatigue data on Al 2014-T6, will be determined and analyzed. The project is near completion and the data gathered will be incorporated into the CT-133 Aircraft Structural Fatigue Program, as part of the final closeout activities. Additionally, the OLM spectra will be compared to the coupon test spectra for aircraft usage tracking. This information will be used to recommend new inspection intervals, if the CT-133 is ever re-activated.

CP-140/A -Aurora/Acturius

Maj. J.Y. Caron and Capt. R.P. Sabourin, DAES, DND.

The CP-140 fleet ASIP consists of fatigue and crack growth monitoring. The CP-140 has reach 100% FLI at the most fatigue critical location and as such is flown by inspection. Inspections are performed as required by crack growth tracking. The CP-140 has an SDRS (Structural Data Recording System) installed which provides usage monitoring, records NZ exceedances and strain gauge readings for 3 wing locations and one horizontal stabilizer location. There is an SDRS validation program in progress to ensure that the readings are accurate. Usage information for the CP-140 is documented every three months. At the end of every fiscal year, the quarterly report provides statistical usage information broken down to the squadron level. The CP-140 is currently undergoing a change in mission codes. Originally only 6 mission codes were defined. A recent study showed that these codes were inadequate for tracking usage and accordingly the six original mission codes have been replaced by 17 new codes. The new codes have been developed to better define the missions of the CP-140. During the next fiscal year, a review of the current mission mix will be conducted.

The CF participated in the P-3 Service Life Assessment Program (P-3 SLAP), which was an international program between the CF, the USN, the RAAF, and the Netherlands. As part of the program, full-scale fatigue tests (FSFT) of the wing-fuselage, and empennage were conducted. At the end of both tests, residual strength tests (RST) were performed. Both the empennage and the wing-fuselage FSFT failed during the RST prior to achieving the 100% design limit load case. The RST failure for the wing-fuselage test resulted from a crack in the centre wing lower panel weep hole. The RST failure of the empennage test article resulted from fatigue cracks in a FS 1185 stringer and FS1221 aft spar cap. To reduce the risk

of a similar failure occurring on the CP-140, flight operational restrictions have been implemented and special inspections of these locations have been conducted on all aircraft. Additionally, SLAP identified a fatigue related problem at the lower wing splices. ATESS is working on developing an inspection technique for the multi-layer splices.

There are several fatigue related projects currently underway for the CP-140. NRC is currently conducting a component test of WS 167 and a coupon test of FTI Forcetec retainers for the fleet. The WS 167 component test will evaluate the effects of cold working pre-fatigued material. This component test will identify the life improvement factor for cold working pre-fatigued material. Once this has been determined, it will be used in D/DTA analysis for WS 167. The goal of the coupon test program is to determine the life improvement factor resulting from replacing the existing dome nut holes that have been fatigued with the Forcetec retaining system. The inboard nacelle lower fillet panel dome nut fasteners have been replaced with Forcetec retainers. Testing is also planned to evaluate the effects of countersink fillers in joints and the effectiveness of safety cuts. These projects are to be conducted at RMC.

Canadian Contributions to the P-3C Service Life Assessment Program (SLAP)

M. Roth, QETE, and L. Hounslow, ATESS

As noted above, several countries have embarked on a collaborative program known as the P-3C Service Life Assessment Program (SLAP) involving a full-scale fatigue test (FSFT) of a P-3C maritime surveillance aircraft designed in the mid-1960s. The objective of the fatigue test was to identify fatigue related life-limiting factors, to provide fatigue life data and crack growth characteristics of the airframe, and to determine measures needed for continued safe and economic operation.

The test article was created from a US Navy P-3C, which entered service in 1969. It had accumulated 10,987 flight hours and 16,543 landings before being turned over as the P-3C FSFT article. During its thirty-year history, it experienced several tours of duty, numerous field and depot level inspections, and many modifications. The structural configuration of the test article was representative of a typical P-3C aircraft, except that prior to testing, the left wing received a major material improvement. The test article was tested to simulate 38,000 flight hours of the 85th percentile mission profiles.

During 2003-2005, Canada's primary contribution to the SLAP program was the teardown of the FSFT right-hand wing, which was performed at ATESS. The teardown started in June 2003 and was completed in December 2004. The teardown was divided into four phases. Phase I consisted of a detailed visual inspection. Phase II involved in-situ NDT inspections using techniques developed by Lockheed Martin and the Canadian Forces for the P-3C wing. Defect confirmation using other NDT disciplines was carried out as required. Phase III consisted of the teardown activities where all fasteners were removed and each section was disassembled into individual components. Phase IV post teardown activities were divided into NDT inspections and fractographic analyses. Eddy current techniques were used as the primary method of inspection for all holes, with various other NDT methods used to aid in defect confirmation. All the findings were recorded and entered into the SLAP teardown database. In preparation for the fractographic activities, an area surrounding each crack indication was cut at ATESS from the components such that the defect was not affected.

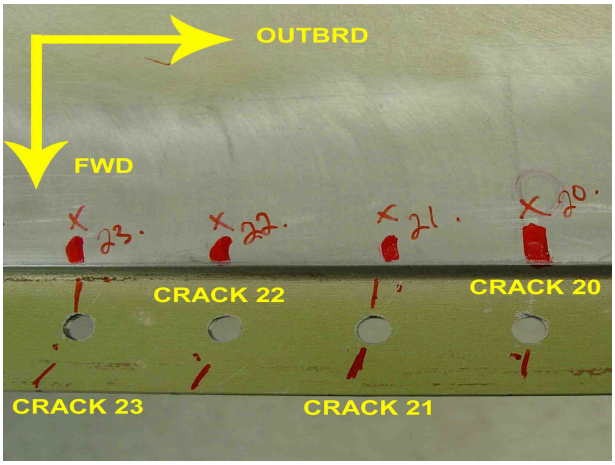

Figure 63. View looking up of the lower wing panel 3 showing locations of the cracks in splice 2/3. Crack 21 was investigated.

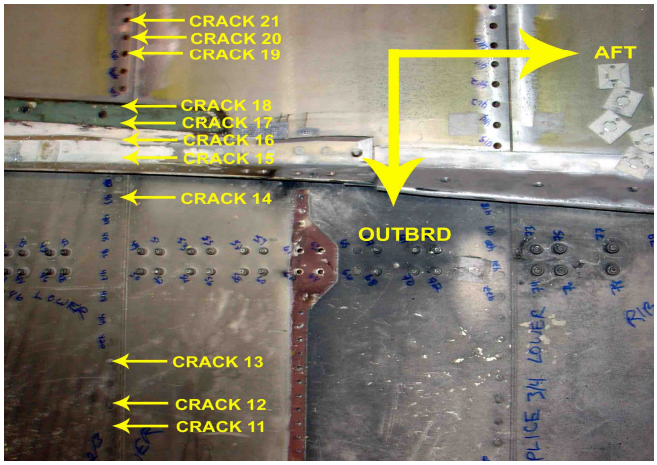

Figure 64. View looking up showing location of 0.263" 5 o'clock crack and 0.067" 11 o'clock crack.

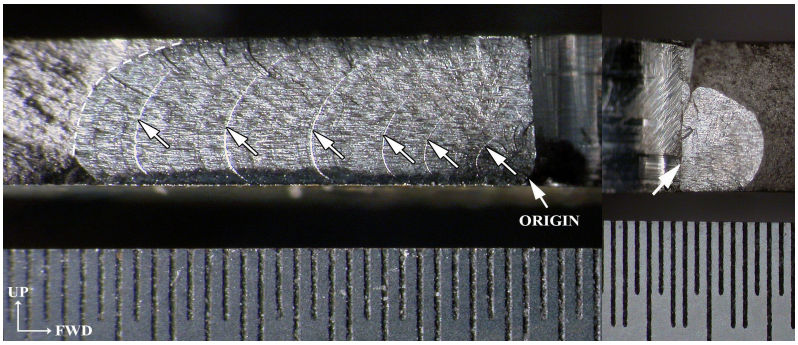

Figure 65. Overall view looking inboard of 0.263" 5 o'clock crack and 0.067" 11 o'clock crack. 5 o'clock crack initiated at lower surface at some damage (possibly partial deburring). 11 o'clock crack initiated in hole close to lower surface. All six marker bands in the 5 o'clock crack were observed using the SEM, but none in the 11 o'clock crack.

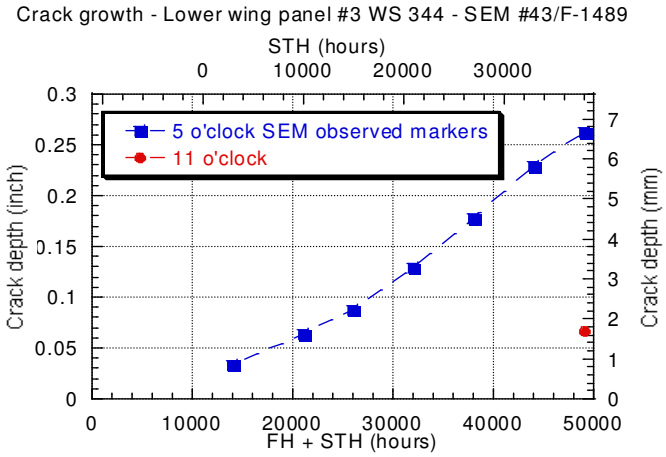

Figure 66. Crack growth curve for the 5 o'clock crack. The last points correspond to the crack depths at the end of the test.

The fractographic work was divided in two parts. The first one, labelled general fractography, consisted of opening all crack indications found during the teardown NDT inspections, identifying the cracking mechanisms, measuring the crack sizes, identifying the features at the origin, and populating the SLAP database. Over 500 cracks were thus opened and documented. A certain number of holes with no crack indications were also opened. If a crack was found, it was characterized as described above. The second activity was a detailed fractographic analysis of 22 cracks, either critical or representative of different areas in the wing, to determine the rate of crack growth. This was made possible by the incorporation of six marker blocks during the test. That data was required to validate analytical models and formed the basis on which the life of the airframe could be safely extended. The procedures followed and some of the findings are described under the Canadian entry "Fractography Investigation and Determination of the Rate of Growth of Cracks from the F/A-18 IFOSTP and the P-3C SLAP Full Scale Fatigue Tests" and in the paper "Fractography and Analysis in Support of a Full Scale Test" to be presented at the ICAF 2005 symposium.

Lower skin panel 3, splice 2/3 was the most severely damaged area of the wing where over 50% of the fastener holes were found to be cracked. Figure 63 and Figure 64 show views of this area with some of the cracks identified. Figure 65 shows a typical fractograph where all six marker bands are clearly visible. Figure 66 shows typical growth rate data for this crack as a function of flight hours plus test (simulated flight) hours.

The final report for the teardown of the right-hand wing of the P-3C SLAP fatigue test article includes the logistics involved, the teardown plan, the conduct of the teardown, the findings, conclusions, and the disposition of parts [32].

NRC Support to P-3C / CP140 Service Life Assessment Program (SLAP)

M. Yanishevsky and D. Backman SMPL-IAR-NRC

The WS167 and BL65 component specimens, Centre Crack Panel (CCP) fatigue crack growth specimens, Dome Nut Cold Work repair fatigue life coupons, and Cold Worked Hole fatigue life testing, as well as teardown activities of the Kestral and post test Right Hand Wing (ATESS) and Probability of Detection NDI studies form part of the Canadian SLAP activities.

The component and coupon tests of design details simulate regions on the aircraft, which have low fatigue lives based on analyses. The goal of these tests at NRC is to establish the fatigue lives of the assemblies, determine critical details of the outer and centre wing, identify where fatigue cracks will develop naturally, monitor their growth characteristics, and determine the effectiveness of cold working as a hole repair or fatigue enhancement option. As well, the tests are to provide a measure of the damage and crack detection capability of in-service NDT inspection techniques. Strain gauges have been installed in strategic areas to ensure that a representative strain distribution is induced in the components and to scale the loading spectrum to the same strain levels as the full-scale test.

Testing of Butt Line BL65, Figure 67, and Wing Station WS167 components was completed and the data used to anticipate damage in the FST. A rarely found 1 to 1 match was found between the component tests, the right "old" wing and the left "new" wing in the areas of representation. The BL65 achieved 6 lifetimes with only 9 naturally occurring failure sites detected during spectrum fatigue testing. To promote additional failure sites, three artificial flaws were introduced in the Lower Wing Skin panel at 4 lifetimes; however, an additional 2 lifetimes of subsequent fatigue loading were not able to encourage cracks to develop and propagate from these sites. The BL65 component achieved 104% of the highest anticipated service load during a RST. Post-test disassembly of the component revealed 13 additional cracks that were either inaccessible or hidden between layers of structure. The inspection results from these components emphasized the effectiveness of ultrasonic inspections for detecting damage in hidden layers. In contrast, the WS167 component failed at ~3 lifetimes with 22 identified failure sites; post-test teardown inspection at QETE revealed an additional 28 sites with 35 total cracks, all below the threshold of detection without fastener removal and/or teardown.

Fatigue testing of the CCP specimens Figure 68, using spectra representing three critical areas, was performed and the crack growth rate data used to establish proper prediction of the response of the structure to fatigue spectrum testing.

An open hole coupon test program was conducted to determine the benefit of using FTI Inc split sleeve hole cold expansion technology in Al 7075-T6 web material for low edge distances of e/D=1.36 (Figure 69) and nominal edge distances of e/D=1.75. The baseline specimens had oversized holes while the specimens to be cold worked had an EDM slot introduced at the edge of the central holes and were pre-fatigued so that after drilling to initial size for cold working, a 0.4 mm crack remained. Fatigue testing to a representative spectrum, showed that for both cases life improvement factors in the order of 13 to 18 were achieved when comparing the "worst" cold work specimen lives to "best" baseline lives for the two configurations. Comparison of "average" lives would have increased the Life Improvement Factors to ~26.5. Examination of the fracture surfaces suggests that cold expansion of the hole will often shift the critical area from the hole surface to a region adjacent to the hole or over to the specimen edge, Figure 70. This evidence indicates that cold expansion of holes will have implications on inspections and conduct of fatigue analyses. Updated analyses and inspections will need to take into consideration potentially unknown secondary and tertiary crack nucleation sites, which are typically not characterized during original aircraft life substantiations and certifications.

Initial indications are similarly very encouraging from a Dome Nut Hole fatigue coupon test program where cracks ~0.5 mm in length were allowed to form naturally toward satellite holes and were not fully removed during cold work with FTI Inc Forcetec bushings, where multiple life improvements appear to be achievable. At the time of writing, the first Forcetec specimen had completed 8 lifetimes of testing and the pre-existing cracks under the Forcetec bushing show no measurable evidence of propagation. New crack nucleation sites have not been found to date.

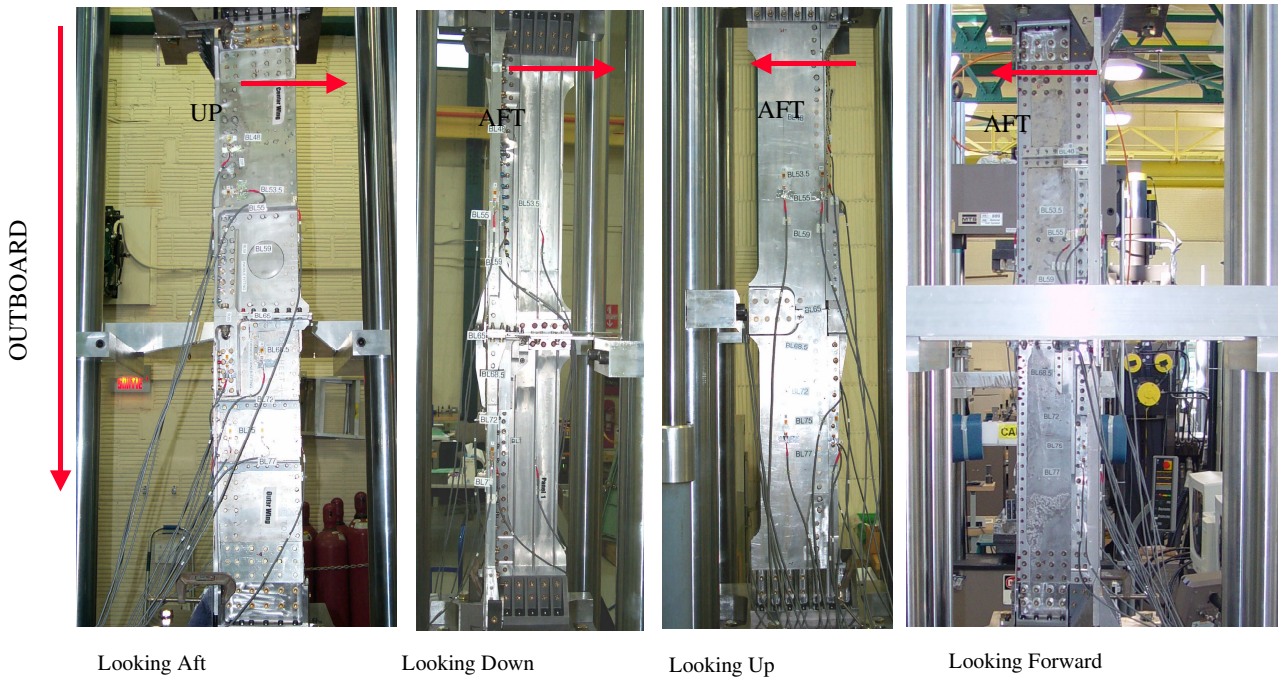

Figure 67. The BL65 main lower wing spar component installed in the loading frame.

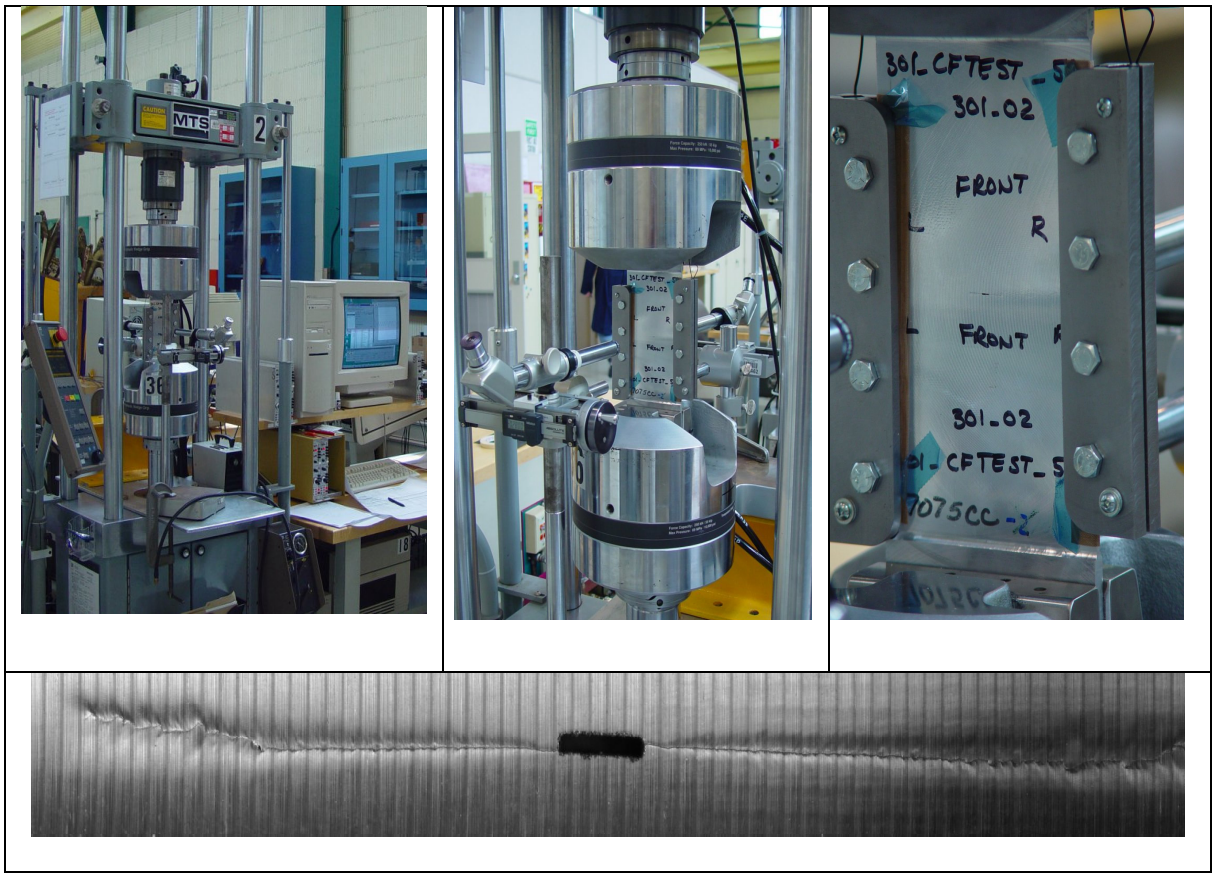

Figure 68. Centre Crack Panel tests used to establish spectrum fatigue crack growth rates for different critical locations and assessing the effects on crack growth of 50th and 85th percentile spectra. Note in the lower photo the plastic zones and tortuous crack path at longer crack length responsible for retardation effects (photo taken using Edge of Light).

A second WS167 component is undergoing spectrum testing to establish the potential of FTI Inc. split sleeve and Forcetec cold expansion to improve the fatigue life. In this test, spectrum fatigue prehistory was introduced to simulate the time when cold expansion repair is implemented across the CP-140 fleet. The component is currently undergoing full inspection with additional Eddy Current bolt-hole inspections prior to and after cold expansion repair of all the holes. A new Digital Image Correlation (DIC) technique is being assessed to determine whether it can be used to quantify the cold work effect of the FTI cold expansion technologies and help quantify the impact of cold expansion on representative close proximity and low edge distance holes. The DIC technique has already been shown to be effective in mapping large area strains, with minimal efforts in surface preparation. Full details of these SLAP activities at NRC may be found in Refs. [33, 34, 35, 36 and 37].

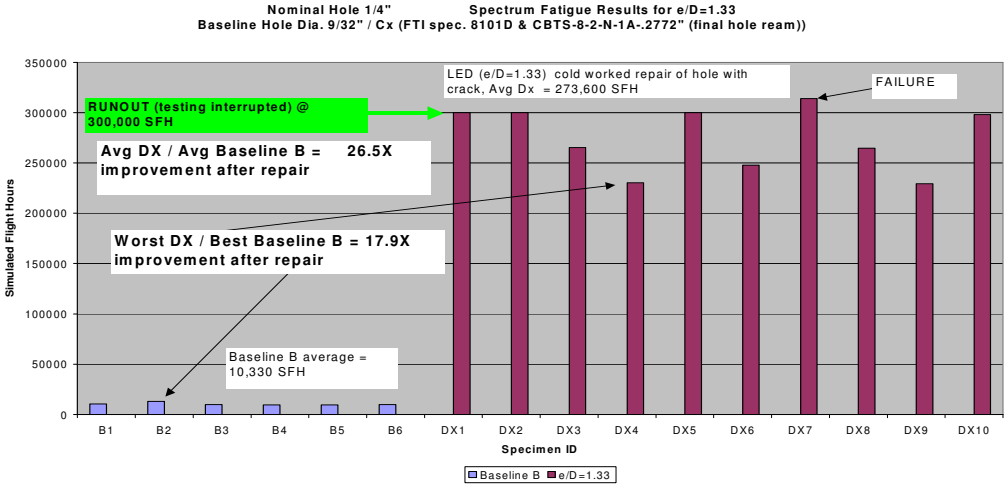

Figure 69. Comparison of cold expanded and baseline low edge distance (e/D=1.33) fatigue results.

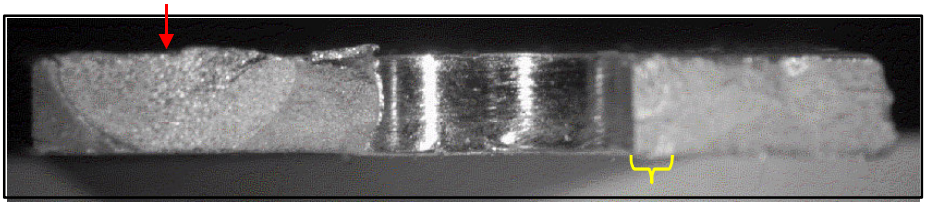

Figure 70. Fracture surface of low edge distance sample DX-9. The main fatigue crack (red arrow, at left) nucleated at a distance midway between the specimen edge and the central hole. Note that the original fatigue crack (in yellow, right side of hole), allowed to remain during cold expansion, did not propagate significantly during subsequent spectrum fatigue testing.

JOINING TECHNIQUES

Numerical Modeling of a Single Aluminium Sheet Containing an Interference Fit Fastener

N.C. Bellinger, SMPL, IAR, NRC

An investigation has been carried out of the 3D stress field around an interference fit fastener hole [38]. Two specimens were tested, each consisting of a single aluminium sheet and an interference fit fastener. A photo-elastic coating was bonded to the outer surface (fastener head side) on one specimen and the inner surface (nut side) of the other. An interference fit fastener was installed in a single sheet and then photo-elastic analysis was used to measure strains under different tensile loads. Four different 3-dimensional finite element (FE) models of the sheet and fastener/nut structure with and without a coating were generated. A numerical technique was proposed to analyze the fastener clamping torque, which was employed in the contact numerical simulations. Multiple load steps in the FE models were used to simulate the entire joining and then tensile loading stages. A good correlation was achieved between the experimental results and finite

element predictions for the maximum shear strain, Figure 71. The full-field contours of the maximum principal stress under different clamping values and tensile loads were also studied.

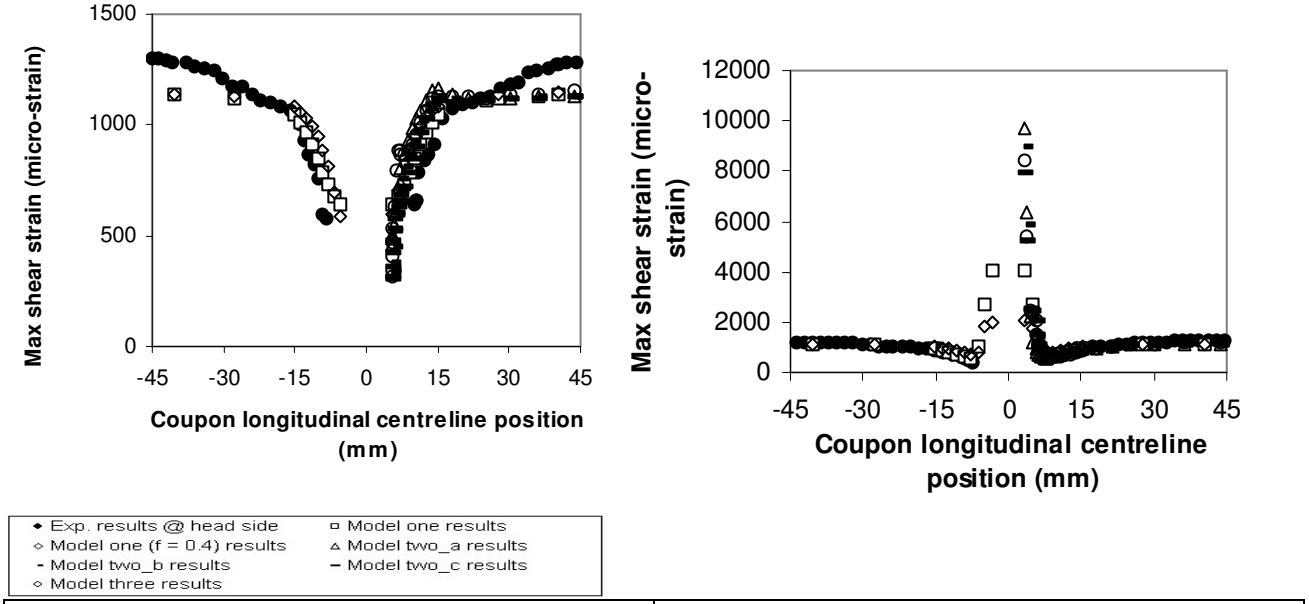

(a) Sheet outer (fastener head side) surface | (b) Sheet inner (nut side) surface

Figure 71. Comparison of the experimental coating and FE results along the sheet longitudinal center-line position on the sheet outer and inner surfaces when the sheet tensile load of 49642 N.

Fatigue Behaviour of Welded 2195 Al-Li Alloy

M.C. Chaturvedi and D.L. Chen, University of Manitoba

In view of the use of 2195 Al-Li alloy in the construction of super-light-weight external fuel tanks for space shuttles, bulkheads of reusable single-stage-to-orbit launch vehicles and in combat ground vehicles, the dependence of tensile properties, fracture toughness and fatigue resistance of this alloy on specimen orientation and welding is very important and was studied [39]. The following conclusions were drawn:

1. The 2195-T8 Al-Li alloy, with pancake-shaped grains and primary strengthening precipitates of T_1 (Al_2CuLi) phase having platelet shapes on {111} matrix planes, contained predominantly a brass-type texture, {110}<112>.
2. After welding with a 4043 filler alloy, the fusion zone (FZ) consisted primarily of T (AlLiSi) particles embedded in the filler matrix, while in the heat-affected zone (HAZ) T_1 phase dissolved, which was replaced by T_B (Al_7Cu_4Li) phase and micro-cracks along the grain boundaries.
3. The post-weld heat treatment (PWHT) caused the spheroidization of primary T phase and the precipitation of small secondary T particles in the FZ, and the dissolution of T_B phase and the re-precipitation of T_1 phase in the HAZ. However, the micro-cracks in the HAZ remained.
4. Due to the presence of the crystallographic texture, the specimen orientation had a strong effect on yield strength, fracture toughness and fatigue threshold, with the lowest values at 45^o to the rolling direction, see Figure 72.
3. The welding resulted in a reduction in tensile properties and fatigue strength, see Figure 73. The PWHT brought about an increase in yield strength due to the modification of microstructures in both FZ and HAZ. However, no improvement in the fatigue strength was observed owing to the existence of micro-cracks in the HAZ.
4. Tensile fracture surfaces exhibited mainly shear steps in the T8 base alloy, cleavage cracking in the welded joint, and cleavage cracking combined with the intergranular micro-void coalescence after the PWHT. Fracture surfaces after fracture toughness testing showed strong cleavage-like cracking coupled with dimple-like features. For the specimens oriented at 0° and 90° to the rolling direction, secondary cracking was observed. Fatigue cracks initiated basically from the specimen surface, and fatigue striations were a typical feature in the crack growth regime in the T8 alloy. However, after welding, with or without the PWHT, the fatigue crack initiation occurred at the defects and the crack propagation was basically characterized by cleavage-like cracking without fatigue striations.

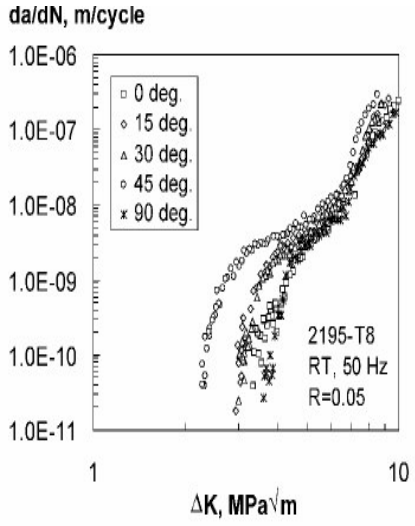

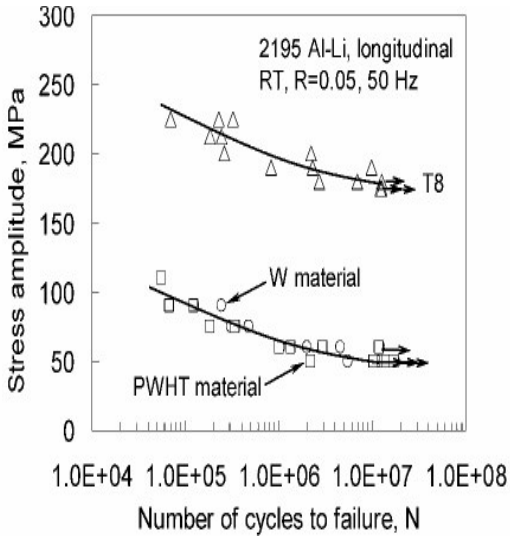

Figure 72. Near-threshold fatigue crack growth behavior of the 2195-T8 base alloy, tested at RT, 50 Hz, and R = 0.05.	**Figure 73. Effect of welding with a 4043 filler alloy (with and without PWHT) on S–N curves of the specimens tested at RT, 50 Hz and R = 0.05.**

COMPOSITE MATERIALS AND STRUCTURES

Fatigue Testing of Fibre Metal Laminates (FMLs)

Jeremy Laliberté, NRC-IAR-SMPL

The Fibre Metal Laminate Durability Project was concluded in 2005 and greatly increased the level of understanding of the damage tolerance behaviour of Glare (glass reinforced aluminium) laminates within Canada. Several spin-off projects are under development, or already operational, including life extension studies at Carleton University and the Technical University of Delft, the application of virtual crack closure theories to FMLs at Ryerson University and advanced processing of FMLs at NRC-IAR.

At this year's ICAF symposium a review poster paper covering all of the fatigue testing conducted under the project will be presented including previously unpublished results. The brief review presented herein covers recently completed or ongoing work at Bombardier, NRC-IAR and Carleton University. This information will also be presented in greater detail in the full paper.

Fatigue testing was conducted on a series of bonded lap splices designed by Bombardier Aerospace. The details of the splice geometries themselves are proprietary, however, all configurations have some of the features of the generic splice shown below (Figure 74).

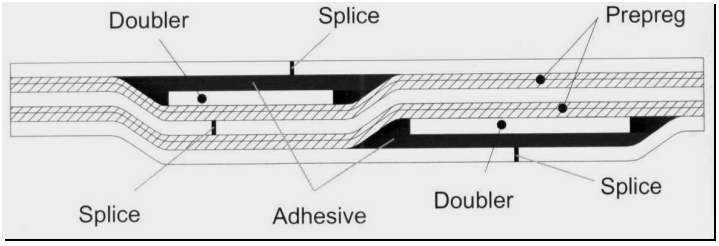

Figure 74. Generic bonded FML splice.

The bonded splices were tested either in the pristine condition or following 60 days of exposure to accelerated salt fog corrosion. Maximum constant amplitude stresses were 10 ksi, 15 ksi, 20 ksi or 25 ksi depending on the configuration of the splice. Figure 75 shows the effects of corrosion on the fatigue life of one particular configuration.

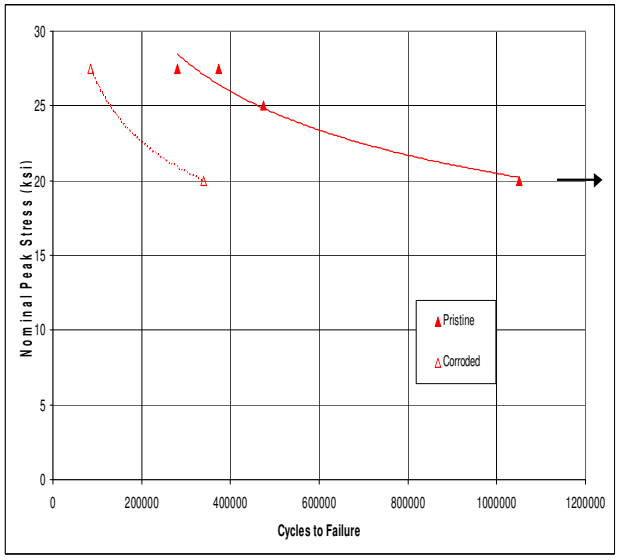

Figure 75. Typical pristine versus corroded S-N data for bonded FML splices.

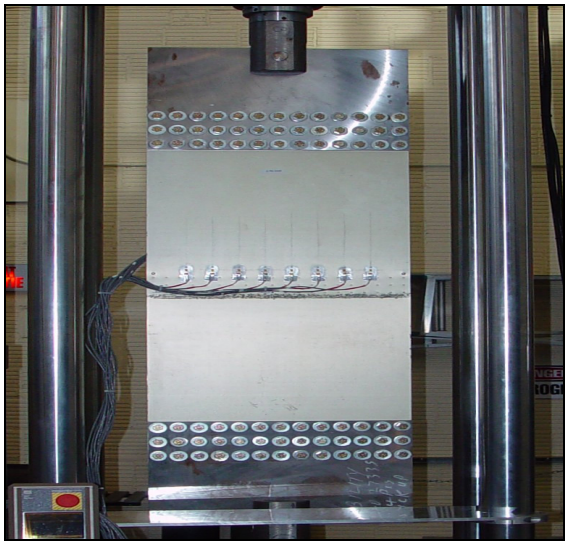

Figure 76. NRC-IAR corroded lap splice fatigue test set-up

Fatigue tests of riveted FML lap joints were carried out using a riveted splice specimen developed following the work of Mueller [40]. Previously IAR, Carleton University and Bombardier Aerospace collaborated on the testing of pristine lap joints of the same configuration. The more recent work was intended to evaluate the effects of corrosion damage on the same splice configurations in Glare 3 2/1 and Glare 3 3/2. Some details of the test follow:

- 20 in wide 3-row riveted lap joint
- 1-in row and rivet pitch
- NAS1097AD4-4 rivets
- Running load of 544 lbf/in at 4 Hz frequency, R = 0.03
- Accelerated salt-fog corrosion exposure for 60 and 90 days

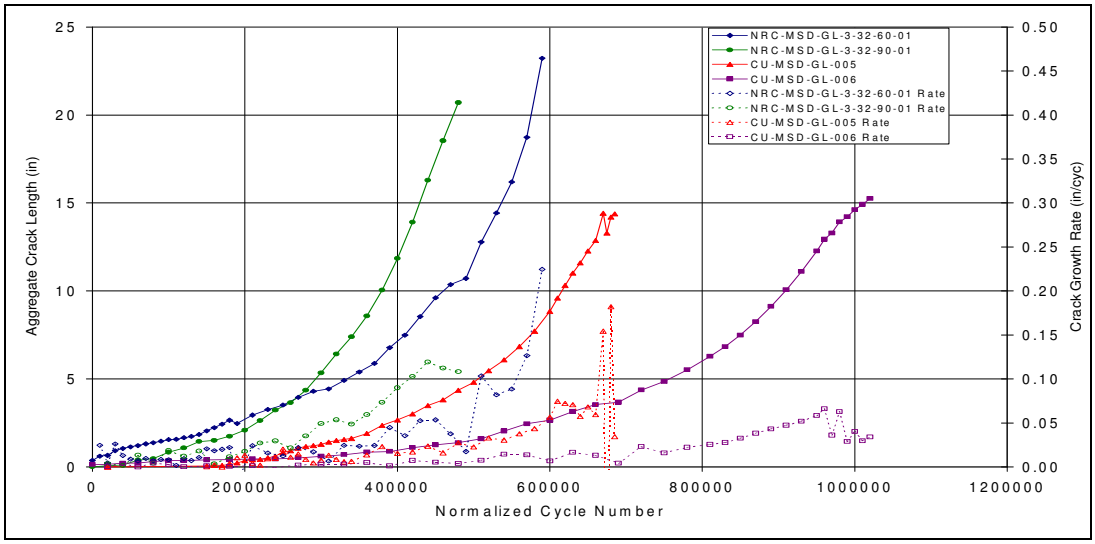

Figure 77. Comparison between aggregate length and crack growth rates for pristine and corroded wide Glare 3 3/2 specimens.

The test rig is shown in Figure 76 above. The specimen was instrumented with 16 strain gauges (8 each side) located nominally 1 inch above the upper rivet row. Fatigue crack measurements were made using a traveling microscope. A comparison between the aggregate crack length and crack growth rates is shown in Figure 77 and demonstrates the moderate reduction in fatigue life due to corrosion in these splices.

GLARE Life Extension Studies

P.V. Straznicky, Carleton University

As part of a larger research effort into the optimization of riveted joint designs used for GLARE, a non-linear finite element investigation was undertaken on the influence of rivet installation on the formation of residual stresses. As a first step, a 3-dimensional finite element model of the split-sleeve cold expansion process was created to compare the formation of residual stresses in monolithic aluminium and GLARE laminates. Subsequently, the model was extended to simulate the rivet installation process. The observed influence of the fibre layer on the residual stress distribution in GLARE was two fold. First, during radial expansion of the fastener hole, displacement compatibility between adjacent layers causes load to be redistributed by the elastic fibre layers as the aluminium layers began to yield. This resulted in a larger region of plastic deformation and residual compressive stresses in GLARE compared to monolithic aluminium. Second, during elastic spring-back, the less resilient aluminium layers resist the elastic spring-back of the fibre layers, providing additional residual compressive stresses near the fastener hole. Additionally, in the rivet forming simulations, the increased resilience of the fibre layers also resulted in increased rivet clamping forces which could have significant consequences related to frictional load transfer and fretting fatigue.

SURFACE TREATMENTS

Corrosion Protective Treatments for Aging Aircraft

B. Arsenault, IMI-NRC

A protective coating is being developed to address aging aircraft problems. The approach involves a metallic coating able to inhibit stress corrosion cracking (SCC), pitting corrosion and fatigue corrosion occurring on aircraft primary structures made of aluminium (Al) alloys sensitive to localized corrosion. The coating is required to maintain the original fatigue properties of the alloy while providing good adhesion and corrosion protection.

This on-going project will provide data in terms of fatigue, SCC protection, localize corrosion protection and bond strength in order to demonstrate that the technology is capable of meeting flight safety issues.
Furthermore, the technology is developed for:

- On-site coating deposition for aircraft maintenance solutions
- Manufacturing capabilities for improvement of spare components.

The targeted benefits are to provide protection against SCC and fatigue corrosion to structures in severe environments and to reduce the maintenance costs and downtime while extending the life of the aircraft.

The Effect of Warm Water Surface Treatments on the Fatigue Life in Shear of Aluminium Joints

P.R. Underhill, A.N. Rider and D.L. DuQuesnay, RMC.

The effect of warm water treatment on the fatigue life of 2024 T3 aluminium alloy adhesively bonded with FM73 epoxy adhesive was investigated [41]. As expected, the fatigue life was shown to depend on the surface preparation of the bonds. Fatiguing the specimens in wet conditions led to a slightly shorter life than under dry conditions Figure 78. There was a correlation between performance in the wedge test and fatigue life for these bonded systems, Figure 79 and Figure 80. Warm water treatment of the aluminium leads to an improvement in both of these properties. The improvement in fatigue life can be attributed to a significant improvement in the wetting of the surface by the adhesive. This moves the failure surface away from the surface into the bulk of the adhesive, Figure 81.

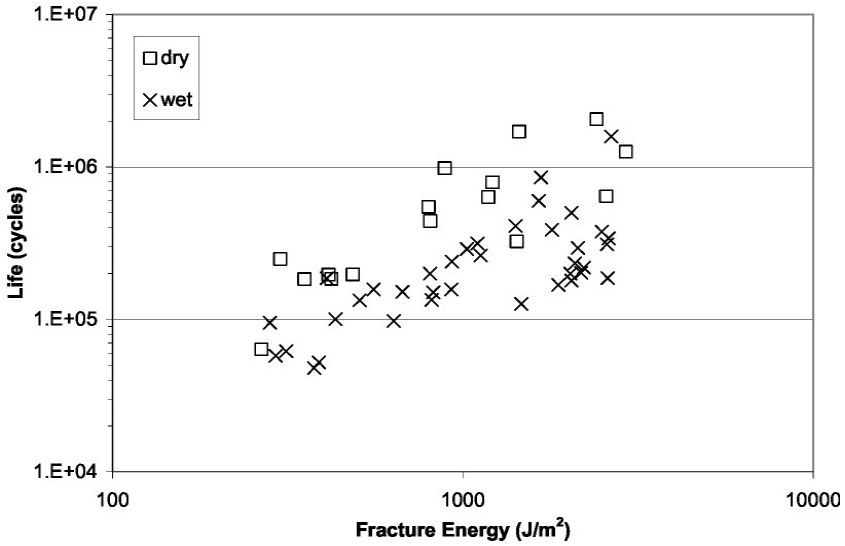

Figure 78. A comparison of wet vs. dry fatigue life as a function of fracture energy as measured in the wedge test after 6 days of exposure at 50°C and 95% R.H.

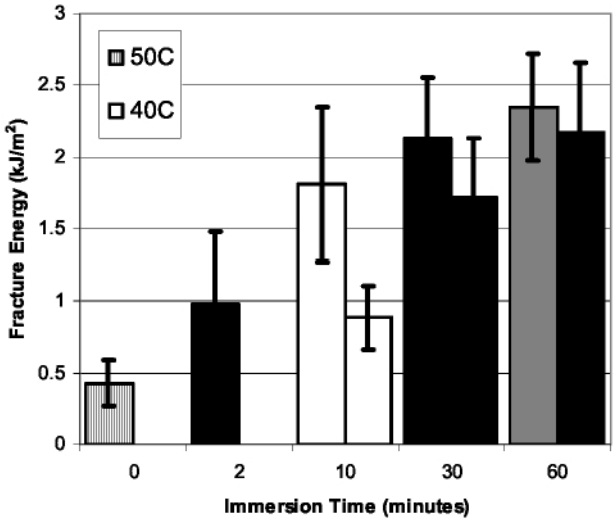

Figure 79. Fracture energy of wedge test specimens made from bare 2024 aluminum alloy treated by immersion in warm water after 6 days exposure to 50°C, 95% R.H. environment.

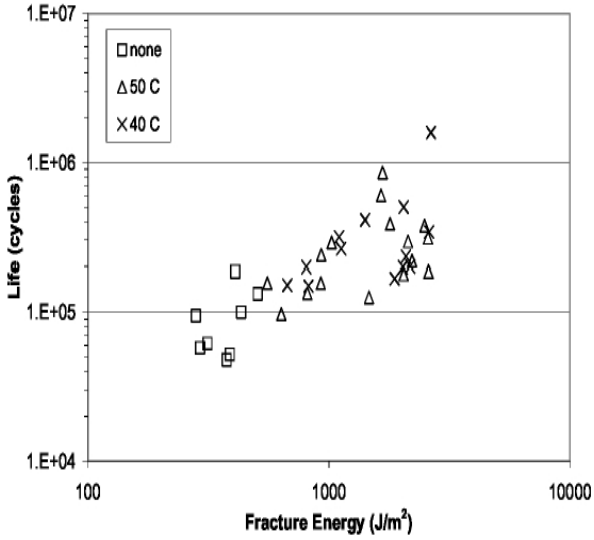

Figure 80. Fatigue life under wet conditions as a function of fracture energy as measured in the wedge test after 6 days of exposure at 50°C and 95% R.H. Symbols represent the temperature of the warm water pre-treatment.

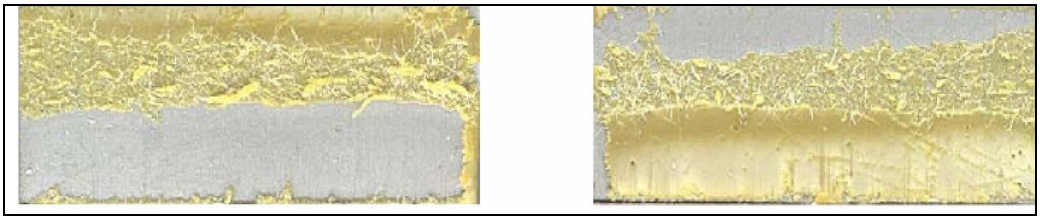

Figure 81. Both failure surfaces of a typical fatigue specimen. Tensile shear loads were applied in the vertical direction.

GAS TURBINE MATERIALS AND STRUCTURES

Fracture Mechanics Analysis of Fatigue of A Single Crystal Superalloy

X.J. Wu, SMPL, IAR, NRC

For description of the anisotropic characteristics of single crystal materials, the continuously distributed dislocation theory (CDDT) was used to derive a closed form solution for elastic-plastic cracks in single crystal materials. Under uniform stress, the crack tip opening displacement (CTOD) and energy release rate of a Mode-I crack in an anisotropic elastic-perfectly-plastic material are given, respectively, as:

$$u_2 = \frac{4a}{\pi} t_2^F F_{22}^{-1} \ln \frac{c_2}{a} \tag{1}$$

$$G = \frac{4a}{\pi} (t_2^F)^2 F_{22}^{-1} \ln \frac{c_2}{a}, \tag{2}$$

where F_{22} is a material constant defined in the Stroh formalism, t_2^F is the yield strength of the material in the loading direction, and the dislocation distribution length (half crack length plus the crack-tip plastic zone size) c2 is given by

$$\ln \frac{c_2}{a} = \ln \left(\cos \frac{\pi t_2^0}{2 t_2^F} \right)^{-1}. \tag{3}$$

Under small scale yielding, the CTOD reduces to

$$u_2 = \frac{K^2}{2 F_{22} t_2^F}$$

The significance of CTOD is emphasized by the correlation of fatigue crack growth rates in both [110] and [100] directions with this parameter [42 and 43].

Single crystal turbine blades are mostly cast in the [001] direction. Fatigue testing of notched CMSX-4 specimens showed that fracture originated mostly at interdendritic pores, and the crack front advanced in a circular shape, Figure 82. An assumption was made that the initial crack took an elliptic form from the pore, and grew first under constant stress in vacuum before it broke through to the surface, and then continued as a long crack in the applied stress fields. Based on the Paris equation fitted to the crack growth rate data and the fracture mechanics solution for the stress intensity factor K, the fatigue life (subsurface plus surface crack growth) was be evaluated, as shown in Table 4. The conclusion is that fatigue fracture can be traced to interdendritic pores and its life can be accounted for by considering crack growth from the pore. Note that in most of the cases, a quite significant portion of the fatigue life has been assumed to be spent in the growth of internal cracks.

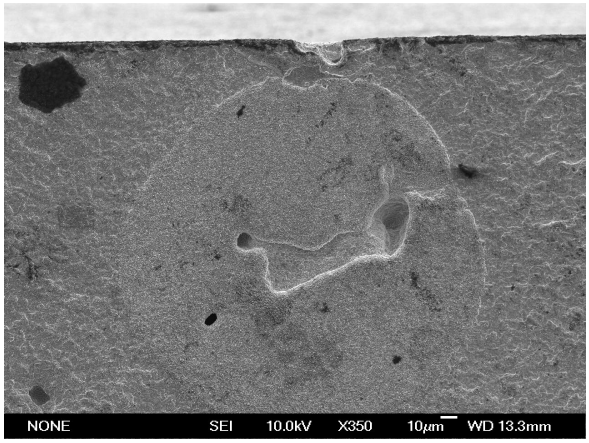

Figure 82. Sub-surface initiation in CMSX-4 at 650°C after 6,500 cycles.

Table 4. Notch Fatigue Life of CMSX-4

Orientation /Test No.	F_{max} (kN)	Major axis (μm)	Minor axis (μm)	Depth (μm)	Test life	Cal. Life
X/3	6.2	100	10	80	62,000	22,800 (17,000)
B/4	6.2	90	10	130	6,500	11,100 (4,600)
A/6	6.2	100	25	250	25,500	49,000 (30,000)
A/8	6.2	40	15	0	21,661	32,000
A/9	6.2	50	30	200	5,270	6,500 (4,000)
B/11	6.2	50	5	350	13,717	14,900 (12,800)

*Note that the number in the bracket indicates the life of internal crack growth.

Fatigue Behaviour of Inconel 718 Superalloy

L. Xiao, D.L. Chen and M.C. Chaturvedi, University of Manitoba

Symmetrical push-pull low cycle fatigue (LCF) tests were preformed on Inconel 718 (IN-718) containing 12, 29, 60 and 100 ppm boron (B) at 650°C [44]. The following results were obtained:

With different concentrations of boron this alloy exhibited a relatively short period of initial cyclic hardening at low cyclic strain amplitudes, followed by a regime of saturation or slight cyclic softening at 650°C, Figure 84. The initial cyclic hardening phase was shortened with increasing strain amplitudes. At the high strain amplitudes the initial hardening vanished, and was replaced by cyclic softening until macroscopic crack growth occurred.

The alloy exhibited serrated flow in the plastic regions of the cyclic stress-strain hysteresis loops, characterized by successive stress drops, Figure 84. This phenomenon was not observed when the cyclic strain amplitude was low. The alloy with 60 ppm B displayed the highest saturated cyclic stress amplitude, while an alloy with 12 ppm B had the lowest at a given cyclic strain amplitude.

Boron had a considerable effect on the fatigue lifetime of IN-718, Figure 83. The LCF life increased with an increase in concentration of B from 12 ppm to 29 ppm. The alloy with 60 ppm B possessed the best fatigue properties among the four studied, in the regime where the fatigue life was longer than about 300 cycles. However, the LCF lifetime decreased as the B concentration increased from 60 ppm to 100 ppm.

Fractographic examination showed that the crack growth path was predominantly intergranular with 12 ppm B. As the B content increased from 12 ppm to 29 ppm, the fracture mode exhibited a mixture of intergranular with transgranular cracking, with intergranular fracture still prevalent. Some plastic deformation traces were observed on the fracture facets of the alloy with 29 ppm B. The proportion of transgranular cracking further increased, and some fatigue striations were observed on the fracture surface of the alloy with 60 ppm B. The fracture surface morphology changed from intergranular to transgranular as the B concentration increased. The LCF fracture surface of the alloy with 100 ppm B was characterized by fatigue striations, i.e., predominantly transgranular with only a small fraction of intergranular cracking.

The TEM examination revealed that the typical deformation structure consisted of a regularly spaced array of planar deformation bands in the fatigued IN-718 with different concentrations of B. They represented the traces of two groups of slip bands operating along two {111} slip planes. A ladder-like structure was observed and wavy slip was activated in localized regions in the fatigued specimen with very low B levels. Wavy slip caused a concentration of slip in a few bands within the bulk of the material, and led to fatigue crack nucleation. This favored crack propagation within PSBs, thereby reducing the fatigue life of IN 718 with the lower concentrations of B. Heavily deformed and well-developed planar deformation bands were observed at 100 ppm B.

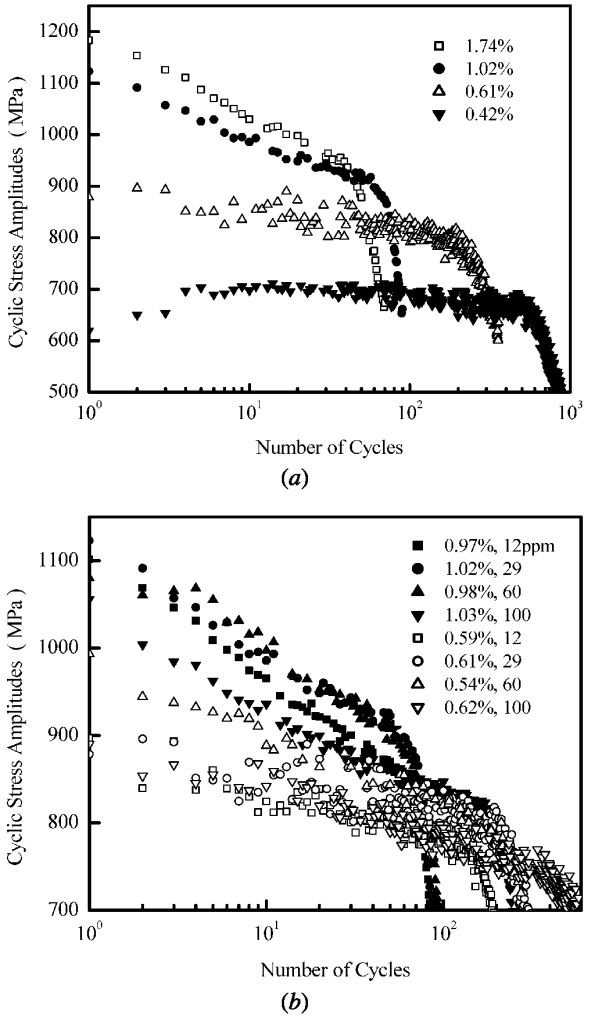

Figure 83. Typical cyclic stress response curves as a function of number of cycles of IN718 at 650 °C: (a) alloy 29 with 29 ppm B fatigued at different cyclic strain amplitudes, and *(b)* IN718 with different concentrations of B fatigued at the same cyclic strain amplitude.

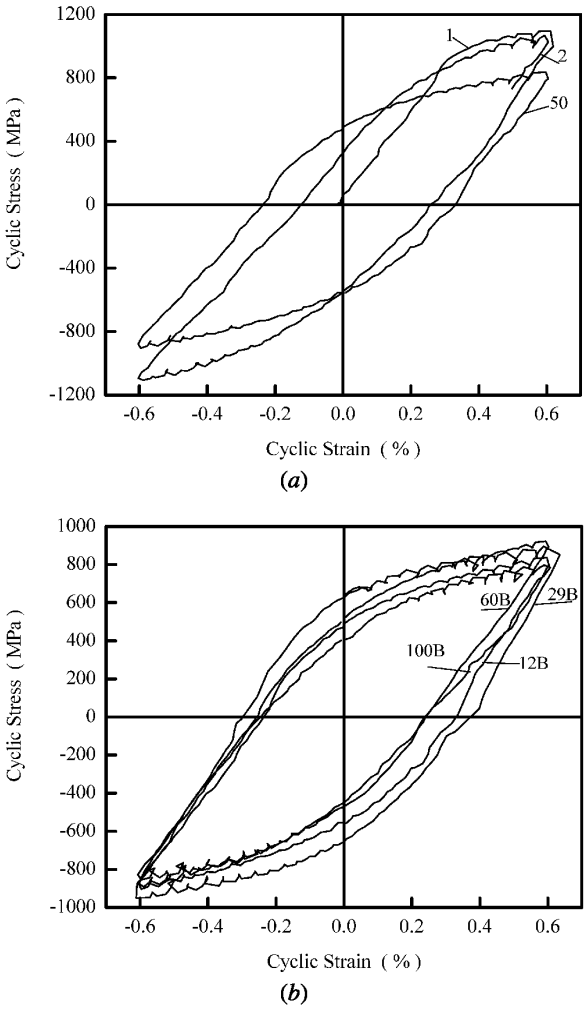

Figure 84. Typical cyclic stress-strain hysteresis loops of IN718 at 650 °C: (a) alloy 12 fatigued at $\Delta\varepsilon_t/2$ = 0.59 pct with different number of cycles; and *(b)* cyclic saturation stress-strain hysteresis loops for alloys with different concentrations of B fatigued at $\Delta\varepsilon_t/2$ = 0.6 pct.

The improvement in the LCF life of IN-718 by B addition could be rationalized by the increase of the direct elastic interaction between dislocations and B atoms in solution and boride particles, and by the increase of grain boundary cohesion due to B segregation which acts to fill vacancies, pin dislocations and diminish grain-boundary diffusion.

Shearing of γ″ Precipitates and Formation of Planar Slip Bands in Inconel 718 During Cyclic Deformation.

L. Xiao, D.L. Chen and M.C. Chaturvedi, University of Manitoba.

Cyclic deformation substructure of Inconel 718 fatigued at RT and 650°C was examined by TEM [45]. A strong tendency to form planar deformation bands was observed in IN-718 fatigued at RT as well as at 650°C, Figure 85. The planar deformation bands consisting of multiple groups of parallel bands formed via the motion of dislocations on {111} planes. The width and spacing of planar slip bands at both the temperatures were almost the same in specimens fatigued at different cyclic strain amplitudes.

The formation of planar slip bands is attributed to the shearing of coherent and ordered γ″ and γ′ precipitates by pairs of dislocations moving on the primary slip planes, which did not cross-slip during cyclic deformation, Figure 86. After the initial cutting of γ″, the trailing dislocations on the same slip plane repeatedly sheared the γ″ precipitates, and the continued cyclic deformation reduced their size to such an extent that they offered very little or no resistance to the movement of dislocations, resulting in the formation of the precipitate-free planar slip bands.

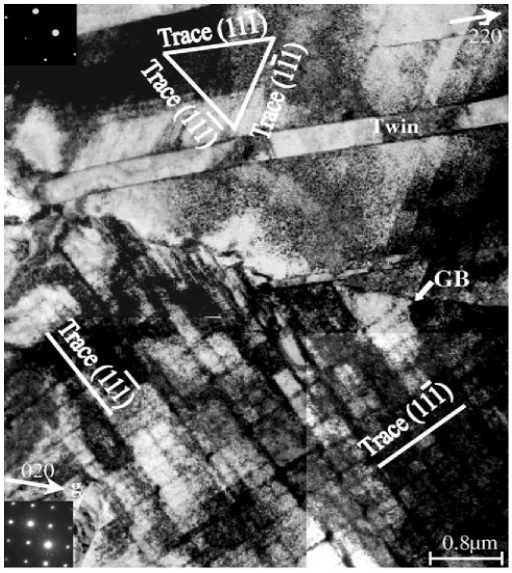

Figure 85. Groups of planar slip bands observed in a specimen deformed at $4e_p/2 = 0.13\%$ at 650 °C.

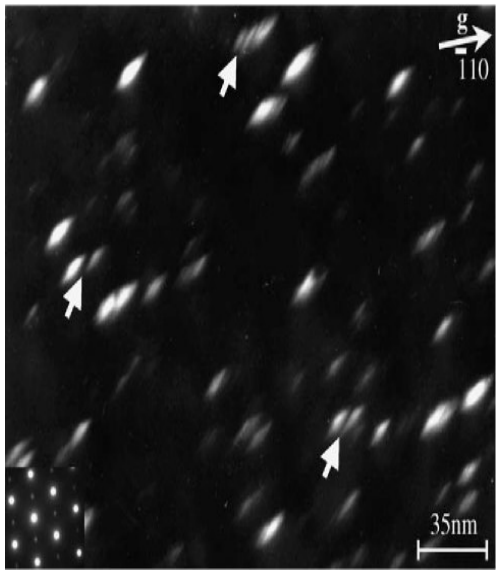

Figure 86. Dark field micrograph with g~ = [110] reflection and the foil in [110] orientation, showing sheared precipitates in a specimen deformed at $De_p/2 = 0.6\%$ at 650 °C.

T56 Series III Engine Turbine Rotor LCF Life Update

W. Beres, SMPL-IAR-NRC

The work on T56 Series III gas turbine engine component life update was initiated in 2001. The main objective was to re-evaluate low cycle fatigue crack initiation life and crack propagation life of the T56 series III turbine rotor. This project was carried out as a collaborative effort between Rolls-Royce Corporation, Indianapolis, USA; the IAR-NRC and DND, Canada; CSIR and SAAF South Africa; DSTO and RAAF, Australia; US Navy and US Air Force. The main contribution

Figure 87. Spacer 1-2 and 2nd stage wheel from the T56 Series III engine.

of the IAR to the project was to design and perform testing of two turbine spacers and two discs in the IAR's spin rig facility. The spin test results were applied to verify the crack initiation and crack propagation lives for these two components.

In the period of 2003-2005 both components were spun in the IAR spin rig facility.

NONDESTRUCTIVE INSPECTION AND SENSORS

Reliability of Nondestructive Testing

D. Forsyth, SMPL-IAR-NRC

Significant effort continues in the development of cost-effective approaches to determining the reliability of nondestructive testing (NDT). A continual feedback approach allows revision of initial reliability estimates based on new information such as field findings or NDT modeling.

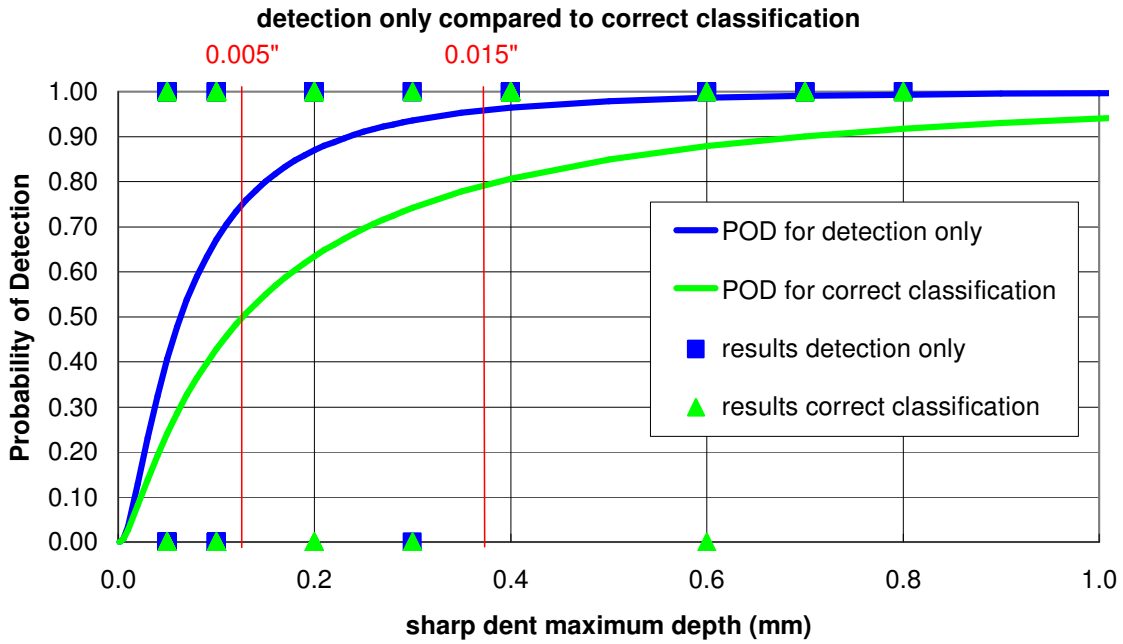

Figure 88. The probability of detection of sharp dents as a function of their maximum depth, compared for detection only against detection and correct classification of findings. The repair limits for this type of damage are either 0.005" or 0.015", depending on the location of the damage.

A study of the reliability of visual inspections of the CH-146 tail rotor blade (TRB) was performed for DND. Controlled damage was created in CH-146 TRB's, and these specimens were mounted on CH-146 airframes and inspected by DND personnel on base. The results indicated that the maintenance manual was not written in a way to incorporate the reliability of the inspections: the most structurally significant damage is believed to be a "nick/scratch", and the manual limits are in terms of depth. The detectability of this type of damage was not a function of depth, but a function of surface length.

It was found that the reliability of detection for sharp dents as required in the SRM was in some cases less than 90% probability of detection (POD) (see the figure below). The reliability of detection for "unsharp" dents was very high.

A study is being undertaken currently for DND to develop a "generic" capability to provide POD estimates for bolt hole eddy current inspections. This study combines the use of specimens from aircraft with natural fatigue cracks, a controlled set of fatigue crack specimens to be manufactured, and experimental design and EC modeling. While the cost of this study will be similar to a more traditional POD study, the output will include a validated model of bolt hole eddy current inspections and a procedure to interpolate new POD information for situations similar to those directly included in the experiment. This provides a much better return on investment to DND.

A Method for Lift-off Independent Eddy Current Testing

C. Mandache, SMPL-IAR-NRC

IAR and DND collaborated to develop a lift-off independent method for conventional eddy current testing (ECT) (patent pending). The inevitable variations in separation between EC probe and specimen are called lift-off, and the signal from this variable is often a limiting factor in the sensitivity of ECT. The new method of analysis of ET signals virtually eliminates this variable, and can be implemented on existing ECT equipment.

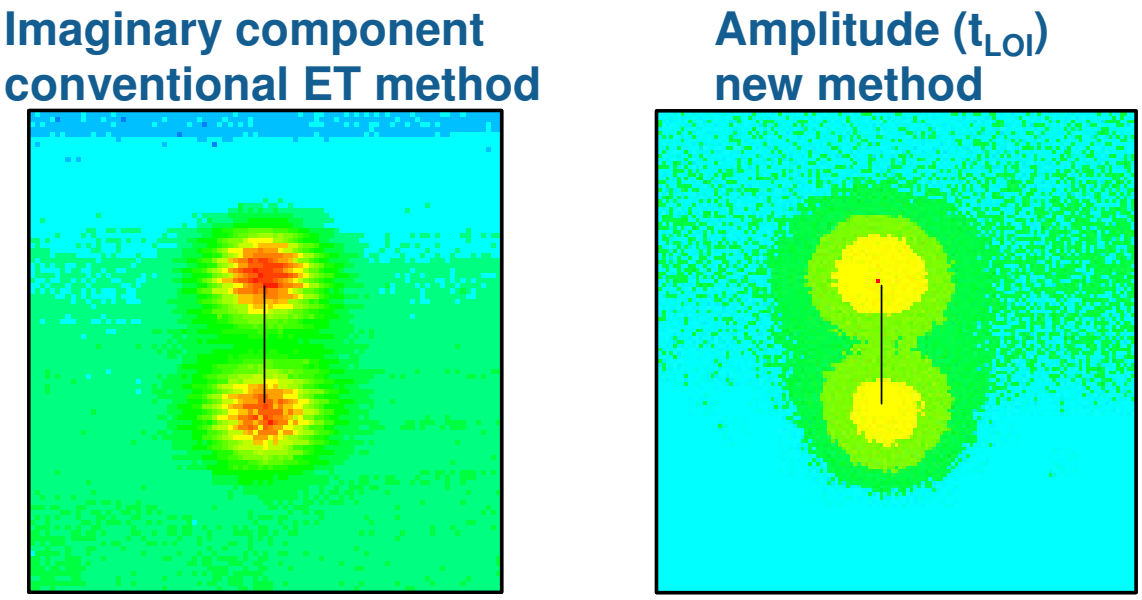

Figure 89. A comparison of conventional ET (left) and new, lift-off independent ET (right) for a specimen with a crack (black line) and lift-off. Background variation is virtually eliminated, and signal to noise much improved, by the lift-off independent method.

Data Fusion for Prognostics and Health Management

D. Forsyth, SMPL, IAR, NRC

The full benefit of sensors and conventional NDT for prognostics and health management (PHM) can only be achieved if the diagnosis can measure indicators of approaching failures. Most data fusion applications so far have been based on classifying outputs: i.e. crack or no crack. IAR is implementing continuous output data fusion engines to provide predictive metrics from sensors and conventional NDT for input into prognostics. These methods have been used to fuse multiple NDT data from inspections of fuselage joints for thickness loss due to corrosion, which is a measurement not well suited to conventional classifier-based fusion. An example result is shown in Figure 90.

Thermal Imaging of Fretting Damage In-situ

D. Forsyth, SMPL-IAR-NRC

In support of a collaborative effort to develop models of fretting fatigue, numerous NDT techniques were evaluated for their potential to detect fretting damage on hidden surfaces. It was found that passive thermal imaging of specimens undergoing loading was sensitive to fretting damage, even at very early stages in life. Coupons of 0.063" thick Al sheet, overlapped and joined with rivets, were cyclically loaded in tension and monitored with a thermal camera. An example of heat produced by fretting after only 10 cycles is shown in Figure 91.

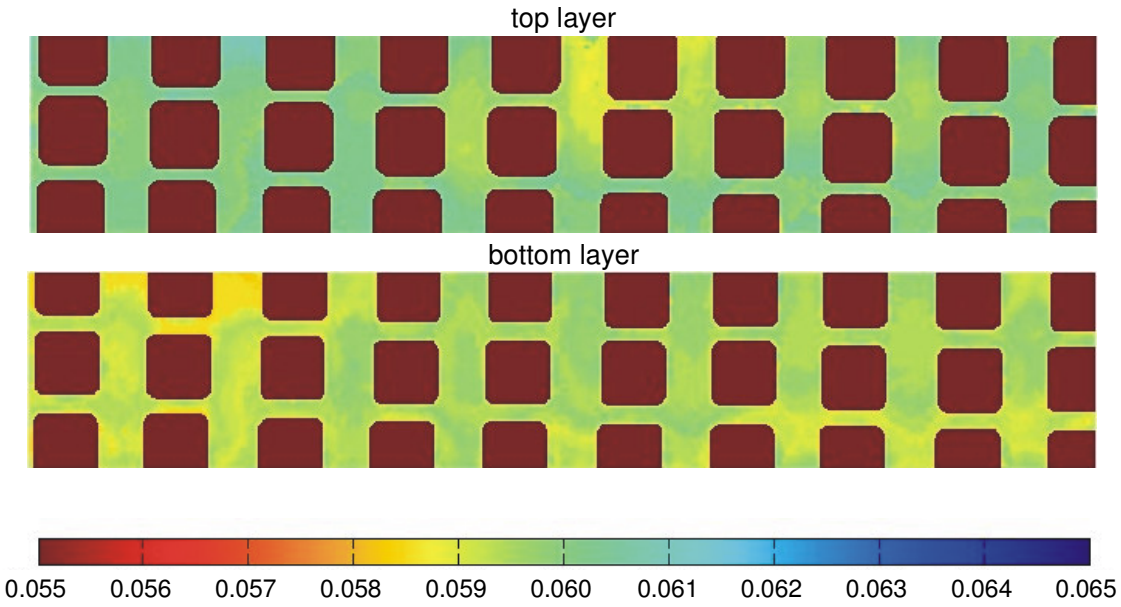

Figure 90. Results of thickness estimation on the top and bottom layers of the lap joint specimen, using data from a commercial two frequency eddy current instrument and data fusion algorithms developed at IAR. The rivets are excluded from the analysis.

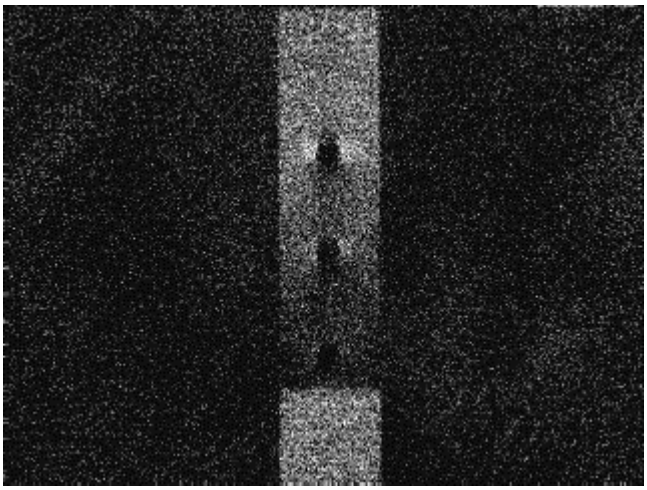

Figure 91. The raw thermal image of specimen 10 at 10 cycles, showing hot areas on either side of the top and middle rivets.

ACKNOWLEDGEMENTS

The authors are grateful to all contributors and their organizations for having submitted their inputs without which this review would not be possible.

REFERENCES

1 J.P. Komorowski, Canadian National Review ICAF 2003.

2 D. Paraschivoiu, Instrumentation of a Fatigue Full-Scale Test Article, 18th Aerospace Structures and Materials Symposium, Canadian Aeronautics and Space Institute, Toronto, 26-27 April 2005.

3 K. Narayan, K. Behdinan, and P. Vanderpol, An Equivalent Uniaxial Fatigue Stress Model for Analyzing Landing Gear Fuse Pins, 18th Aerospace Structures and Materials Symposium, Can Aero and Space Institute, Toronto, 26-27 April 2005.

4 M. Liao, and J. P. Komorowski, "Effect of Prior Exfoliation Corrosion on Fatigue and Fracture Behaviour of Aging Aircraft Structures and Materials", LTR-SMPL-2002-0136, June 2002.

5 M. Liao, N. C. Bellinger, and J.P. Komorowski, "Modeling the Effects of Prior Exfoliation Corrosion on Fatigue Life of Aircraft Wing Skins", Int. J. of Fatigue, 25 (2003) 1059–1067.

6 M. Liao, T. Benak, D. Backman, M. Brothers, P. Vesely, and T. Marincak, "Static Testing of Coupon Machined from C-141 Upper Wing Skins Containing Exfoliation Corrosion – Preliminary Results", LTR-SMPL-2004-0016, 2004.

7 M. Liao, G. Renaud, D. Backman, D. S. Forsyth, and N.C. Bellinger, "Modeling of Prior Exfoliation Corrosion in Aircraft Wing Skins". The Second International Conference on Environment-Induced Cracking of Metals, September 2004, Banff, Albert, Canada.

8 M. Liao, G. Renaud, N.C. Bellinger, D. Backman, and D.S. Forsyth, "Effects of Exfoliation Corrosion on Static and Fatigue Behaviour of Aircraft Materials and Structures -- Testing and Modeling Studies". The 8th Joint NASA/FAA/DoD Conference on Aging Aircraft, January 2005, Palm Springs, California, USA.

9 A. Merati, "A study of nucleation and fatigue behaviour of an aerospace aluminium alloy 2024-T3", International Journal of Fatigue, Vol. 27, 2005, pp. 33-44.

10 D.L. DuQuesnay, P.R. Underhill and H.J. Britt, Fatigue Failure of Adhesively Patched 2024-T3 and 7075-T6 Clad and Bare Aluminum Alloys accepted for publication in Fatigue and Fracture of Engineering Materials & Structures (FFEMS), 2005.

11 M. Yanishevsky, D. Backman and J. Rogers, "Test Protocol - Compression Testing of "Pristine", "Z" Cut-out "Damaged", and "Z" Cut-out "Damaged and Repaired" C-141 Wing Panels, LM-SMPL-2004-0014, January 2004.

12 G. Renaud, G. Li, G. Shi and M. Yanishevsky, Extensively-Corroded C-141 Wing Panel Modeling and Patch Design Study, Canadian Aeronautics and Space Institute, 18th Aerospace Structures and Materials Symposium, Toronto, April 2005.

13 M. Yanishevsky, Compression Testing of Composite Patch Repaired C-141 Lower Wing Panels, LTR-SMPL-2005-0089, in progress.

14 G. Li, G. Shi and M. Yanishevsky, Finite Element Analysis of C-141 Lower Wing Panels With and Without Simulated Exfoliation Corrosion Damage Under Compression Loading, LTR-SMPL-2005-0090, in progress.

15 A.E. Nolting and D.L. DuQuesnay, The Effect of Mean Strain on Fatigue Damage Caused by Fully Open Loading Cycles, accepted for publication in Canadian Metallurgical Quarterly, 2005.

16 Q. Zhang and D.L. Chen, A Model for Predicting the Particle Dependence of the Low Cycle Fatigue Life of Discontinuously Reinforced MMCs, Scripta Materialia, 2004, 51(9), 863-867.

17 Q. Zhang and D.L. Chen, A model for low cycle fatigue life prediction of discontinuously reinforced MMCs, International Journal of Fatigue, 2005, 27(4), 417-427.

18 Q. Zhang and D.L. Chen, Effect of particle size on the low cycle fatigue life of discontinuously reinforced MMCs, Proc of the 2nd International Symposium on Aerospace Materials and Manufacturing: Development Testing & Life Cycle Issues (COM 2004), Hamilton, Ontario, August 2004, edited by P.C. Patnaik, M. Elboujdaïni, M. Jahazi and J. Luo, The Metallurgical Society of CIM, 2004, pp.289-300.

19 M. Roth, CF188 ALEX 66.1 Coupon Test program - Crack growth Investigation, QETE Report A014504, March 2005.

20 N. Goldsmith, R. Bayles, M. Roth, E. Ferko, "Fractographic Analysis in Support of a Structural Life Assessment" presented at the International Conference and Exhibition on Failure Analysis and Maintenance Technology in Brisbane, Australia, April 2004

21 R. Bayles, et al., "Fractographic Analysis of Cracks from a Full-Scale Fatigue Test" presented at Aeromat 2004 in Seattle in June 2004

22 R. Bayles, et al., "Fractographic and Analysis in Support of a Structural Life Assessment", to be presented at ICAF 2005

23 QETE IFOSTP Fractography Reports A019800-6 to -8, and -12

24 QETE IFOSTP Fractography Reports A019800-13 to -15

25 QETE IFOSTP Fractography Reports A019800-10, -16 and -17

26 QETE IFOSTP Fractography Reports A013501-9
27 L. Hounslow, M. Bunn, “Final Report - P-3C SLAP RHS Wing Teardown”, ATESS, 15 November 2004
28 M. Liao, D.S. Forsyth, and N. Bellinger, “Risk Assessment of Corrosion Maintenance Actions in Aircraft Structures”, The Proceedings of 2003 USAF Aircraft Structural Integrity Program, Savannah, GA, USA, December 2003.
29 M. Liao, D.S. Forsyth, J.P. Komorowski, M. Safizadeh, Z. Liu, and N. C. Bellinger, “Risk Analysis of Corrosion Maintenance Actions in Aircraft Structures”, The Proceedings of the 22nd International Committee of Aeronautical Fatigue (ICAF 2003), Lucerne, Switzerland, June 2003.
30 M. Liao and J.P. Komorowski, “Corrosion Risk Assessment of Aircraft Structures”, Journal of ASTM International, Vol. 1, No. 8, September 2004.
31 M. Liao and J.P. Komorowski, “Final Report for TTCP Collaboration Program TTCP-AER-TP4-CP4A-3, Risk and Reliability Analysis”, LTR-SMPL-2004-0178, August 2004.
32 L. Hounslow, M. Bunn, “Final Report - P-3C SLAP RHS Wing Teardown”, ATESS, 15 November 2004
33 M. Yanishevsky and M. Brothers, Fatigue Testing and Nondestructive Evaluation of the P-3C Orion (CP140 Aurora) Service Life Assessment Program (SLAP) Wing Station WS167 Lower Front Spar Component, LTR-SMPL-2003-0135, November 2003.
34 M. Yanishevsky and M. Brothers, Fatigue Testing and Nondestructive Evaluation of the P-3C Orion (CP140 Aurora) Service Life Assessment Program (SLAP) Butt Line BL65 Lower Front Spar Component, LTR-SMPL-2003-0270, January 2004.
35 G. Pieton and M. Yanishevsky, P-3C Orion (CP140 Aurora) Service Life Assessment Program (SLAP) Crack Growth Prediction of Centre Crack Panel and Wing Station WS167 Design Detail Using AFGROW and FASTRAN, LM-SMPL-2003-0325, December 2003.
36 M. Yanishevsky, P-3C Orion (CP140 Aurora) Service Life Assessment Program (SLAP) Spectrum Fatigue Crack Growth (FCG) Tests on Centre Crack Panel (CCP) Coupons, LTR-SMPL-2003-0134, June 2003.
J.F. Roberge (Martec Ltd), J.F. Leclerc (Martec), M. Yanishevsky (National Research Council) and A. Hull
(Engineering Material Research), Spectrum Fatigue Evaluation of Cold Expanded CP140 Web Material, Martec Technical Report TR-04-02, February 2005.
37 M. Yanishevsky, P-3C Orion / CP140 Aurora Wing Component Tests - Hole Cold Expansion Fatigue Enhancements, ICAF 2005, Hamburg, Germany, June 2005, to be published.
38 G. Li, D. Backman, N.C. Bellinger, and G. Shi , Numerical Modeling of A Single Aluminum Sheet Containing An Interference Fit Fastener, 18th Aerospace Structures and Materials Symposium, Can. Aero. & Space Institute, Toronto, 26-27 April 2005.
39 M.C. Chaturvedi and D.L. Chen, Effect of specimen orientation and welding on the fracture and fatigue properties of 2195 Al-Li alloy, Materials Science and Engineering A, 2004, 387-389, 465-469.
40 R.P.G. Mueller, An Experimental and Analytical Investigation of the Fatigue Behaviour of Fuselage Riveted Lap Joints, Ph.D. Dissertation, Delft University of.
41 P.R. Underhill, A.N. Rider and D.L. DuQuesnay, The Effect of Warm Water Surface Treatments on the Fatigue Life in Shear of Aluminum Joints, accepted for publication in Int. Journal of Adhesion and Adhesives, 2005.
42 X.J Wu, W Deng, AK Koul, and J.-P. Immarigeon A continuously distributed dislocation model for fatigue cracks in anisotropic crystalline materials. Int. J. Fatigue, 23, S201-S206 (2001).
43 J. Zhao, XJ Wu, R Liu, and Z. Zhang Finite element analysis of a notch root semi-elliptical crack in single crystal superalloy. Engineering Fracture Mechanics 71: 1873-1890 (2004).
44 L. Xiao, D.L. Chen and M.C. Chaturvedi, Effect of boron on the low cycle fatigue behavior and deformation structure of Inconel 718 at 650°C, Metallurgical and Materials Transactions A, 2004, 35A, 3477-3487.
45 L. Xiao, D.L. Chen and M.C. Chaturvedi, Shearing of γ″ precipitates and formation of planar slip bands in Inconel 718 during cyclic deformation, Scripta Materialia, 2005, 52(7), 603-607.